ADDIS ABABA UNIVERSITY
SCHOOL OF GRADUATE STUDIES
COLLEGE OF NATURAL SCIENCES
SCHOOL OF EARTH SCIENCES

GEOPHYSICAL INVESTIGATIONS FOR GROUNDWATER POTENTIAL ASSESSMENT OF VOLCANIC PLAINS OF THE MERMERO AREA; BORENA ZONE, SOUTHERN ETHIOPIA

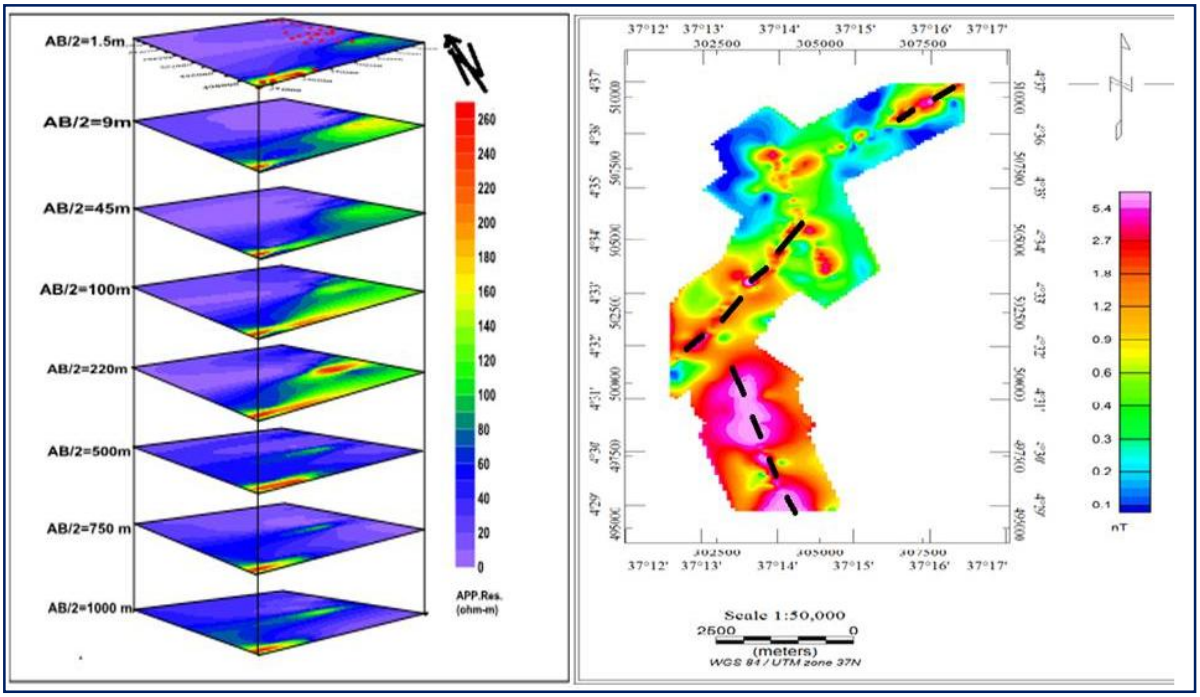

A THESIS SUBMITTED TO THE SCHOOL OF GRADUATE STUDIES OF ADDIS ABABA UNIVERSITY IN PARTIAL FULFILLMENT OF THE REQUIREMENTS FOR THE DEGREE OF MASTER OF SCIENCE IN GEOPHYSICS

BY: DEREJE MERGA

June, 2015
ADDIS ABABA

ADDIS ABABA UNIVERSITY

SCHOOL OF GRADUATE STUDIES

SCHOOL OF EARTH SCIENCES

GEOPHYSICAL INVESTIGATIONS FOR GROUNDWATER POTENTIAL ASSESSMENT OF VOLCANIC PLAIN, MERMERO AREA, BORENA ZONE

BY: DEREJE MERGA URGO

APPROVED BY BORD OF EXAMINERS:

Name	**Signature**	**Date**
Bekele Abebe (PhD) (Chairman)	_____	_____
Abera Alemu (PhD) (Examiner)	_____	_____
Dessie Nadew (PhD) (Examiner)	_____	_____
Tigistu Haile (Prof.) (Advisor)	_____	_____
Tilahun Azagegn (Co-Advisor)	_____	_____

Declaration

I, the undersigned; declare that this thesis is my original Work, has not been presented for degrees in any other University and all sources of material used for thesis have been properly acknowledged.

Name: Dereje Merga

Signature_____

Date_____

This thesis has been submitted for examination with approval as University advisors:

1. Tigistu Haile (Prof.)

   Signature: _____

   Date of approval: _____

2. Tilahun Azagegn

   Signature _____

   Date of approval_____

ABSTRACT

Geophysical investigation methods of Vertical Electrical Sounding and magnetic prospecting were used to investigate groundwater potential zones of Mermero area, Borena zone, Southern Ethiopia. The main objective of this study is to determine the depth of groundwater table, to locate the groundwater potential areas and to identify the subsurface layers.

The data acquired from twenty eight (28) Vertical Electrical Sounding points and 663 magnetic data points, which were interpreted both qualitatively and quantitatively in order to understand the lithostratigraphic section at the specific locality and identify aquifer bearing horizons.

The qualitative analysis of Vertical Electrical Sounding data were performed by using pseudo depth sections and geo-electric section and different apparent resistivity maps. Similarly, the qualitative interpretations of magnetic data were performed by total magnetic variation plot and different magnetic anomaly maps.

Finally, the qualitative interpretation was done by all the above results together with the geologic, topographic maps and borehole information. From the analysis result, geologic structures and groundwater potential zones are identified.

The quantitative interpretations of the Vertical Electrical Sounding data were conducted by modeling the sounding data using Ip2win and Win Resist modeling software and constructing geoelectric sections along selected survey lines, using the result from individual Vertical Electrical Sounding point interpretations.

The depth and lithologic units from the boreholes were used to fix parameters during the modeling of Vertical Electrical Sounding data. The geoelectric sections enabled to identify the overburden thickness and the depth to the aquifer along survey lines whereas the magnetic method complemented the finding of the other geophysical methods regarding structural indication such as faults, fractures and lithologic contacts.

Keywords: Magnetic anomalies, Pseudo–Depth Section, Geoelectric Section, Magnetic and electrical properties of Earth materials, Mermero, Borena.

ACKNOWLEDGEMENT

First of all, I would like to thank the almighty God for everything He does in my life. I have no words to thank my advisor Prof.Tigistu Haile for without his scientific advice and guidance, constructive suggestions and all way round support, his crucial comments and sound suggestions that he gave me in order to accomplish this thesis successfully.

I would like to extend my appreciation to my co-oadvisor Tilahun Azagegn for his scientific advice, unreserved support, comments and positive response, giving sound suggestions he gave me.

My gratefulness goes to Dr.Shimeles Fissiha for their unreserved support, suggestions and crucial comments and also during the primary data collection to accomplish this work successfully. I have great respect in my life for you due to your rational and enthusiasm behavior to help others.

I would like to extend my appreciation to my colleagues Likissa Fanta for his unreserved support, suggestions and crucial comments, assisting and cooperation during primary data collection and for his assisting during making different type of maps.

My deepest gratitude goes to Dr. Wakgar Furi: General Manager of Oromia Water Works Design and Supervision Enterprise (OWWDSE), for his kind of advice, supportive and motivation during my study.

I also like to extend my thanks to the following individuals for their cooperation in sharing their views for my study: Etefa Rundassa, Gelatu Belay, Abu Adem, Solomon Kenea, Asamino Gebayew, Ayantu Dibaba, Million Etefa and Mekdem Dereje for giving unreserved supports.

I am also very thank full for Oromia water works Design and Supervision Enterprise(OWWDSE), for their supportive,particularly during the primary data collection without any completion.

Last but not least, I would like to thank my lecturers for giving me all the basics of science and their courage to help everybody.

Table of Contents

List of Figures

List of Tables

ACRONYMS

DC	Direct Current
GPS	Global Position System
IGRF	International Geomagnetic Reference Field
ITCZ	Inter Tropical Convergence Zone
J_r	Intensity of Remnant Magnetization
MER	Main Ethiopian Rift
NE-SW	Northeast-Southwest
N-S	North-South
nT	Nanotesla
NW	North-West
NW-SE	Northwest-Southeast
OWWDSE	Oromia Water Works Design and Supervision Enterprise
PPM	Proton precession magnetometers
SW-NE	Southwest-northeast
UTM	Universal Transverse Mercator
VES	Vertical Electrical Sounding
Ω-m	Ohm-meter
NMSA	National Metrological Service Agency

1. INTORODUCTION

1.1. Background

Water is one of the basic needs to sustain life. Living things such as humans, animals and plants are dependent on water. Our bodies need to ingest water every day to continue functioning.

Communities and individuals can exist without many things like shelter, even without food for a period, but they cannot be deprived of water and survive for more than a few days. Because of the intimate relationship between water and life, it plays a vital role in the development of a community since reliable supply of water is an essential perquisite for the establishment of a permanent community. Access to clean water is a human right and a basic requirement for economic development.

The largest amount of water on Earth (97.2 %) is contained in the oceans and seas as a saline or salty water but only small amount of it (2.8 %) exist as fresh water on land. This fresh water found on land is distributed as ice caps and glaciers (76.43 %), groundwater and soil moisture (21.96 %), fresh-water lakes (0.32%), saline-lakes (0.29 %) and very small amount of it as streams channels (0.004 %) (Fetter, 2001). The amount of fresh water which is available for domestic, industrial and agriculture purposes is very limited as compared to the total volume of water on the planet Earth. Due to the above reasons, the search for ground water is vital as an immediate and sustainable solution to alleviate the scarcity of water for drinking and other domestic uses in most part of the world. This is also the case in Ethiopia.

Groundwater refers to water that occurs below the Earth's surface resulting from water infiltrating down from the surface. It is the safest kind of water supply. The attractive features of developing groundwater resource are the fact that groundwater is free from pollution and is very useful for domestic use in small towns, farms, and development sites as well as for the reason that it can be made available at a small capital cost and also in least possible time. In arid regions and in areas far removed from municipal water supply schemes groundwater becomes the only reliable source of clean water for domestic, industrial, livestock and agricultural uses.

The general objective of the research focuses on groundwater potential assessment for the Mermero volcanic plain using electrical and magnetic methods of geophysical investigation methods to determine and locate groundwater potential areas.

Groundwater occurs at various locations below the Earth's surface depending on the physical properties of various formations that exist. Measurement of these physical properties can yield information on whether, say, these formations are water saturated or not. Accordingly there are a number of methods used to investigate the presence of groundwater including geological, hydrogeological, geophysical and geocehemical investigations.

Among these various techniques to explore for groundwater, geophysical methods are well suited for the exploration of groundwater. Out of the various geophysical methods that can be used, the electrical resistivity and the magnetic method are more powerful for they respectively provide a quantitative measure of the conducting properties of subsurface materials which in turn largely depend on the moisture content and on the possible structural conditions that control their movement. Because of its relatively higher depth of investigation, operational speed, lower cost and adequate delineating power for mapping the presence of water bearing horizons and their depth beneath the surface, the electrical resistivity method with the vertical electrical sounding variation has established itself as an important and standard tool for the purpose. The method is one of the most sensitive geophysical methods to determine the presence of water saturated horizons in the subsurface, the depth to these zones and also, when appropriate measurement schemes are employed, groundwater flow pattern. Electrical survey data acquired along properly arranged traverses are also powerful means to delineate the presence of subsurface structures and weak zones that control (enhance) the movement of groundwater. In addition to mapping formations of water saturation beneath the surface, electrical methods have also found application in giving information on the water quality and the possible yield of these zones.

Groundwater occurrence in an area can be variable due to abrupt discontinuity in lithology, thickness, and the properties of the overburden of volcanic rocks and the weathered bedrock. Consequently, groundwater exploration within such geologic setting requires integration of geophysical data types to effectively characterize the hydro geologic zones and to enhance successful identification of well locations. In situations where subsurface structures and

discontinuities play a major role in the movement of groundwater, methods like the magnetic survey are indispensable tools for mapping the presence and role of these structures.

In the final analysis, the thesis is expected to create awareness on the productive aquifer of the area so as to guide both the government and individuals involved in groundwater development on the possible areas and depth that more boreholes could be drilled for potable and sustainable water supply. This will be achieved by obtaining information on the subsurface aquifer distribution, formation and type, and controlling structures using Vertical Electrical Sounding (VES) and magnetic methods of prospecting.

1.2. Statement of the Problem

The study area-Mermero lowland plain is located in one of the drought prone areas of Borena Zone, Oromia Regional State; Southern Ethiopia. Almost all of the population in the area is engaged with pastoral farming whereby the search for grazing land and water determine their settlement location at any particular time and their movement. Hence, the people are clustered near existing wells to get water because the rainfall in the area is generally erratic and scarce. Since there is no any river, stream or spring over large part of Borena area in general and the study area in particular hand dug wells and drilled boreholes are the only sources of drinking water for the people and their livestock to have permanent settlement. There is also no perennial surface water in the study area. For instance the absence rainfall in the years 2010-2011 forced the dwellers to lead their daily life by assistance from government and local and international NGO's for their food security. From year to year an acute water shortage is prevailing. As the study area is well-known with the Borena cattle breeding/pastoralist population, the life of the local people and their livestock rely only on the availability of groundwater resources.

The search for groundwater resources potential of the area was not adequately carried out in the past. But the studies to explore and exploit these groundwater resources began in earnest in recent times through a number of projects funded by the Ministry of Water Resources and run by the Oromia Water Works Design and Supervision Enterprise (OWWDSE). Because of the metamorphic geology of the area, believed to be containing less groundwater as a

whole, most studies were not exhaustive and have failed to give results. Through studies it was understood that the volcanic rocks which cover a good portion of the area are the potential horizons that could bear the groundwater of the areas. The depth to groundwater saturation, the thickness and presence of the overburden and the volcanic rocks, which are believed to hold much of the groundwater potential of the area, the degree of weathering of these rocks are the main problems for the sitting of preferred location of the production boreholes.

Out of the various locations within the Borena area, the Mermero volcanic plains (Figure 2.1) are chosen as a subject of the current research work because of the rich fertile soil, extensive grazing land and the large livestock population the area supports. Furthermore, from geologic studies it was found that the volcanic rocks of this area are found to be extensive and potentially water bearing.

1.3. Objectives of the study

1.3.1. General Objective

The general objective of the research focuses on groundwater potential assessment for the Mermero volcanic plain using electrical and magnetic methods of geophysical investigation methods to determine and locate groundwater potential sites in the study area.

1.3.2. Specific Objectives

- To identify the major subsurface units/ layers.
- To identify groundwater potential areas,
- To determine the depth to groundwater bearing horizons,
- To identify the geologic structures and weak zones that serve as a storage areas or conduits for groundwater movement,
- To determine the depth to the bottom confining crystalline basement rocks/ aquiclude whenever possible,
- Suggest preferred locations for sinking of boreholes to extract the groundwater,

1.4. Methodology

In order to achieve these research objectives, a number of steps have been followed. These included reviewing different previous works, not only geophysical works (on the groundwater exploration and identification of geophysical structures) but also geological and hydro-geological literatures on the study area.

These were followed by collecting field data using two specific geophysical methods. The methods employed are the vertical electrical sounding (VES) and magnetic methods of prospecting. Specifically, data from both methods were collected along four selected traverses well distributed to cover the study area. The vertical electrical sounding (VES) data are analyzed using appropriate software like RESIST, IP2Win, and were presented using the plotting software like SURFER and Auto CAD. and while The magnetic data are analyzed using a combination of Microsoft Excel spread and the Oasis Montaj, SURFER and the handy Paint software. Consequently curves, maps and models are produced and interpreted to arrive at the objectives of the research work.

The detailed methodological approach of the thesis is as indicated in figure 1.1

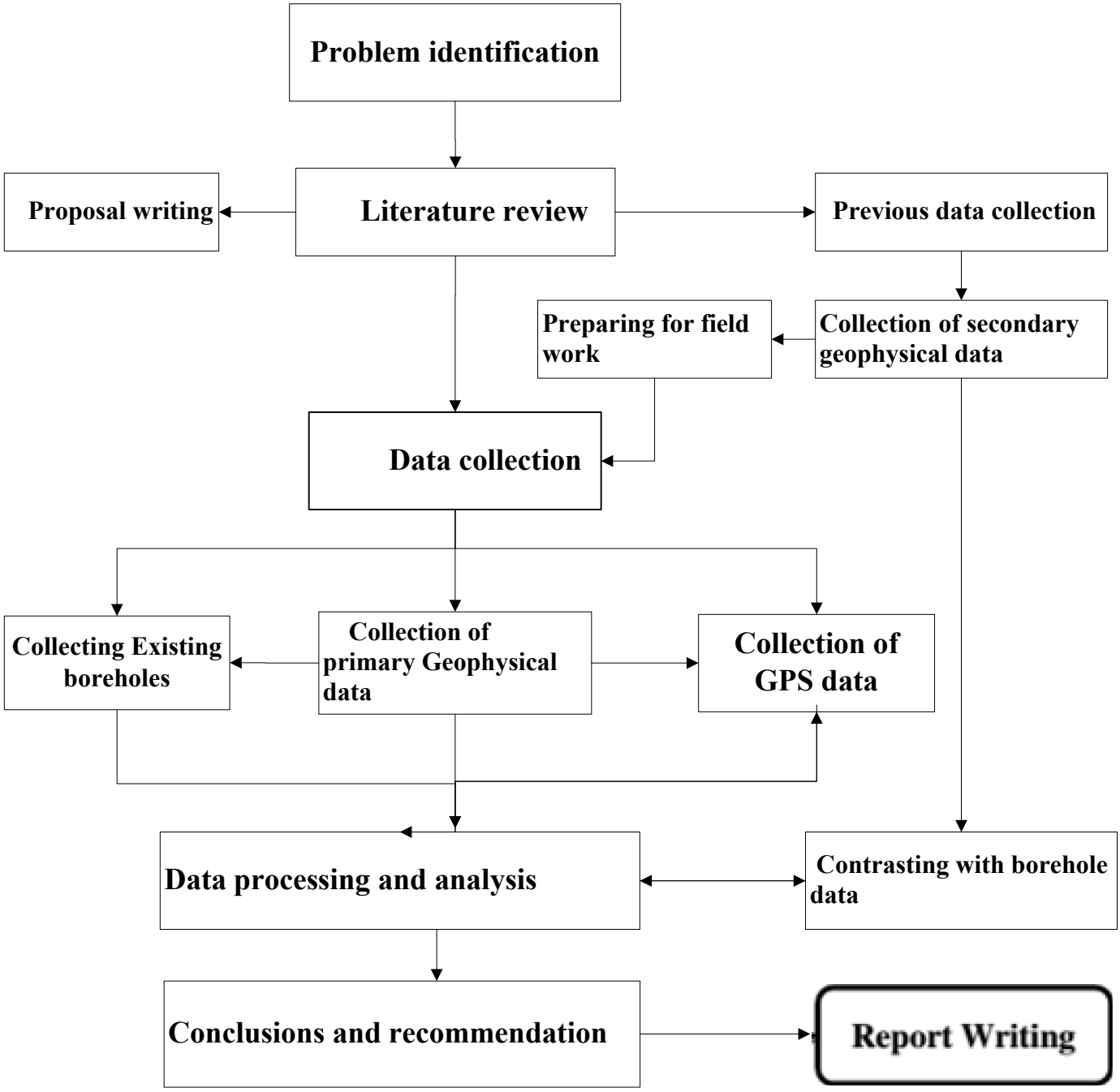

Figure 1-1: Flow model of the project.

1.5. Basic Research Questions

- What is the general geological setting of the Mermero area?
- Which geophysical method is appropriate to investigate groundwater potential of the study area?
- How to identify the geologic structures and weak zones of the area and their role in controlling the storage and movement of groundwater?
- Where to locate the preferred locations for sinking of test/productive boreholes?
- How to identify the groundwater table of the area?

1.6. Research Hypothesis

To fully utilize the groundwater resources of an area the implementation of detailed hydrogeological investigations is important, i.e. detailed and integrated investigation on the groundwater potential resource must be conducted. To improve the hydrogeological investigations, the application of geological and geophysical methods are crucial to solve a number of associated problems like locate areas of presence of volcanic rocks, determine the thickness of overburden and the degree of weathering and fracturing of the volcanic rocks, determine areas of groundwater saturation, and their depth and the preferred location for sitting of productive boreholes.

1.7. Significance of the study

In general the main essence of this project is to identify the presence of groundwater in the volcanic rocks of the Mermero plain, identify zones of groundwater saturation, their thickness and depth, thickness of overburden in the area by combining the knowledge of the geology of the study area also using integrated geophysical (electrical and magnetic) methods.

Furthermore, the objective of the work will be to identify which of these two geophysical methods is a fundamental tool specifically for the current project area just to locate productive drilling sites for the extraction of groundwater resource more appropriately and to give benefits for the advancement of science. So that the local communities in particular and the scientific communities in general could gain a lot from the study result.

1.8. Literature review

In the proposed area, many investigations were carried out at local level by different organizations to exploit the groundwater resources for rural and urban domestic water supply. Oromia Water Resources Bureau and NGO's operating in the area conducted most of these studies for location of well sites for the water supply of rural and urban settlements. The investigations were aimed at identifying potential areas for mostly domestic water supply.

Oromia Water Works Design and Supervision Enterprise (OWWDSE) have commenced Borena Groundwater investigation projects in the year of 2006. The investigation consisted of three phases and at present only the first and second phases of work are accomplished. The third phase is proposed to continue in future. These earlier studies indicated that the groundwater bearing aquifer in Borena area is the highly weathered and fractured basalt lying in most of the nearly flatlands and is moderate to high yielding (Abebe Ketama, 2011). Through these studies, the groundwater flow direction is deduced to be from West, North and south toward the Rirriba valley (Figure 2.1) and finally flows south towards the Kenyan border. The groundwater is sourced from modern age precipitation.

The Ethiopian Geological Survey (EGS) and Ministry of Water and Energy had conducted regional hydrogeological and geological studies of the area. The geological mapping exercise of the Yabello, and Moyale sheet by the EGS. The other regional study is that of Ministry of Water and Energy which aims at Genale Dawa river basin Master Plan Project (2004) investigation. This study indicates that extensive fracturing that occurred in the past geologic time during the development of the present rift system controls the groundwater system in the proposed area. This study also briefly described the hydrogeological characteristics of different geologic units found in the study area.

International Livestock Centre for Africa has also conducted a synthesis of pastoral research, development and change in the Borena plateau of southern Ethiopia (Helland et al., 1980b). This study also covers some part of the current research area. The research composed of an inter-disciplinary project, but focused on rangeland and land use investigations. It states that water resource is the fundamental future that has shaped the Borena society. Deep wells in particular are a focal point for social organization and retinal, (Helland et al., 1980b).

1.9. Organization of the thesis

The thesis is organized in six chapters. Chapter one deals with general introduction, Objectives, methodology and literature review. Chapter two gives the physical description of the study includes the location, Physiography and drainage, geology, climate and hydrogeology of the study area**.** Chapter three overview of theoretical background of the geophysical methods employed in the work, i.e. Vertical Electrical Sounding (VES) and magnetic methods of prospecting. Chapter four data acquisition and processing .Chapter five deal with discussion and interpretations of the processed data. Chapter six deals with conclusions and recommendations of the study.

2. GENERAL DESCRIPTION OF THE STUDY AREA

2.1. Location and Accessibility

The research area is found in the Mermero area, Borena Zone, Oromia Region, southern Ethiopia. The Mermero area is located about 150 km in west of Yabello town and about 60 km south of Telltale town. It is located between latitude of 4° 27'46" and 4°52'28" N and longitude of 37° 02' 56" and 37° 22'45"E with a 720 km distance from Addis Ababa (Figure 2. 1). It is bounded by the Ethio-Kenyan border in the south of the study area. The site is accessed by an all weathered detour access road from the asphalt road that goes from Addis Ababa to the border town of Moyale that passes via towns of Yabello and Mega; which are found at the north eastern and eastern adjacent of the study area. All weather roads, secondary and tertiary roads connect different part of the study area.

2.2. Physiography and Drainage

At the regional scale, the Mermero area is bounded by the chain of Mermero Mountain in the adjacent west, and the Kukesa and Elkune hills and high grounds in the north. In the east, the landscape opens into wide grazing plain area towards the Gocha area that slopes gently towards south. Geomorphologically the area is situated in the middle of the Bulal catchment (figure2.2). The dendritic nature of the drainage patterns at the locality of the study area area is the result of the flat configuration of the landscape. Further towards the south, the landscape gets relatively rugged and the drainage patterns converge to the main drainage channels.

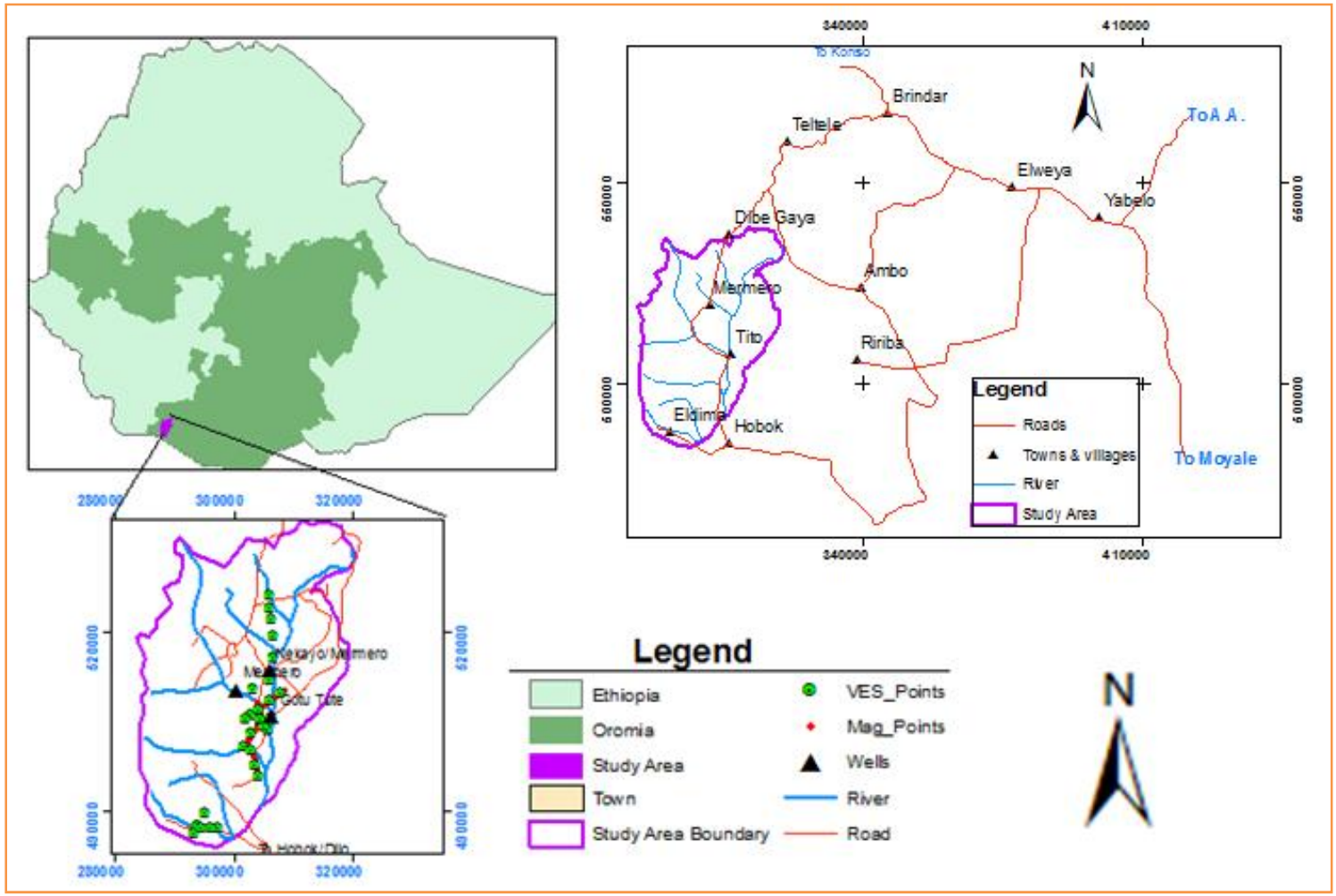

Figure 2-1: Location Map of the Study Area

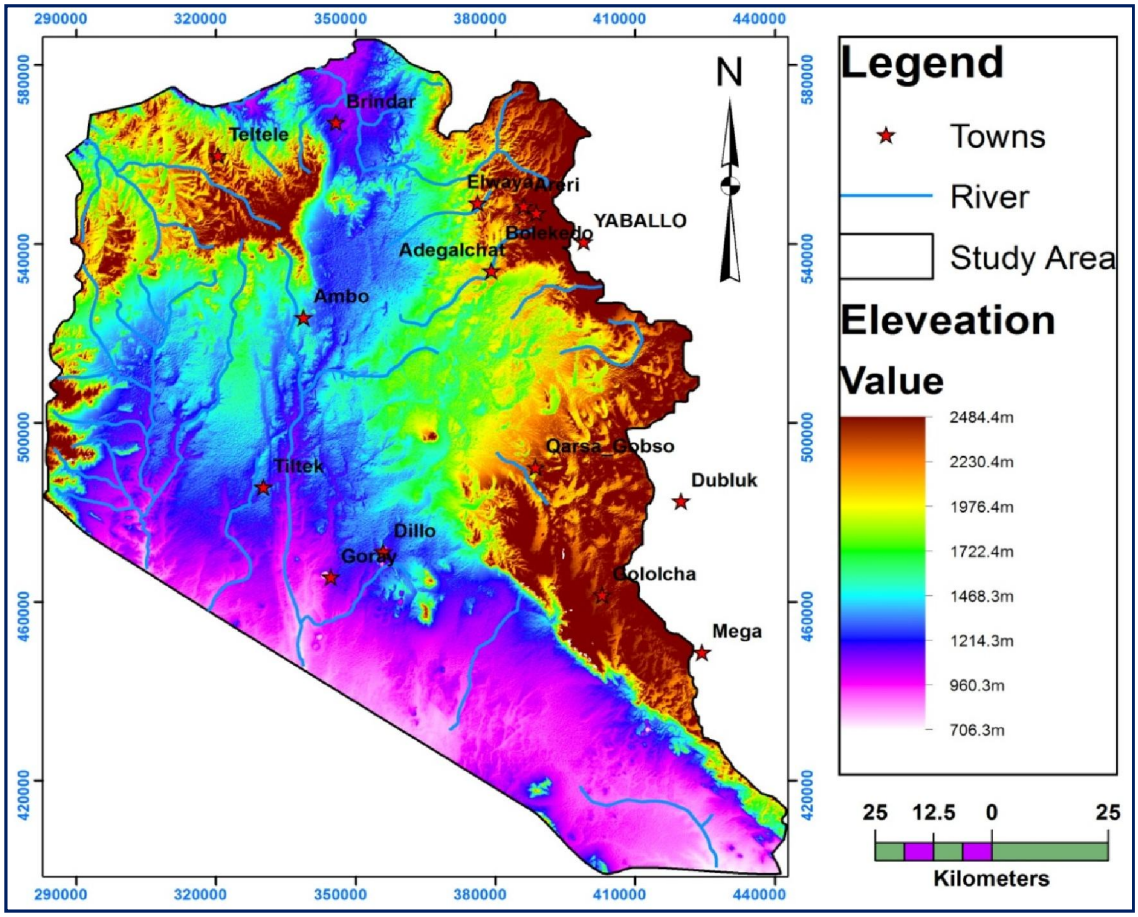

Figure 2-2: Physiography and Drainage Map of Borena

2.3. Climate and Vegetation

The climatic condition of the study area is similar to that over the Borena zone and it is characterized by arid to semi-arid climate. According to the National Metrological Service Agency (NMSA, 1996), the moisture for precipitation in the area originates from south-east equatorial air stream, which moves Inter Tropical Convergence Zone (ITCZ). It is characterized by arid to semi-arid climatic condition with two rainy seasons. These are from March to May and from September to November, but rarely with little rainfall from June to August.

The mean annual temperature of the area, estimated according to the data of three stations, varies from 37°C to 21°C.

The mean annual aerial rainfall of the study area is estimated to be about 593mm. The mean annual maximum temperature of the study area varies from 23°C to28°C; while the mean minimum temperature varies from 13°C to16°C (OWWDSE, 2011).

The vegetation cover of the area is mostly continuous, dense and tall grass with thorny shrubs, wild seasonal, and scattered small trees. There is no any agricultural works in the area by the pastoralists.

2.4. Geology of the Study Area

2.4.1. Regional geo logy

In Southern Ethiopia in general, three major chronostratigraphic units are known to occur namely: Precambrian crystalline basement, Mesozoic sedimentary rocks and Cenozoic volcanic rocks with sporadic sediments and superficial deposits (Kazmin, 1972 and Davidson, 1983). The metamorphic complex and associated plutonic rocks make up the crystalline basement, which are the northern and southern continuation of the Mozambique belt and the Arabian Nubian shield respectively (Kazmin, 1978; Senbeto Chewaka et al., 1981). The extensive sedimentary rocks are results of marine transgression and regression of Indian Ocean in the Mesozoic. The voluminous volcanic rocks with subordinate fluviatile and lacustrine sediments overlying unconformably the crystalline basement are results of extensional tectonics responsible for the formation of the East African Rift (Davidson, 1983; Mohr, 1986; Gidey Woldegebriel, 1987; Ebinger et al., 2000). Although three major time stratigraphic units are known in southern Ethiopia, the Mesozoic sedimentary rocks are virtually absent in the presently mapped areas.

The East African Rift System including the Main Ethiopian Rift is a classical volcano-tectonic feature on the planet Earth with significant physical details visible from outer space. In the sector between the Ethiopian and Kenyan domal uplifts, the East African Rift system is represented by more than 300 km “broad rift” zone (Davidson and Rex, 1980; Davidson, 1983; Gidey Woldegebriel and Aronson, 1987). It is characterized by overlapping either north-south, northeast-southwest, northwest-southeast trending two or more rift systems which is more than three times the breadth of the MER or Gregory Rift away from the zone of overlap.

The rift system in southern Ethiopia mainly encompasses the branches of Turkana Rift in the west, Chew Bahir Rift, Rirriba Rift (Davidson, 1983; Gidey Woldegebriel, 1987) and Mega Rift (Hailemeskel Awoke et al., 2007). The surface expression of the northeast southwest trending Main Ethiopian Rift splays into north south trending Chamo and Segen basins separated from the Gelana Basin by the Amaro Horst. Until recently the southern

end of the Main Ethiopian Rift was considered to be a few kilometers from the Amaro horst, around 5^0 N latitude. However both field mapping and satellite image interpretation unequivocally demonstrated that the Main Ethiopian Rift continues southward to join the Rirriba Rift. Moreover, around Mega a series of northwest-southeast trending high scarp steep normal faults with considerable strike length defining outstanding horsts and grabens were recognized by Hailemeskel Awoke et al., (2007) that define the Mega Rift of the broadly rifted zone of southern Ethiopia proceeding further southeast into Kenya and northwest into Sudan represented by similarly oriented rifts and grabens.

2.4.2. The Geological Setting of Mermero Area

Geologically the Mermero area (including the area where geophysical survey was conducted) lies on volcanic plains underlain by basement rocks similar to the other Borena lands. The volcanic rocks are observed as boulders in the area. The exposed basaltic formation over the area is highly vesicular basalt which is confirmed from the drilled well lithology. The part of the basement rock which lies below the volcanic rocks is weathered and fractured with different degrees at different places.

The observed and identified geological make up of the area as it was mapped and described by Oromia water works design and supervision Enterprise geological report (OWWDSE, 2008), is arranged from bottom to top as: Banded gneiss, Quaternary vesicular basalt, Quaternary Scoraceous basalt, Scoria, Elluvial and Alluvial deposits.

The area is thus underlain by Proterozoic Metamorphic rocks and intrusives that are covered by Phanerozoic (pre-rift to post-rift) volcanic and superficial deposits.The volcanic comprises two major rock units. These are the vesicular basalt and the upper basalt. The superficial deposits comprise two units which are the alluvial and elluvial.

2.4.2.1. The Upper Basalt (TUb)

This unit is predominantly exposed in the western half of the mapped area, in the form of elevated ridges that mark the western boundary of the Rirriba fault Zone. It covers a total area of 103.19 km^2 which is about 22.5 percent of the total 460 km^2 area.

One hill forming outcrop of this unit in the Mermero area, is more acidic looking on its upper part than basalt which can be the sialic rock occasionally found capping the upper basalt as reported by Woldegebriel Genzebu et.al.,(1994) in the geology of the

Ageremariam Sheet. They reported that the upper basalt is sometimes capped by the Sherenga (a type locality in their mapped area) Rhyolite, as in the Segen basin which is found north of the study area.

2.4.2.2. Bulal Vesicular Basalt (BVb)

It is exposed in the eastern part of the mapped area, making two large bodies separated by incursion of elluvial deposit on the central portion of the eastern part of the area. The total surface area coverage of the vesicular basalt is about 249 km^2 that is nearly 31 % of the total area of the well field. Its average thickness is not well yet.

Floats of cobble and boulders of vesicular basalt, with carbonate in the vesicles and exhibiting alteration of olivine into other secondary mineral were observed in the mapped area. The size of the floats indicates that it is nearly in situ or was transported very little. At some other localities the rock was found as an in situ outcrop exhibiting very closely spaced jointing resulting in a sort of naturally crushed gravel. Intermixing of aphanitic basalt, sometimes with gradational varieties, was also observed occasionally.

It is generally gray to dark gray, fine to medium grained commonly very fresh and young looking. At places the vesicles are filled with secondary minerals such as quartz, calcite, and zeolits giving the rock amygdaloidal appearance.

2.4.2.3. Elluvium (QEl)

This is the largest unit in the Mermero well field. Its areal coverage is nearly equal to the area of all the remaining three units together. It covers a total area of 220.2 km^2 that is about 48 percent of the total 460 km^2 mapped area. According to the well-log data its average thickness is 50m.

This unit represents a superficial soil cover developed as the result of weathering of surfacial rocks. It is black, dark grayish, and grayish brown predominantly silty to silty clay soil with floats of vesicular basalt, aphanitic basalt, and rectangular acidic rock that was mentioned as the occasionally occurring Sialic rock that caps the upper basalt. The grayish brown colored soil is the result of alteration of this acidic rock, where the alteration of feldspar and some mica results in such colored soil.

The presence of floats of all kinds of rocks in the elluvial deposit is a clear indication of its development over variable parent material where the physico chemical condition permits.

Though the above mentioned rock units differ in age and texture they are all basaltic, and it can be concluded that it is derived from basaltic parent material.

2.4.2.4. Alluvium (QAl)

The alluvial deposit covers about 40 km^2 is which is only about 9 percent of the total area. It is found in the central part of the mapped area along a stream channel that drains south, widening at two points towards west along the confluence of tributary streams and their flood plains formed by runoff that flows down steep sided mountains of the upper basalt. The stream course is made up of gravel, with cobbles and boulders deposited on low energy side of meandering/ oblique places while the flood plains are predominantly covered by silty and clayish soil with minor rock fragments.

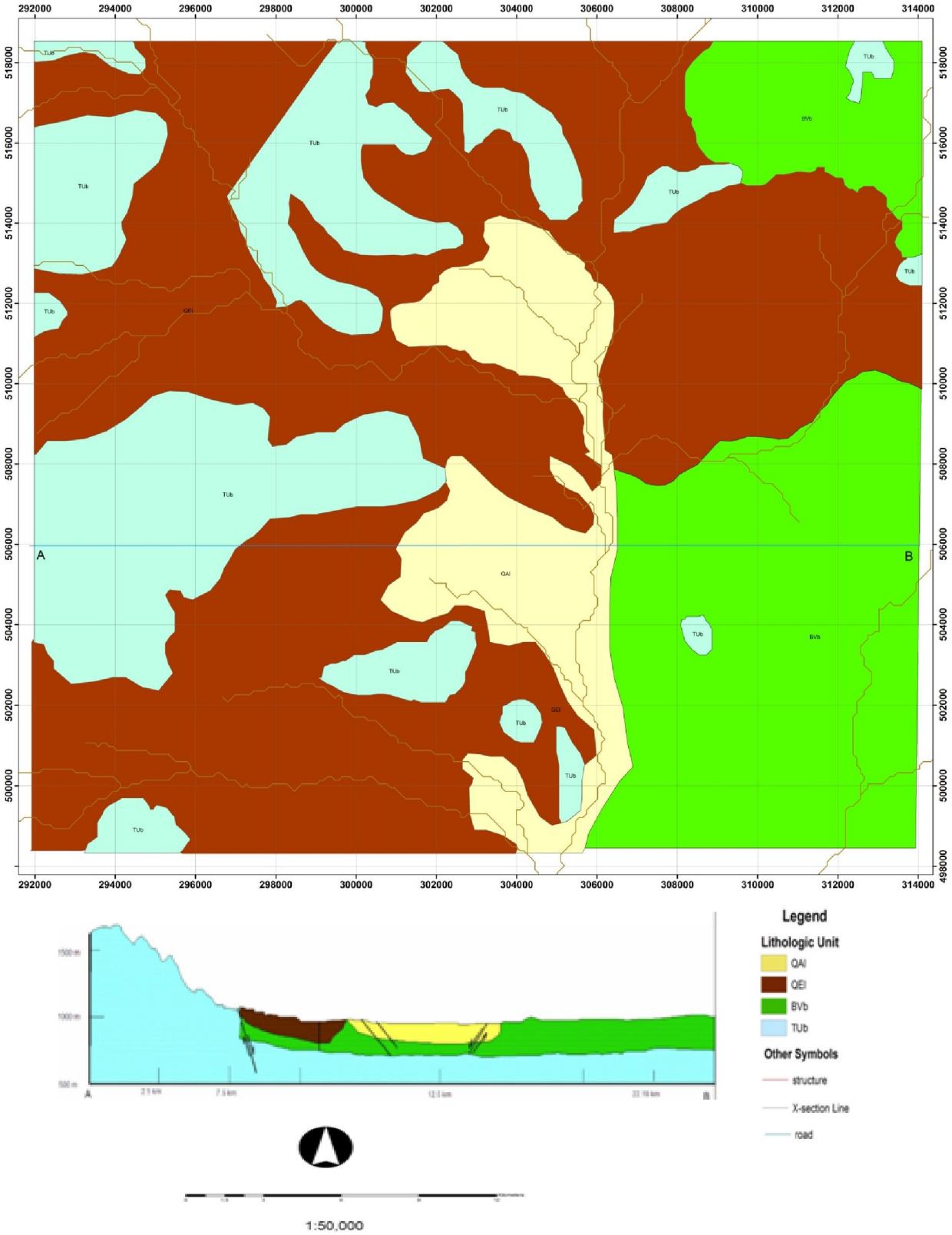

Figure 2-3: Geological map of Mermero area (OWWDSE, 2011).

2.5. Hydrogeology

The different in mineralogy, texture and structure of the volcanic rocks leads to have variable water bearing capacity. Groundwater circulation and storage in the volcanic rocks depend on the type of porosity and permeability formed during and after the rock formation (Tamiru Alemayehu., 2006). The occurrence of groundwater in the basement and volcanic rocks is governed by the volume and behavior of faults, fissures, and flow breccias, porous zones between successive lava beds, cracks and joints (Belete et al., 2000). The primary porosities such as vesicles and flow contacts or interflow spaces in the volcanic rocks are also factors that determine the water bearing capacity in addition to the aforementioned secondary porosities.

The groundwater occurrences in the metamorphic rocks are in the fractured and weathered parts of the rock. In the case of volcanic rocks, the sizes of fractures are the predominant factors whereas for metamorphic rocks; the storage capacity is determined by the type of weathering products and the thickness of the consequent weathered layer. Metamorphic rocks are mostly impervious and serve as aquicludes and the only water bearing zones in many of them are the upper loose and weathered parts. Hence metamorphic rocks are characterized by secondary permeability which decreases with depth, the groundwater yield to wells decrease rapidly as depth increase.

The weathered and fractured vesicular basalt rocks, the contact between the fractured and massive basalts and the upper weathered and fractured part of basement rock that lies below the volcanic rock are the potential aquifers for the drilled wells in the area due to their high permeability and porosity for the percolation of groundwater to the saturated zone.

2.5.1. Drilling Results and Aquifer Parameters

Only one well was tried to drill which even could not reached the intended target depth by reasons of groundwater back pressure and weak capacity of the drilling equipment. Hence, BTW2 test well was terminated at a depth of 141m, before intercepting the basement or reaching deeper depth.

Though this well has not been tested, indicative information during the drilling showed potential yield of about 15l/s. The shallowest depth to groundwater water table within the project area is 17.6 m b.g.l. The potential aquifers in this well field area are considered to

be within the weathered and fractured zones of both the Bulal basalt and upper basalts of the area, underlying the thick alluvial deposit. The alluvial deposits acting as highly permeable infiltration media to the underlying aquifer is recorded to have thickness in the range of 20 to 60m.

According to the previous study, OWWDSE, 2011, since both the geophysical and drilling works remained at shallower depths, the basalt section has not been penetrated more than about 80m (partial penetration) underlying the alluvial of about 60m thick at the locality.

Table 2-1: Basic Wells Parameters – Mermero

Well Code	Depth (m)	SWL (m, b.g.l)	Q(l/s)	Dd(m)	T(m2/d)	Remarks
BTW2	141	17.6	>15*			larger diameter well to be drilled and tested

* Estimated from drilling

2.5.2. Aquifer Geometry and Extent

Attempt has been made to trace the geometry and extent of the aquifer unit in this target area by the aid of geological mapping, geophysical surveys and test drilling. Except for the obstruction created as a result of the East ward continuations of the foot of the Mermero Mountain, at the adjacent West of the proposed well field area, the area currently studied as potential well field zone has nearly a square shape with about 11 kms. dimension in its sides.

Geophysical surveys and drilling operations launched to obtain information on the vertical and lateral extents of the volcanic aquifer in the area have only indicated that thick alluvial deposit with thickness in the range of 20 to 60m rest over the basalt unit. The basalt section has not been penetrated more than about 80m. Both works remained at shallower depths.

2.5.3. Depth to Water Strike, Static Water Level and Groundwater Flow System

The shallowest depth to water strike (79m b.g.l) corresponding to the shallowest depth to static water table (17.6m b.g.l) is recorded within Mermero potential well field area. Similarly, the highest confining pressures head of 61 m measured within well BTW2 is also regionally the highest.

The high groundwater head created as a result of the position of water table at high elevations over the Northern adjacent areas drives the groundwater flow through the well field area towards the South direction within Bulal sub-catchment.

2.5.4. Water Quality

By virtue of its geomorphological situation being close to the recharge zone of the project area, the proposed Mermero potential well field area has good water quality. The index water quality parameter (TDS) measured in test well BTW2 and existing Wobok BH-1 boreholes during phase I, showed values of 345 mg/l and 597 mg/l) respectively against the drinking water guideline value of 1776 mg/l set by the Ministry of Water Resources(2002).

3. THEORY OF THE GEOPHYSICAL METHODS

3.1. General

The application of geophysical methods in hydrogeological problems is based on the fact that groundwater conditions at a location are mainly described through characterizing the existence and distribution of permeable layers (like sand, gravel, fractured rock) and impermeable or low-permeable layers (like clay, till, solid rock) in the subsurface.

To obtain a geophysical image of these underground structures, sufficient contrast of physical properties is required. Electrical conductivity, dielectric constant, and magnetic susceptibility (to some extent) are the most relevant petro-physical properties used as diagnostic parameters in geophysical exploration for groundwater. The influence of porosity, water saturation, and clay content on these petro-physical properties is the key factor.

Owing to their intrinsic correlation to the aforementioned physical properties of subsurface rocks, the geophysical methods chosen for this particular research project were Vertical Electrical Sounding (VES) and Magnetics method of prospecting.

The resistivity method is used for detecting groundwater presence and differentiating subsurface layers whereas the magnetic method supports the electrical resistivity method. From the electrical resistivity method, one can deduce hydro geological information such as the availability of water and water quality.

3.2. Theory of Electrical Resistivity Method

Electrical resistivity methods have been used in a number of groundwater exploration surveys when the resistivities of the rocks are needed to be inferred. The resistivity of shallow subsurface of the Earth which yields much of our groundwater resources depends on the clay content, formation porosity, amount of water in the rock and the salinity of the water in the rocks. The electrical conductivity of these rocks will increase when they are saturated well with water compared to unsaturated and dry rocks. The resistivity of the saturated rocks in the upper part of the earth's crust, decreases with increasing their porosity and the degree of salinity of the saturated fluids. In contrary to the above, the presence of clay and conductive minerals can also reduce the resistivity of rocks which can be resolved by using other geophysical techniques, geological or well information. In

resistivity surveying especially in vertical electrical sounding (VES), conduction in rocks is mainly due to pore fluids acting as electrolytes. Water in its pure form is poor conductor but most water contains dissolved salts which facilitate current flow.

The resistivity of geological materials exhibits one of the largest ranges of all physical properties from 1.6 x $10^{-8}\Omega$m for native silver to $10^{16}\Omega$m for pure sulphur (Reynolds, 1997). The basic procedure in resistivity surveying is to measure the potential difference on the surface associated with a known current that is made to flow into the earth. Normally, a four electrode system is systematically arranged and expanded systematically about the point on the surface to obtain depth information.

3.2.1. Basic Principles of the Direct Current (DC) Electrical Resistivity Method in Groundwater

Groundwater, through the various dissolved salt it contains, is ironically conductive and enables electric currents to flow into the ground. By measuring the ground and subsurface resistivity therefore it gives the possibility to identify the conditions necessary for the presence or the absence of water. In resistivity surveying, especially in vertical electrical sounding (VES), conduction in rocks is mainly due to pore fluids acting as electrolytes. Water in its pure form is poor conductor but most water contains dissolved salts which facilitate current flow. Resistivity of rocks generally depends on the water content (porosity), the resistivity of the water, the clay content and the content of metallic minerals Bernard (2003). The following considerations help in the determination of the resistivity of rocks.

- A hard rock without pores or fractures is very resistive to the flow of electric current. This is generally observed in hard fresh Precambrian rocks.
- Dry sand without water is very resistive.
- Porous or fractured rock bearing free water has resistivity, which depends on the resistivity of the water and on the porosity of the rock.
- Impermeable clay layer, which is wet, has low resistivity but may not contain enough yields for successful groundwater exploitation.
- Mineral ore bodies (iron, sulphides) have very low resistivity due to their electronic conduction; usually lower or much lower than 1Ohm-m (Bernard, 2003).

To identify the conditions necessary for the presence of groundwater from resistivity measurements, the absolute value of the ground resistivity must be considered. Usual target for aquifer resistivity can be between 50 Ohm-m to 2000 Ohm-m (Bernard, 2003).

In hard rock environment, which is considered very resistant to the flow of electric current, a low resistivity anomaly will be the target for groundwater.

In a clay or salty environment that is normally considered conductive, a comparatively high resistivity anomaly will most probably correspond to fresh water and thus will be the target in the case for groundwater exploration for domestic use.

Resistivity values of earth materials cover a wide range. The variety of resistivity has been the essential reason why the technique can be used for different applications (Loke, 2001).

The electrical conductivity of rocks can be studied by measuring the electrical potential distribution produced at the earth's surface due to an electric current which is injected in to the ground through electrodes for the cause of DC current. The types of currents introduced in to the ground are direct, commutated or low frequency alternative currents and the potential differences are measured using non-polarized electrodes. The direct current sources are used to inject current in to the ground using two current electrodes to measure the generated electric field as a potential difference using other two potential electrodes. . If we consider the media that the current entered as a homogeneous isotropic ground, the flow of current in the medium is based on the principle of conservation of charge and is expressed.

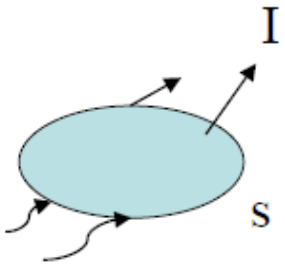

$$(I_C)_S = -\frac{dQ}{dt} \qquad (3.1)$$

where (I_c) – is the current flow due to charges out of the closed surface's'

Q – is charge enclosed by 's'

In terms of current density **J** and charge density q, $(I_c)_s$ and Q are given by

$$(I_C) = \oint \vec{J}.ds \tag{3.2}$$

$$Q = \int_V q.dv \tag{3.3}$$

where V is the volume bounded by the surface's'. Using equations (3.2) and (3.3) in equation (1)

$$\oint_S \vec{J}.ds = -\frac{d}{dt}\int_V q.dv \tag{3.4}$$

Applying the divergence theorem on the left hand side of the above equation,

$$\oint_S \vec{J}.ds = \int_V (\nabla.\vec{J})dv$$

Interchanging the differentiation and integration sequence on the left hand side of the equation

$$\int_V (\nabla.\vec{J})dv = -\int_V \left(\frac{\partial q}{\partial t}\right)dv$$

Or

$$\int_V \left(\nabla.\vec{J} + \frac{\partial q}{\partial t}\right)dv = 0 \tag{3.5}$$

Since equation (3.5) must be valid for any volume, it follows

$$\nabla.\vec{J} + \frac{\partial q}{\partial t} = 0 \tag{3.6}$$

Where this equation (3.6) is the law of continuity equation

$$\nabla.\, J = 0 \tag{3.7}$$

Since the stationary field is conservative, **E** (the electric field) may be related to the scalar vector function **V** as:

$$E = -\nabla V \tag{3.8}$$

The relation between the current density and the electric field intensity is given by Ohm's law as

$$J = -\sigma E = \frac{1}{\rho}E \tag{3.9}$$

$$J = -\frac{1}{\rho}(-\text{grad}\mathbf{V})$$

where ρ is a scalar function of the point of observation and *J* is in the same direction as *E* for isotropic medium.

$$\nabla\frac{1}{\rho}.\nabla v + \frac{1}{\rho}\nabla.\nabla V = 0 \tag{3.10}$$

This equation is called fundamental equation of electrical prospecting with direct current. For homogeneous medium, ρ is independent of the coordinate axis and equation above is simplified as

$$\nabla.\nabla V = 0 \; or \; \nabla^2 V = 0 \tag{3.11}$$

This equation is called the Laplace equation. Therefore the electrical potential distribution for direct current flow in homogeneous isotropic medium satisfies the Laplace equation. The above equation has different forms in different coordinate systems. For example using spherical coordinate system it can be expressed as

$$\frac{1}{r^2}\frac{\partial}{\partial r}\left(\frac{r^2\partial V}{\partial r}\right) + \frac{1}{r^2 sin\theta}\frac{\partial}{\partial\theta}\left(sin\theta\frac{\partial V}{\partial\theta}\right) + \frac{1}{r^2 sin^2\theta}\frac{\partial^2 V}{\partial\phi^2} = 0 \tag{3.12}$$

The DC resistivity survey is conducted with two current electrodes (AB) called source and sink in which the current I (A) is injected into the ground and two potential electrodes (MN) where the potential difference $\nabla V(V)$ is recorded.

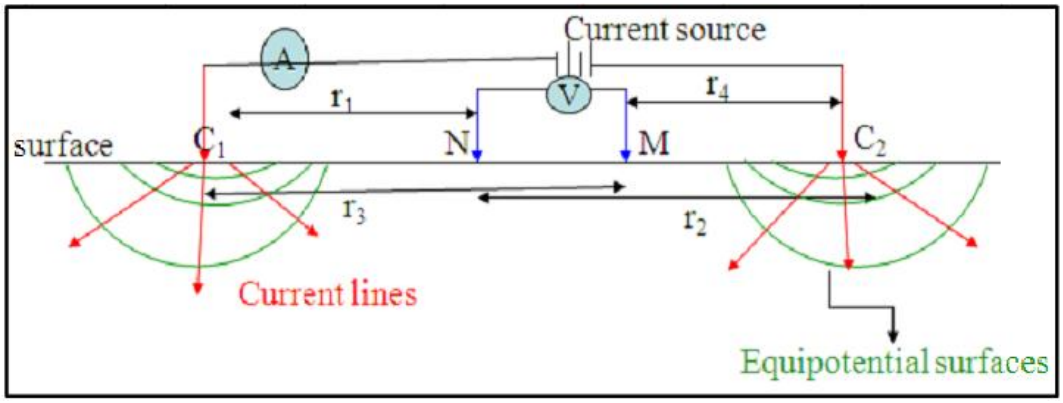

Figure 3-1: The arrangement of current and potential electrodes.

Assuming that the air above the ground has zero conductivity, the Laplace equation in spherical coordinate is used to find the relation between the potential at r, distance from the current electrodes and this equation is reduced to

$$\nabla^2 V=\frac{d^2V}{dr^2}+\frac{2dv}{rdr}=0 \quad (3.13)$$

Since the potential varies as the function of r,$\frac{\partial v}{\partial \theta}$ and $\frac{\partial v}{\partial \phi}$ will be zero.

By multiplying the above equations with r^2becomes

$$\frac{r^2d^2v}{dr^2}+2r\frac{dv}{dr}=0 \quad (3.14)$$

Integrating both sides of this equation becomes

$$V=\frac{-C_1}{r}+c_2 \quad (3.15)$$

where C_1 and c_2 are integration constants to be solved by using the following boundary conditions.

a. $v \to 0\ as\ r \to \infty\ then\ c_2=0$
b. $\frac{dv}{dz}=0\ at\ z=0$ and
c. the current flow through the hemispherical surface in the lower half ,so that I=$2\pi r^2 J$ but J=ɒE=-ɒ$\frac{dv}{dr}$ and $\frac{dv}{dr}=\frac{c_1}{r^2}$

J=- ɒ$\frac{c_1}{r^2}$ so that I=$-2\pi ɒ C_1$ or $C_1=\frac{-J\rho}{2\pi}$ where ρ and ɒ the resistivity of the ground and the conductivity of the homogeneous isotropic ground respectively. Therefore the above equation can be written as:

$$V = \frac{I\rho}{2\pi}\left(\frac{1}{r}\right) \; or \; \rho = 2\pi\left(\frac{V}{I}\right) \quad (3.16)$$

When the distance between the two current electrodes is finite, the potential at any nearby will be affected both by current electrodes. Therefore the potential at N due to c_1 is

$V_{1=}\frac{I\rho}{2\pi}(\frac{1}{r_1})$ and due to c_2 at N is $V_2 = -\frac{I\rho}{2\pi}(\frac{1}{r_2})$ (3.17)

The current between two electrodes are equal in magnitude but opposite in sign. The total potential at N is given by

$$V_N = \frac{I\rho}{2\pi}(\frac{1}{r_1} - \frac{1}{r_2}) \quad (3.18)$$

Similarly the potential at M due to $C_{1\ and} C_{2\ is}$

$$V_M = \frac{I\rho}{2\pi}(\frac{1}{r_3} - \frac{1}{r_4}) \quad (3.19)$$

The potential difference measured between the two potential electrodes (MN) is

$$\Delta V = V_N - V_M = \frac{I\rho}{2\pi}(\frac{1}{r_1} - \frac{1}{r_2} - \frac{1}{r_3} + \frac{1}{r_4}) \quad (3.20)$$

where $r_1, r_2, r_3 \; and \; r_4$ in meters. Therefore, after re-arranging the distances between the current and the potential electrodes according to the well knowing configurations, we can determine the resistivity of the homogeneous ground.

In resistivity sounding, which is also known as Vertical Electrical Sounding (VES), the positions of electrodes changed with respect to a fixed point (known as the sounding point) and the measured values reflect the vertical distribution of resistivity values on a geologic section.

Vertical electrical sounding (VES) consists of a symmetrical electrode array used to determine the resistivity of the subsurface which is assumed to be horizontally stratified layers. The procedure is used to determine the variations in resistivity in the vertical direction and called electrical drilling or commonly vertical electrical sounding (VES). By expanding symmetrically the distance between current electrodes the potential electrodes MN at the same position, provides a sounding curve corresponding to the apparent resistivity versus depth of the location. As the spacing between the current electrode increases, the investigated depth will also increase.

The two most commonly used arrays in electrical sounding survey are the Wenner and Schlumberger arrays. In this work, we have used the data which was collected by using the Schlumberger electrode array techniques.

The advantage of this array is that initially only the spacing between the current electrodes is increased. However, at large current electrode spacing, the measured potential becomes very low and the distance between the potential electrodes is increased. Increasing the potential electrode spacing produces a 'step' in the apparent resistivity curve and it is good practice to obtain an overlap between the curve segments by obtaining two readings at different potential electrode spacing for two adjacent current electrode spacing. Segments obtained at larger potential electrode spacing can be shifted in order to produce a smooth curve (Gibson and George, 2003).

In electrical prospecting to determine the depth and the electrical resistivity of a series of horizontal or nearly horizontal ground, In order to solve this problem, we should calculate the potential and the electric field, due to a point source of current, at any point on the surface of a stratified earth. This has advantages because of enables one to use axial symmetry of the potential filed about the vertical axis through the current source and the additive ness of the potential is also be used.

Let as choose a cylindrical system of coordinate with the origin at the point source a direct current located on the surface. The subsurface consists of infinite number of layers separated by horizontal boundary planes, the deepest layer existing to infinite depth and the other layers have finite thickness $h_i=h_1,h_2,h_3\ldots\ldots h_n$ and resistivity $\rho_{i=}\rho_1,\rho_2,\rho_{3\ldots..}\rho_n$

Each of the layers is electrically homogeneous and isotropic. The derivative of the potential based on the above conditions was first due to Stefanescu et al., (1930).

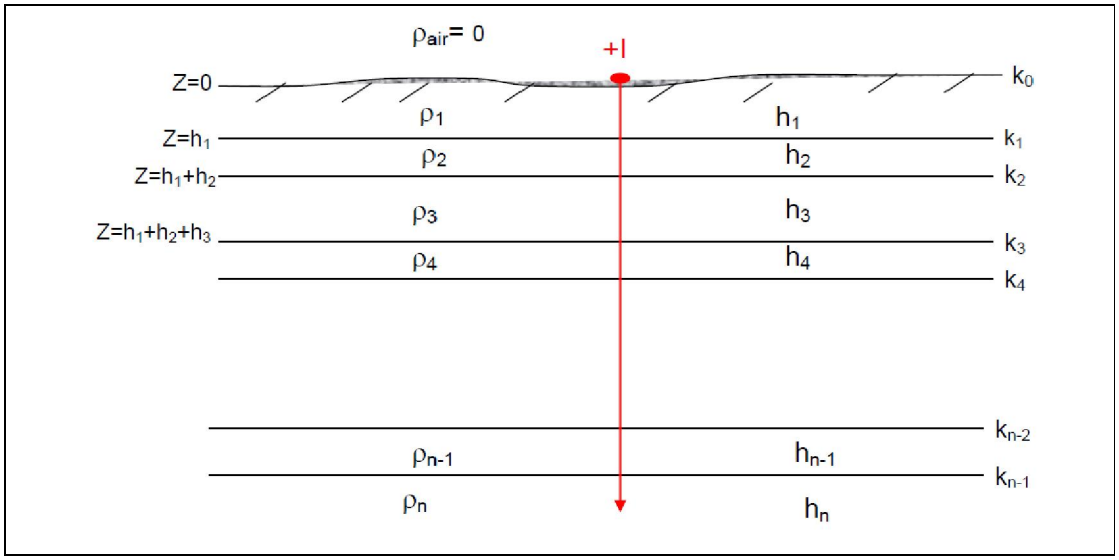

Figure 3-2: A multi-layer earth and problem presentation for solution of the potential.

The electrical potential V for direct current satisfies the Laplace equation, i.e

$$\frac{\partial^2 v}{\partial x^2}+\frac{\partial^2 v}{\partial y^2}+\frac{\partial^2 v}{\partial z^2}=0 \quad \textbf{(3.21)}$$

The potential field has a cylindrical symmetry with respect to the vertical axis line through the current source. Therefore, Laplace equation in cylindrical coordinate is most appropriate.

For a solution symmetrical with respect to the vertical axis

$$\frac{\partial v}{\partial \theta}=\frac{\partial^2 v}{\partial \theta^2}=0 \quad (3.22)$$

$$\frac{\partial^2 v}{\partial x^2}+\frac{1}{r}\frac{\partial v}{\partial r}+\frac{\partial^2}{\partial z^2}=0 \quad \textbf{(3.}23)$$

The particular solution of equations can be obtained using the method of separation of variables and can be assumed to be the form of

$$V(r,z)=U(r)W(z) \quad (3.24)$$

By substituting the above equations and dividing through by the product in to $U(r)W(z)$ gives

$$\frac{1}{U(r)}\frac{\partial^2}{\partial r^2}U(r)+\frac{1}{rU(r)}\frac{\partial U(r)}{\partial r}\frac{1}{w(z)}\frac{\partial^2 W(Z)}{\partial z^2}=0 \quad (3.25)$$

The equation satisfied if and only if

$$\frac{1}{U(r)}\frac{\partial^2}{\partial r^2}U(r)+\frac{1}{rU(r)}\frac{\partial U(r)}{\partial r}=\lambda^2 \quad (3.26)$$

$$\frac{w(z)d^2}{dz^2}\frac{1}{w(z)}=-\lambda^2 \quad (3.27)$$

Where λ is the arbitrary constant.

The solution of the above equation is given as follows

$$W(z)=C_{1e^{-\lambda z}} \ and \qquad W(z)=C_{1e^{\lambda z}} \quad (3.28)$$

$$U(r)=C_3 J_o(\lambda r) \quad (3.29)$$

Where $\boldsymbol{J_o}$ **is** the Bessel function of order zero.

The combination of the above equations is

$$V(r,z)=c_4 e^{+\lambda z}\boldsymbol{J_o}(\lambda r) \quad (3.30)$$

$$V(r,z)=c_4 e^{-\lambda z}\boldsymbol{J_o}(\lambda r) \quad (3.31)$$

where c and λ are both constant in the last of these equations.

Since, by theory of differential equation, every linear combination of the particular solution is also a solution, one can make λ to rough all possible values from zero to infinity and

allowing the constant "c" to very independence of λ the general solution of the above two equation can be obtained as

$$V(r,z) = \int_0^\infty [\Phi(\lambda)e^{+\lambda z} + \Psi(\lambda)e^{-\lambda z}]\, \boldsymbol{J_o}(\lambda r)\, \mathrm{d}\lambda \qquad (3.32)$$

From basic theory, the potential generated by a single point source of current intensity "I" located at the surface of an electrically homogeneous earth is given by:

$$V = \frac{I\rho}{2\pi}\frac{1}{\sqrt{r^2+z^2}} \qquad (3.33)$$

Where λ is the resistivity of homogeneous earth. These equations can be written as the integral form by using the so-called Lipchitz integral (also called the Weber integral Formula) in the theory of Bessel function as

$$\int_0^\infty \boldsymbol{e}^{\lambda z}\boldsymbol{J_o}(\lambda r)\mathrm{d}\lambda = \frac{1}{\sqrt{r^2+z^2}} \qquad (3.34)$$

So that the equations gives as

$$\boldsymbol{V} = \frac{\boldsymbol{I\rho}}{\boldsymbol{2\pi}}\int_0^\infty \boldsymbol{e}^{-\lambda z}\boldsymbol{J_o}\,(\lambda r)\mathrm{d}\lambda \qquad (3.35)$$

From the above equation the combined solution will be the solution of the equation, that is

$$V(r,z) = \frac{\boldsymbol{I\rho}}{\boldsymbol{2\pi}}\int_0^\infty [\boldsymbol{e}^{-\lambda z} + X(\lambda)\boldsymbol{e}^{+\lambda z} + \Theta(\lambda)\boldsymbol{e}^{+\lambda z}]\, \boldsymbol{J_o}\,(\lambda r)\mathrm{d}\lambda \qquad (3.36)$$

Where $\Theta(\lambda)\ and\ X(\lambda)$arbitrary function.Solution of equation is are valid in all layers of the surface. So the potential due to the point source of current at the surface of horizontally layered earth must in each layer satisfies.

$$Vi = \frac{\boldsymbol{I\rho}}{\boldsymbol{2\pi}}\int_0^\infty [e^{-\lambda z} + X_i(\lambda)e^{+\lambda z} + \Theta i(\lambda)e^{+\lambda z}]\, J_o\,(\lambda r)\mathrm{d}\lambda \qquad (3.37)$$

This equation is called the Stefanescu Integral, with "i" referring to the several layers of the subsurface.

3.2.2. The Apparent Resistivity

If the ground is homogenous, the potential difference measured is as a function of the true resistivity of the homogeneous earth and the geometric factor. But in reality the ground is locally in the homogeneous and the potential difference depends on the current applied, the resistivity of the subsurface medium and the geometrical factor (k) determined by electrode array or configurations types. The resistivity calculated from such non homogenous ground is not a true resistivity rather it is called apparent resistivity (ρa) which can be related to the parameter as

$$\rho a = k\frac{\Delta \mathrm{V}}{I} \qquad (3.38)$$

This apparent resistivity has to be interpreted using curve matching or inversion techniques to find estimated resistivity versus depth of the subsurface. This are many type of electrode configurations used in ground surveys of which the most commonly used array are Wenner, Schlumberger and the Dipole-Dipole. Since, the electrode separation relate to the investigation depth and lateral solution power required, one can choose the best electrode configuration for planed survey at the initial of the survey. The expression for apparent resistivity in each of the array types will be different due to the difference in the geometrical factor (K) of each any type.

Take the Schlumberger array in which the electrodes are symmetrically placed a point at the center of the array as shown in the figure 3.3 below.

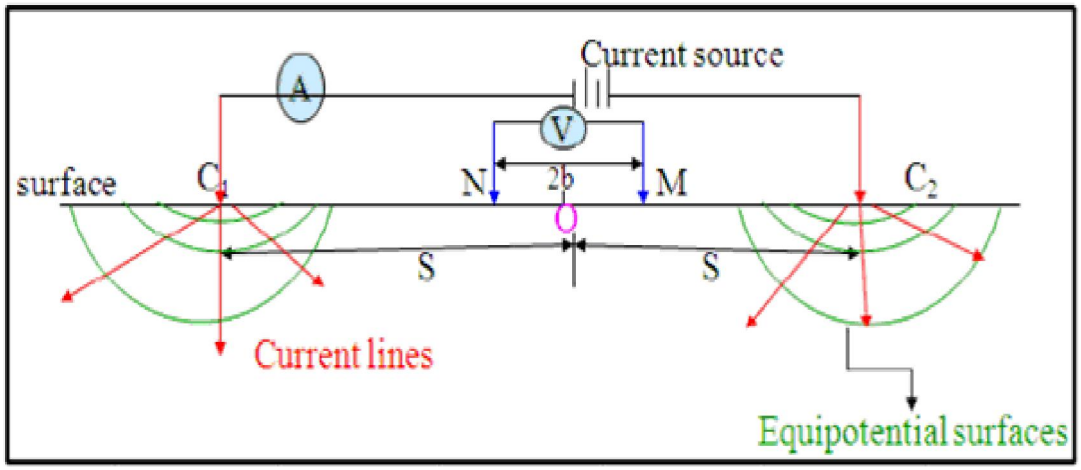

Figure 3-3: Electrode arrangement for the schlumberger array

Where r_1=s-b_1,r_2=s+b,r_3=s+b and r_4=s-b,'O' is the center of array

The potential difference using the above equations is

$$\Delta V = \frac{I\rho}{2\pi}\left[\left(\frac{1}{S-b}-\frac{1}{s+b}\right)-\left(\frac{1}{s+b}-\frac{1}{s-b}\right)\right] \quad (3.\ 39)$$

$$\Delta V = \frac{I\rho}{2\pi}\left[\left(\frac{1}{s^2-b^2}\right)\right] \quad (3.40)$$

$$\rho a = \pi\left(\frac{s^2-b^2}{2b}\right)\left(\frac{\Delta V}{I}\right) \quad (3.\ 41)$$

Where the geometric factor is

$$K = \pi\left(\frac{S^2-s^2}{2b}\right)\left(\frac{\Delta V}{I}\right) \quad (3.\ 42)$$

3.2.3. Interpretation of VES data

The interpretation problem for Vertical Electrical sounding data is to use the curve of apparent resistivity versus electrode spacing, plotted from field measurements on bi-log scale graph paper, to obtain the parameters of the geo-electrical section: the layers

resistivity and thicknesses. From a given set of layer parameters, it is always possible to compute the apparent resistivity as a function of electrode spacing (the VES curve). Unfortunately, for the converse of that problem, it is not generally possible to obtain a unique solution. There is interplay between thickness and resistivity; there may be anisotropy of resistivity in some strata; large differences in geoelectric section, particularly at depth, produce small differences in apparent resistivity; and accuracy of field measurements is limited by the natural variability of surface soil, rock and by instrument capabilities. As a result, different sections may be electrically equivalent within the practical accuracy limits of the field measurements.

To deal with the problem of ambiguity, Vertical electrical sounding (VES) field curves can be interpreted qualitatively using simple curve shapes, semi-quantitatively with graphical model curves, or quantitatively with computer modeling.

3.2.4. Master Curves

Layer resistivity values can be estimated by matching to a set of master curves calculated assuming a layered Earth, in which layer thickness increases with depth.

3.2.5. Master curves of two layer earth model

Any two- layer curve for particular value of k, or for a particular ratio of layer resistivity must have the same shape on the logarithmic plot as the corresponding standard curve. It differs only by horizontal and vertical shifts, which are equal to the logarithms of the thickness and resistivity of the first layer. For two layers, master curves can be represented on a single plot.

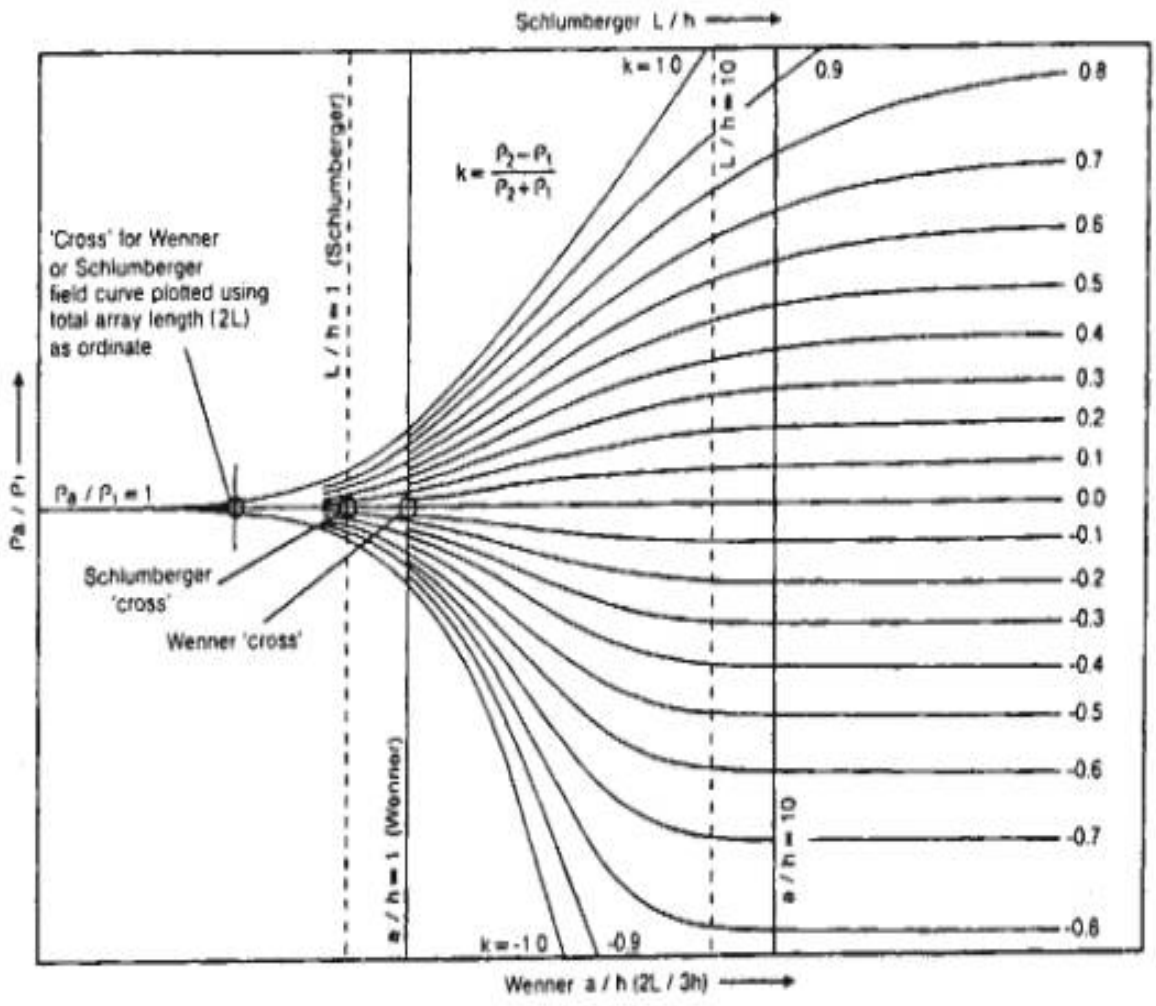

Figure 3-4: Two-layer master set of sounding curves for the Schlumberger array (Zohdy 1974a, 1974b)

Master curves: log-log plot with ρ_a / ρ_1 on vertical axis and a / h on horizontal (h is depth to interface)

- Plot smoothed field data on log-log graph transparency.
- Overlay transparency on master curves keeping axes parallel.
- Note electrode spacing on transparency at which (a / h=1) to get interface depth.
- Note electrode spacing on transparency at which (ρ_a / ρ_1 =1) to get resistivity of layer 1.

- Read off value of k to calculate resistivity of layer 2 from:

$$K=\frac{\rho_2-\rho_1}{\rho_2+\rho_1} \qquad (3.\ 43)$$

Inversion

Curve matching is also used for three layer models, but book of many more curves. Recently, computer-based methods have become common:

- Forward modeling with layer thicknesses and resistivities provided by user
- Inversion methods where model parameters iteratively estimated from data subject to user supplied constraints.

3.2.6. Magnetic Profiling

The magnetic method is a versatile, easy-to-operate geophysical tool, applicable to many different subsurface exploration problems. It has a lot in common with the gravity method both theoretically and with regard to field work.

Magnetism of rocks is related with the magnetism of the rock-forming minerals. Diamagnetic minerals like quartz and calcite have negative susceptibilities in the order of 10^{-5}. Minerals like feldspars and micas are paramagnetic and have higher (positive) susceptibilities (10^{-4} - 10^{-2}).The positive susceptibility of ferromagnetic minerals like magnetite (k ~ 1 - 10) and titanomagnetites is even larger by some orders of magnitude and, in general, most important for the magnetization of rocks. Very roughly, the susceptibility of rocks in an ascending order may be addressed as follows: (k ~ 0.0001) sedimentary rocks - metamorphic rocks (0.001) acid volcanic and plutonic rocks - basic plutonic rocks (0.01) basic volcanic rocks (0.1). Strong remnant magnetization is abundantly observed with young volcanic rocks, while in sedimentary and metamorphic rocks the remnant magnetization is in general much lower than the induced magnetization.

Water is diamagnetic ($k = -9.05 \times 10^{-6}$) and has no importance for the actual magnetization of a rock. However, playing an important role in the alteration of rocks and being a carrier of iron-bearing and generally chemically active solutions, water can change the magnetization of rocks during geological times. Both an intensity increase and an intensity decrease are possible. Magnetization changes of rocks by contaminated groundwater may be addressed in environmental geophysical surveys.

Magnetometer is a sensitive instrument which is used to map spatial variations in the earth's magnetic field. In the proton magnetometer, a magnetic field which is not parallel to the earth's field is applied to a fluid rich in protons causing them to partly align with this artificial field. When the controlled field is removed, the protons precess toward realignment with the earth's field at a frequency which depends on the intensity of the earth's field. By measuring this precession frequency, the total intensity of the field can be

determined. The physical basis for several other magnetometers, such as the cesium or rubidium-vapor magnetometers, is similarly founded in a fundamental physical constant. The optically pumped magnetometers have increased sensitivity and shorter cycle times (as small as 0.04 s).

Magnetic surveys are used to locate and delineate:

- Magnetic iron ore deposits,
- Metallic ore deposits which may have either magnetite or pyrrhotite associated with them, and
- Geological structures like contacts, faults, dykes.

Magnetic surveys are used in groundwater studies to map the depth to the magnetic basement rock and also it provide a valuable aid to lithological mapping, as the character of a magnetic anomaly is indicative of the rock. Moreover, it can also be applied in mapping structural features, which often provide a conduit for the accumulation of groundwater and, at times, act as barriers.

Table 3-1: Typical Magnetic Susceptibilities some common rocks and minerals in rationalized SI units (Milsom, 2003)

Common rocks		Ores	
Slate	0-0.002	Hematite	0.001-0.0001
Dolerite	0.01-0.15	Magnetite	0.1-20.0
Greenstone	0.0005-0.001	Chromite	0.0075-1.5
Basalt	0.001-0.05	Pyrrhotite	0.001-1.0
Granulite	0.0001-0.05	Pyrite	0.0001-0.005
Rhyolite	0.00025-0.01		
Salt	0.0-0.001		
Gabbro	0.001-0.1		
Limestone	0.00001-0.0001		

3.2.7. Principles of magnetic method

The force between two poles of strength m_1 and m_2, situated a distance 'r' apart is given by:

$$F = \frac{m_1 m_2}{\mu r^2} \bar{r} \qquad (3.44)$$

where,

$\bar{r}$= unit vector from m_1 *to* m_2

μ = permiability = $\mu_r \mu_o$

μ_r= relative permeability

μ_o=permeability of free space=$4\pi x 10^{-7} henry/m$

r=separation between m_1 *and* m_2

3.2.8. Magnetic induction/ Flux density

A magnetic field strength gives rise to a magnetic flux, just as electric field strength can give rise to an electric charge flux (current). The magnetic flux density that is the flux per unit area, also called magnetic induction, is denoted by B, and the field strength by H. The magnetizing force (field strength) gives rise to the flux density that is the cause of the magnetic field is the magnetizing force, thus

$$B = \mu H \qquad (3.45)$$

Where, μ is the absolute permeability of the medium on which H is acting. In SI units, the magnetizing force or field strength (H) is measured in ampere per meter [Am-1]. The unit of magnetic flux is volt-second (V-s), also named Weber [Wb].Hence, the unit of flux density B is [Vsm-2] or [Wbm-2] which is also called tesla[T]. The magnetic fields that we measure in practice are flux densities. For most geophysical purposes, the tesla is too large as a unit and flux densities are more conveniently expressed in nanotesla [nT =$10^{-9}T$]. One nT is equals the basic unit of B, namely gamma [The absolute permeability (μ), being equal to B/H has its dimensions from

$$\mu = \frac{B}{H} = \frac{V.sec\,m}{m^2 A} = 0hm\,\frac{sec}{m} = Ω.\,Sec.\,m^{-1} \qquad (3.46)$$

The absolute permeability of vacuum is denoted by μ_o, its value in SI unit is: $4\pi x 10^{-7} \Omega.sec.m^{-1}$ .Thus in vacuum the flux density due to a magnetizing force H will be

B=μ_oH

For most practical purpose, the absolute permeability of air, and even most rocks, may be taken to be μ_o.

3.2.9. Nature of the Geomagnetic Field

The geomagnetic field of the Earth is composed of three parts:

1. The main field or Diploe field B_D , which is produced in the fluid outer core of the earth and accounts for the very large regional variations in the total field intensity and direction.
2. The external magnetic field B_{ext} , which is produced by electric currents in the earth's ionosphere consisting of particles ionized by solar radiation and put into motion by the solar tidal force.
3. The anomalous magnetic field or rock magnetism B_{rm} , which is produced by ferromagnetic minerals and rocks in the earth's crust (Telford et al.). The earth's total magnetic field B_T is given by

$$B_T = B_{ext} + B_D + B_{rm} \quad (3.47)$$

3.2.10. The Earth's Magnetic Field

The Earth's magnetic field is akin to that of a dipole situated at the center of the earth with its magnetic moment pointing towards the Earth's geographical south. The Earth's magnetic field vector **F** is completely specified at any point by its elements. Shows the elements of the Earth's magnetic field.

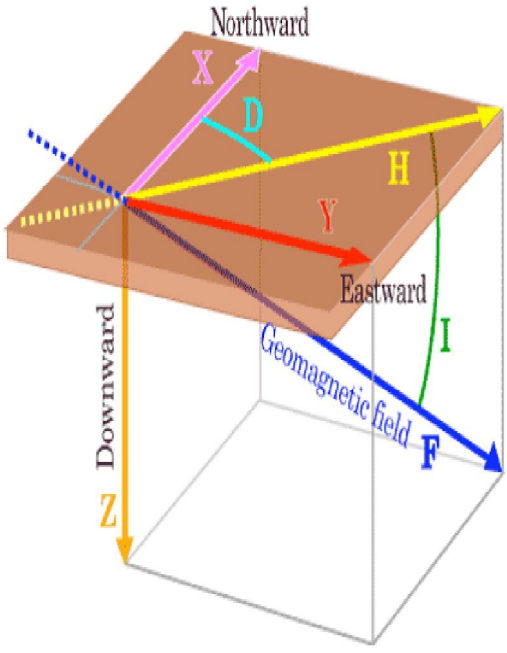

Figure 3-5: Elements of earth's magnetic field (Reynolds, 1997)

According to figure 3.5 the earths total field is F takes an angle I (the inclination) with the horizontal plane. It can be measured by a dip needle and is also called magnetic dip.

The angle D is the angle between geographic north and magnetic north,or the declination of H (here,H is the horizontal component of the total field vector,F) east or west of true north. In the northen hemisphere the magnetic field is directed downwards towards the north magnetic pole and in the southern hemisphere it is directed up wards and away from the south magnetic pole. At the magnetic equator the magnetic field is horizontal and at the magnetic poles the field is vertical i.e, the strength of the earth's field varies from 25,000-30000nT in the equatorial regions while 60,000-70,000nT in the polar regions.

The amplitude of the total field varies more rapidly along the N-S direction as compared to the east–west. On the above figure, Z is the vertical component of the total field (F). It is directed downwards in the northern hemisphere (positive) and up wards (negative) in the southern hemisphere. H, which is the horizontal component of F, is directed towards magnetic north for both the southern and northern hemispheres.

3.2.11. Relative permeability of susceptibility and magnetization

In a medium other than vacuum we write $\mu = \mu r \mu 0$

$$B = \mu H \quad (3.48)$$

$$B = \mu r \mu 0 \, H \quad (3.49)$$

$$B = \mu 0 H + \mu 0 (\mu r - 1) H \quad (3.50)$$

$$B = \mu 0 H + \mu 0 \kappa H \mu r \quad (3.51)$$

$H\mu r$ = relative permeability of the medium

The ratio of two permeability: ($\mu r = \frac{\mu}{\mu_o}$) and therefore it is a pure number. It is called the relative permeability of the medium, and κ is called susceptibility which is a dimensionless quantity. For a vacuum, $\mu = 1$ and $k = 0$.

This additional field strength that may be said to be present at points of space occupied by a medium subject to a field strength H is known as intensity of magnetization M induced by H. The direct relation is given by:

$$M = KH \quad (3.52)$$

The total field within a body written as

$$B = \mu o \, (H + M) \quad (3.53)$$

Therefore the x, y and z components of B, in a orthogonal coordinate system, we have that.

$$Bx = \mu o\,(Hx+Mx)$$
$$By = \mu o\,(Hy+My) \qquad (3.54)$$
$$Bz = \mu o\,(Hz+Mz)$$

Equation (3.53) implies that, a magnetic body placed in a magnetic field becomes magnetized by induction. The magnetization (M) is proportional to the inducing external magnetizing force. The constant proportionality K is the magnetic susceptibility. It is a dimensionless quantity.

3.2.12. Noise and correction for magnetic variations

All magnetic data sets contain elements of noise and will require some form of correction to the raw data to remove all contributions to the observed magnetic field other than those caused by sub-surface magnetic sources. In ground magnetometer surveys, it is always advisable to keep any magnetic objects (keys, penknives, some wristwatches, etc), which may cause magnetic noise, away from the sensor. It is also essential to keep the sensor away from obviously magnetic objects such as cars, metal sheds, power lines, metal pipes, electrified railway lines, walls made of maffic rocks, etc.

There are several ways of correcting magnetic data according to the various magnetic variations. For the secular variation of magnetic data a model is known as International Geomagnetic Reference Field (IGRF) has been prepared from comparison of individual magnetic responses in different areas of magnetic observatories. So, it has become standard processing practice for magnetic survey that the applicable IGRF (updated to the time of the survey) is subtracted from the observed values of the total magnetic intensity. The most significant correction is for the diurnal variation in the Earth's magnetic field.

The necessary corrections are mostly attempted by the reoccupation of the base station which is located in or near the survey area. Variations in magnetic field due to magnetic storms can be so rapid, unpredictable, and of such large amplitude, that normally no corrections can be made. Magnetic surveying is therefore generally discontinued under these conditions.

In all magnetic data, diurnal and IGRF correction can be applied. The most significant correction is for the diurnal correction in the Earth's magnetic field. Base station readings taken over a survey period of facilitate the compilation of diurnal correction.

$$DC = Y \pm \left(\frac{BS_{2-BS_1}}{T_{2-T_1}}\right)(T_{r-}T_1)$$

Where, DC= Diurnal correction

Y= Total magnetic field

BS_2 =Reading at base station 2

BS_1 = Reading at base station 1

T_1=observation point at station 1

T_2=observation point at station 2

$T_{r=}$Observation time of each measuring point

In order to produce the magnetic anomaly, the data have to be corrected to take into account the effect of latitude and, to a lesser extent, longitude. As the Earth's magnetic field strength varies from 25000nT at the magnetic equator to 69000nT at the poles, the increase in magnitude with latitude needs to be taken into account (Reynold, 1997).Survey data at any given point can be corrected by subtracting the theoretical filed value obtained from IGRF, from the measured value.

4. DATA ACQUISTION AND PROCESSING

4.1.Survey Traverse line

The area was planned to be studied for detailed investigation to understand the lithologic units, groundwater potential zones, geological structures and the physical properties of surface rocks. The methods chosen for the survey consist of vertical electrical sounding(VES) and magnetic method of prospecting technique.

The total volume of work in Mermero area are twenty Eight (28) Vertical Electrical Soundings and 663 magnetic data points and is given in Table 4.1. Figure 4.1 shows the location and orientation of the survey lines and the positions of Vertical Electrical Sounding (VES) points. All the traverse lines are cross each other as shown in figure 4.1.

Table 4-1: Volume of work in Mermero area (VES & Mag)

Survey Line	VES	MAG (data pts)
TRV1	4	91
TRV2	4	72
TRV3	9	265
TRV10	11	235
Total	**28**	**663**

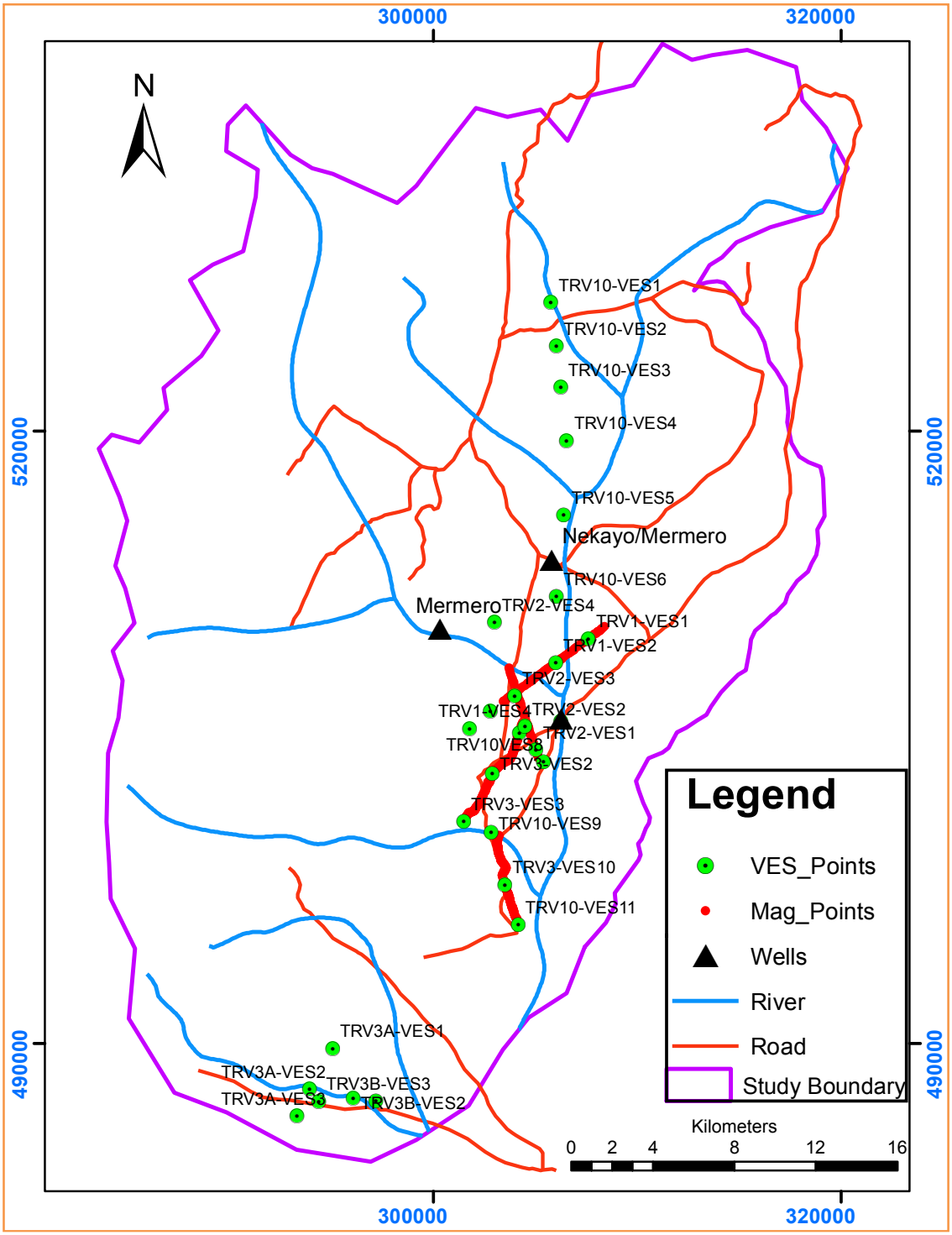

Figure 4-1: location map of geophysical traverse lines (VES and Magnetic).

4.2. Data acquisition and Instrumentation

4.2.1. Vertical electrical sounding

Vertical electrical sounding was carried out along four tranverse lines oriented approximately south west and East west within the area and the observations were made around 2km sounding station spacing. The choice of a spot to place a sounding was mainly dictated by the suitability of the point for the survey logistics, the condition of the surrounding ground and accessibility, and also the fitting of its position along the particular traverse.

As the result, the separation distance between the points may vary from one traverse to the other and sometimes within the same traverse line. Regarding the outer electrode separation, maximum effort has been made to reach end –to-end distance of 2000m (AB/2=1000m) in order to attain the larger depth of penetration and as such succeeded for most of the stations

4.2.2. Instrumentation

The geoelectric data were acquired using IRIS Instrument SYSCAL R1 PLUS switch-72 which is new all-in one multiple resistivity imaging system. If features an internal switching board for 72 electrodes and an internal 200W power source. It is compact, easy to use and field proof.

The SYSCAL R1 PLUS Switch-72 (Resistivity/IP measurement and Imaging unit) of the IRIS Instrument. A latest earth resistivity measuring unit with seventy two electrode console for 2D resistivity imaging and also incorporating consoles for current out puts and measuring sections for convectional resistivity sounding and profiling surveys. Handheld GPS was used to record the sounding point locations.

The apparent resistivity for different electrode spacing and the location of the VES points are recorded. Data quality was controlled concurrently plotting and examining the VES data in the field. The spread directions were dully recorded and were used during data processing session for anisotropic correction purposes.

4.2.3. Magnetic survey

The total field magnetic survey was carried out along VES lines and observations were made every 20m along all traverse lines of the VES.A total of six hundred sixty three data point were acquired, with the traverse separation similar to that of the VES.

4.2.4. Instrumentation

The instrument used was the Scintrex IGS-2: Integrated Geophysical System with proton precision sensor. As aforementioned, Proton precession magnetometers (proton magnetometers or PPM) are composed of a portable sensor and an electronic unit for display and storage of the data. Proton magnetometers measure the total intensity of the earth magnetic field vector at a resolution of 0.1 - 1 nT. The IGS-2 is operable in cycling (base station), total field or gradient survey modes and for this survey the instrument was used in total filed measurement mode. Magnetometer, which is versatile and rugged tool for such a survey and, handled GPS was used for recording the time and position of the measured point.

The total magnetic intensity, the time, date and the location of the data points were recorded. Data quality was controlled by measuring the data three times to take the average and taking the base station readings at the beginning to overcome the diurnal variation.

4.3. Data Reduction and Processing

4.3.1. VES Data Reduction

The apparent resistivity values are plotted on logarithmic transparent paper. In processing the collected data, the apparent resistivity value on the ordinates and the electrode separation (AB/2) on the abscissa. The resistivity measurement was made by progressively increasing the potential electrode distance (MN) for relatively large increment of the current electrode distance (AB/2). In most cases the sounding curve is segmented due to overlap measurement and cannot be interpreted as it is.

To have precise interpretations the segmented curves were shifted to the small MN curve points, so that the effect could be quantified and corrections could be made in order to obtain a single smooth curve that could be processed with the computer using IP2WIN and then Win Resist software (Velpen, 1995).

4.3.2. Vertical Electrical Sounding (VES) data processing

The field results of the study area presented in both qualitative and quantitative interpretations. In qualitative interpretation the shape of the field curve is observed to get the idea of qualitatively about the number of layers and resistivity of layers.

The segmented curves were shifted to the small MN curve points to have precise interpretation. This interpretation involves the Geo-electrical pseudo section and the slice stacked of electrical resistivity maps depth. The VES data was collected in the field by using the bi-log paper curve method and interpreted using the software's like Win Resist, Resist and Ip2win software's to find out the initial model parameters of the possible layers. The Electrical resistivity method is used to study the resistivity of the subsurface rocks. The vertical (1D) electrical sounding survey was used in this study to identify the water-bearing horizons, the number of layers, their thickness and resistivities.

In the quantitative method of geo-electrical parameter, i.e. true resistivity and layer thickness were obtained to make geo-electrical section using the software AutoCAD 2007. The pseudo section and slice depth was presented using the software's Surfer10.

A slice stacked map for different value of AB/2 reflects the lateral variation of apparent resistivity over a horizontal plane at a certain depth. In other words, these maps indicate distribution of apparent resistivity in the area against distance of current electrodes. The maximum depth penetration of the AMNB method is 1/3to 1/4 of the maximum distance of current electrodes (Frohlich et al., 1996).

In general, Geo-electric sections show the distribution of layer resistivities and thicknesses and are believed to give a closer approximation to the actual geo-electrical setting in the subsurface. In practice, most of the quantitative interpretation would be based on geo-electric sections. In order to prepare the geo-electric sections the final model parameters (resistivity and thickness) are determined by inversion software, IP2WIN.

4.4.Magnetic Data Reduction and processing

4.4.1. Magnetic Data Reduction

Data reduction and processing is the series steps taken to remove both signal and spurious noise from the data that are not related to the geology the area. This process there by prepares the data set for interpretation by reducing the data to only contain signal relevant to the task. These are:

- **Data checking and editing**: involves the removal of spurious noise and spikes from the data that was caused by high tension power cable.
- **Diurnal removal**: corrects for the temporal variation of the Earth's main field which was achieved by subtracting the time synchronized signal, recorded at a stationary base magnetometer from the survey data.
- **IGRF removal**: removes the strong influence of the Earth's main field. This was achieved by subtracting a calculated of main field using Oasis Montaj from the diurnal corrected survey data.

4.4.2. Magnetic Data processing

To make accurate magnetic anomaly maps, temporal changes in the earth's field during the period of the survey must be considered. Normal changes during a day, sometimes called diurnal drift, are a few tense of nT but changes of hundreds or thousands of nT may occur infrequently, magnetic surveys should not be made. The correction for diurnal drift can be made by repeat measurements of a base station at frequent intervals. The measurements at field stations are then corrected for diunar variations by assuming a linear change of the field between repeat base station readings. Continuously recording magnetometers can also be used at fixed base sites to monitor the temporal changes. If time is accurately recorded at both base site and field location, the field data can be corrected by subtraction of the variations at the base site.

5. RESULTS, DISCUSSION AND INTERPRETATIONS

5.1.General

The resistivity sounding surveys are presented in the form of VES curve, apparent resistivity pseudo-sections for the purpose of qualitative assessments and vertical geoelectric section, permitting quantitative interpretations. Again the results of the magnetic survey presented as the total magnetic field anomaly map, residual map, analytic signal map and reduced to pole maps.

5.2.Discussion and interpretation of VES curve

5.2.1. Interpretation of VES curve

The Vertical electrical sounding curve modeling and interpretation is inextricably linked with the principle of equivalence. The principle expresses that the measurement sounding curve is basically related with many physically equivalent models that may differ considerably. The VES data can be interpreted with different number of layers without any preference. Another important property of vertical electrical sounding curves is evident by all appearances; only the minimum number of layers can be deduced implying that thin layers are preferentially suppressed. A rule of thumb indicates that a layer becomes clearly visible in a sounding curve if its thickness is comparable to its depth of deposition (Kirsch, R., 2006).

Once the resistivity and depth for the above mentioned VES were determined by fixing their depth from the boreholes (lithology data) using IP2WIN software, the depth and resistivity of the other VES along these survey lines were estimated by using the principle of parameterization. The resistivity parameters which were estimated form constrained and parameterized 1D inversion of VES data using IP2WIN software, were used as initial model for Win Resist software to find the final resistivity layer parameters. The software Win Resist uses iterations techniques to adjust the fitting between the observed data curve and the initial model parameters. Several reinterpretations for modeled soundings curves were performed to get better model parameters and the iteration process was finalized when the root mean square (RMS) errors was less than 5%.

The illustration is taken from the interpreted VES curves, one each from the survey traverses and these are given in figure 5.1,the rest are annexed.

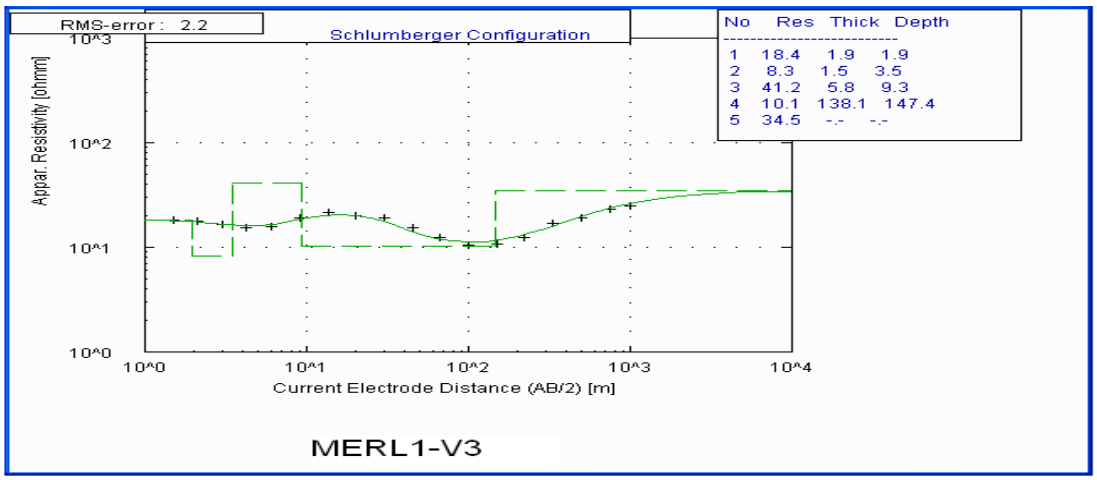
RMS-error : 2.2
Schlumberger Configuration
No Res Thick Depth
1 18.4 1.9 1.9
2 8.3 1.5 3.5
3 41.2 5.8 9.3
4 10.1 138.1 147.4
5 34.5 -.- -.-
Appar. Resistivity [ohmm]
10^3
10^2
10^1
10^0
10^0 10^1 10^2 10^3 10^4
Current Electrode Distance (AB/2) [m]
MERL1-V3

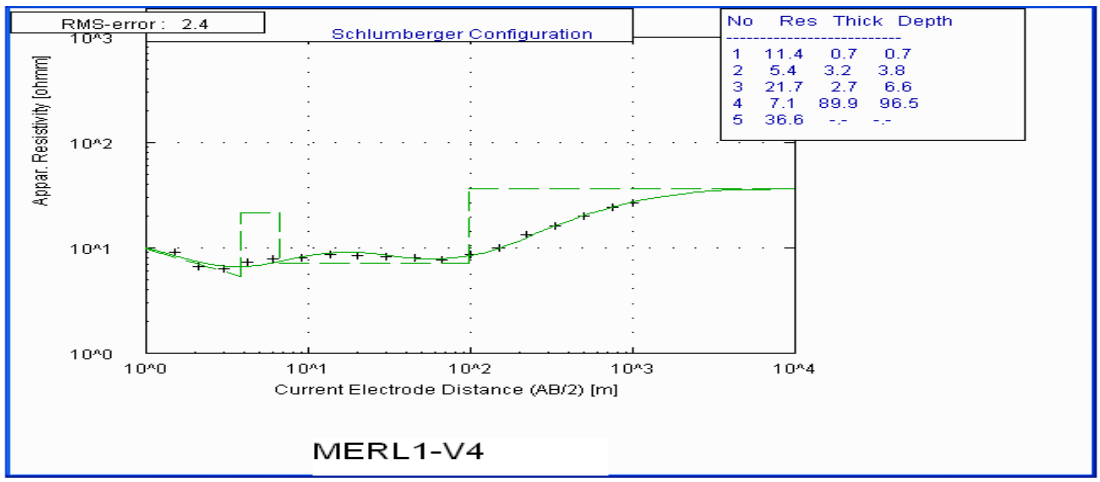
RMS-error : 2.4
Schlumberger Configuration
No Res Thick Depth
1 11.4 0.7 0.7
2 5.4 3.2 3.8
3 21.7 2.7 6.6
4 7.1 89.9 96.5
5 36.6 -.- -.-
Appar. Resistivity [ohmm]
10^3
10^2
10^1
10^0
10^0 10^1 10^2 10^3 10^4
Current Electrode Distance (AB/2) [m]
MERL1-V4

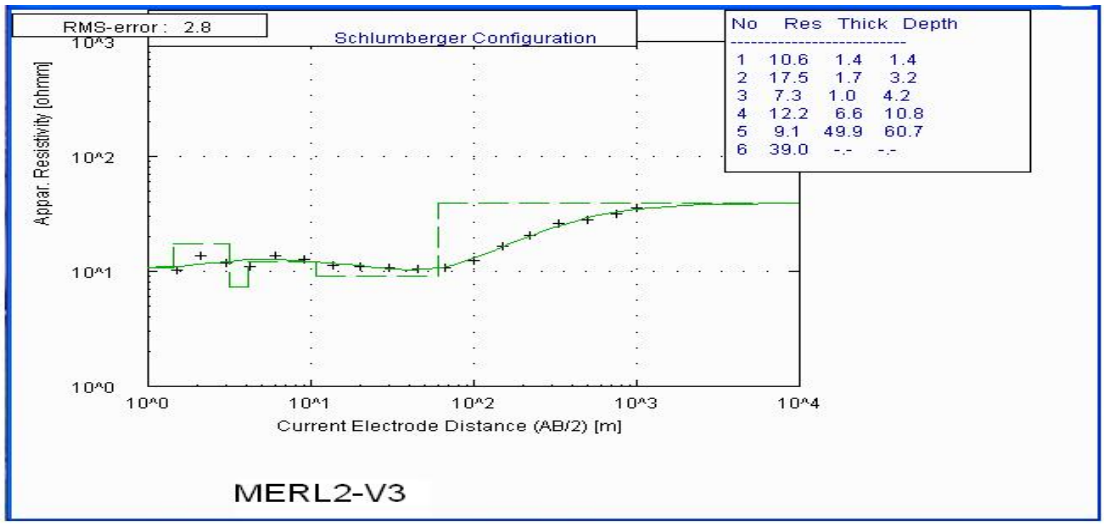
RMS-error : 2.8
Schlumberger Configuration
No Res Thick Depth
1 10.6 1.4 1.4
2 17.5 1.7 3.2
3 7.3 1.0 4.2
4 12.2 6.6 10.8
5 9.1 49.9 60.7
6 39.0 -.- -.-
Appar. Resistivity [ohmm]
10^3
10^2
10^1
10^0
10^0 10^1 10^2 10^3 10^4
Current Electrode Distance (AB/2) [m]
MERL2-V3

TRV3-V2

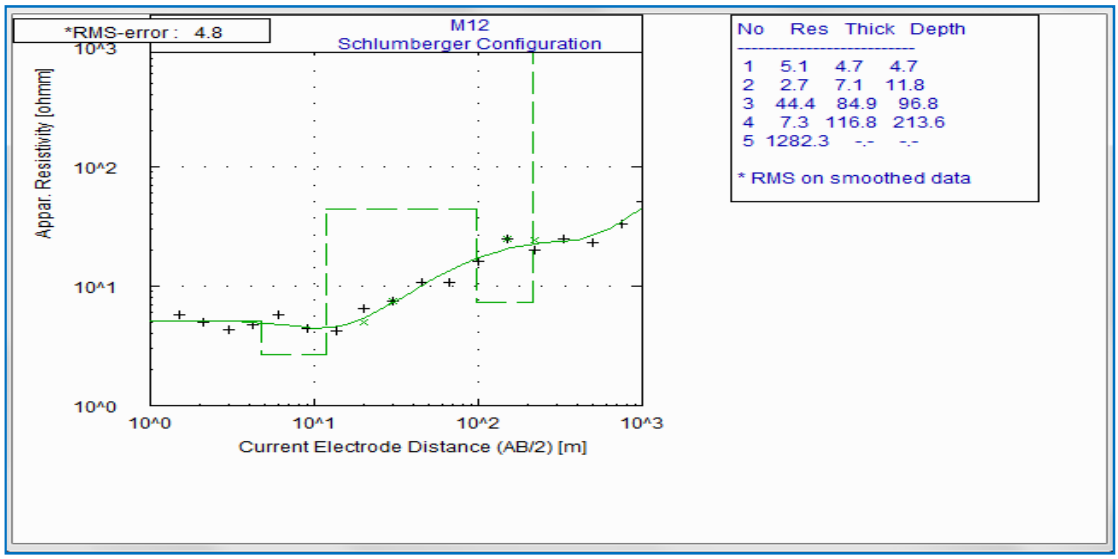

TRV10-V4

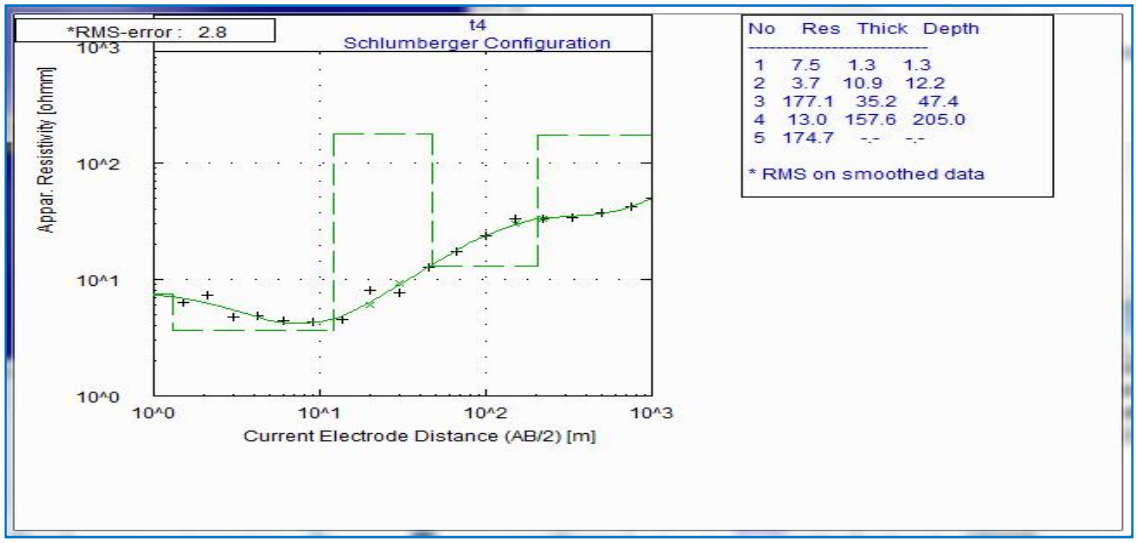

Figure 5-1: Interoperated VES curves for five sounding points.

5.2.2. Stacked plan maps of sliced depth sections

The geo-electrical survey comprises of twenty eight Vertical Electrical Sounding points with a maximum current electrode separation 1000m. The general variation in electrical resistivity of the subsurface is presented in the form of sliced pseudo-depth section is presented in figure 5.2 below. The sounding points are almost evenly distributed so it is believed to give a good representation of the ground overall.

The measured field data have been plotted along each profile line to get pseudo sections using the apparent resistivity (ρ_a) and pseudo depth (AB/2) values and depict the overall resistivity picture on a vertical section. Moreover the plan view of resistivity variations across the area, pseudo-depth slices, for instance, AB/2= (1.5, 9, 45, 100, 220, 500, 750 and 1000 m), are presented. The choice of such spacing depends on the variability between them and to show the lateral variations of resistivity at different pseudo depth.

The knowledge on the lateral distribution of the electrical resistivity at the subsurface shades additional light towards a complete understanding of the geological framework of the area under investigation. Sliced depth sections, when presented in the form of stacked plots, provide sufficient visualization of the overall picture of subsurface electrical parameters and their variation in both lateral and vertical directions. Moreover, it greatly facilitates ones interpretations of discontinuities in terms of geological structure which are of great interest for hydro-geophysical analysis. From the geological map there is also a variation horizontally as well as vertically. This stacked depth supports the vertical and horizontal variations.

The map shows the relative variation of the apparent resistivity value of the whole area laterally as well as vertically at different depth of the spacing of current electrodes. It is seen that the apparent resistivity value varies considerably from 0-260 Ω.m. According to Figure 5.2 the most interesting feature of this sliced plot is the low resistivity zone, (<100Ω-m) that occupies the vast portion of the survey area. Depth wise the low resistivity zone dominates the high resistivity zone except at the spacing at AB/2=220m.

All Vertical Electrical Sounding (VES) points are used for qualitative assessments of the electrical nature of the geologic medium.

The western, northwestern and SSW margins of the target area appear to be conductive approximately (<100Ωm) at the surface and tend to be moderately resistive (<200Ωm) with depth, i.e. at larger current electrode separations.

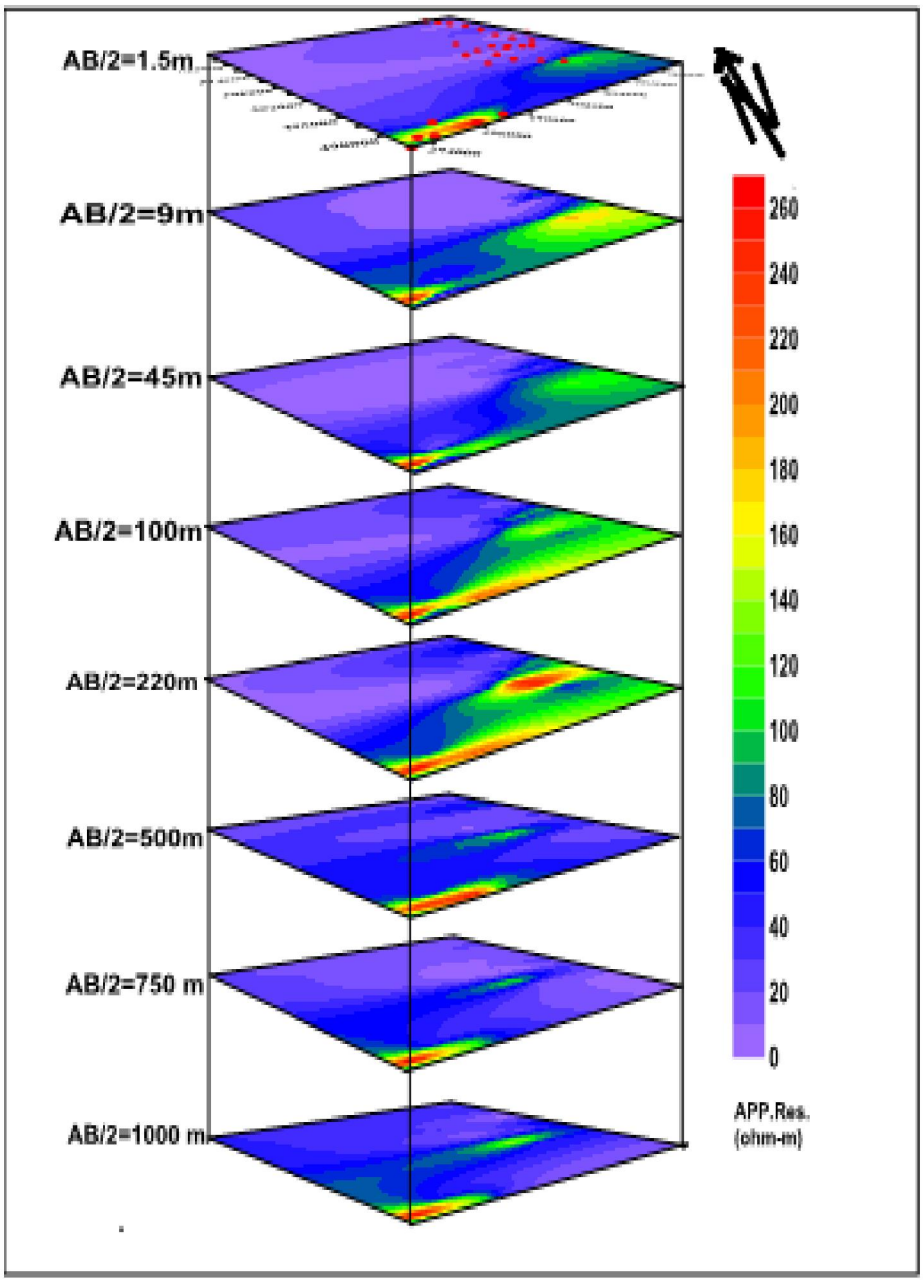

Figure 5-2: Sliced map of stacked section

5.2.3. Pseudo depth section and Geo-electric section along the profiles

The VES data collected from the field, after that reduction and filtering of all the survey are processed. The filtered and reduced VES data along all the survey lines were used to construct the pseudo section in order to identify the distribution of different resistivity values in vertical and lateral direction. That means the apparent resistivity data which is collected from the field, by arranging with the spacing between each VES points along the profile lines. The software used to construct the pseudo- section from the VES data were SURFER10 software. The qualitative interpretation of pseudo-section gives the preliminary idea for identification of high potential groundwater and examination to see relative resistivity variation for preparing geo-electric sections.

In order to identify the distribution of different lithologic units in vertical direction from one dimensional inversion of vertical electrical sounding (VES) data along the survey line the Geo-electric section is constructed. To construct the geo-electric section, firstly the VES data was processed with the software's IP2WIN and WINRESIST where as the plotting was carried out by using AutoCAD2007.The lithologic logs from boreholes that are lying on this profiles were used to fix the thickness of each layer by grouping with the rock samples on their type and the degree fracturing and weathering. The pseudo-depth sections along the survey line were examined to see the relative resistivity variations when preparing the Geo-electric sections.

5.2.3.1. Mermero TRV1 (Profile Line1)

Referring to the site location map figure 4.1, this line one runs in NE- SW direction. The total length of line-1 is 7.5 km. The data are compromised from four (4) VES points. The apparent resistivity pseudo-depth section of line-1, figure 5.3, displays a relatively homogeneous geo-electric image of the subsurface beneath the line. This pseudo-depth section shows an extensively low resistivity ranging (6-16 Ω.m) except the deepest region beneath TRV1-V1 and TRV1-V2 where high resistivity responses were recorded in the north eastern part of the study area ranging from (28-36Ω.m). But the top layer of each VES points shows the low resistivity. The maximum value of the measured apparent resistivity does not exceed 48 Ω.m.

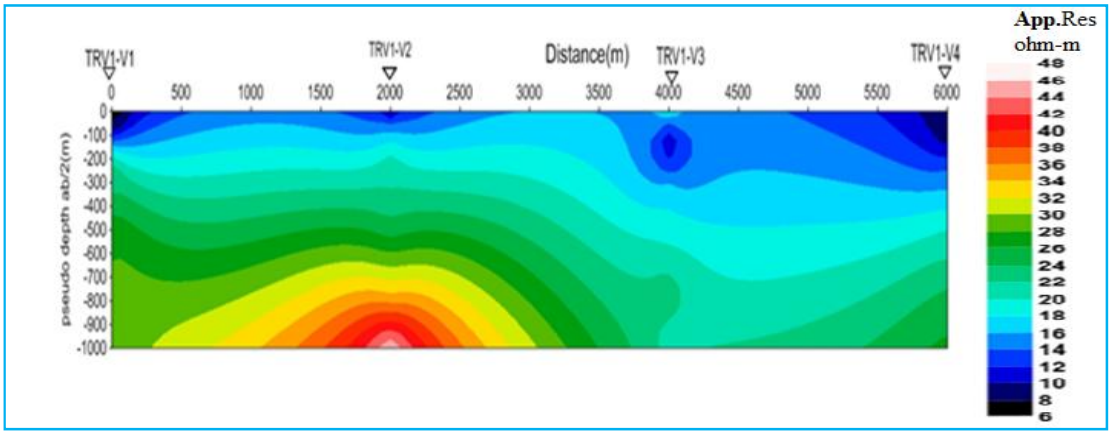

Figure 5-3: Apparent resistivity pseudo-depth section, along line-1

The shallow geoelectrical picture indicates that the resistivity values are generally low (7.4 – 13.4 Ω.m) and laterally uniform.

The corresponding geo-electric section, figure 5.5, presents the interpreted VES parameters for Line-1 of the Mermero target area in the form of stratified layers. Along this southwest–northeast (SW-NE) line, the subsurface is represented by three geo-electric layers. The geologic interpretation of the layers was based on the description obtained from the test bore hole, BTW-2.

As discussed in table 5-1 the lithological description shown a thin top layer with a resistivity range of 8 – 13Ω.m is interpreted as a sandy soil layer with gravel and extremely weathered basaltic rock fragments. This is underlain by a thick layer of another low resistivity range, 7 – 10 Ωm. The maximum thickness of the second layer reaches averagely about 75m towards the NW. But, in the middle of the line, the thickness diminishes to about 20m, possibly affected by the inferred fault. This second layer is attributed to gravel bed with clay.

The subsequent bottom geo-electric layer is correlated to weathered and fractured basaltic horizon. The resistivity signature from this substratum appears to be low indicating abundance of clay material and other conductive phase (water) and hence may represent the likely aquifer bed. The geologic structure, speculated from the qualitative appraisal of the resistivity pseudo-depth section and magnetic profiling, is seen displacing subsurface layers.

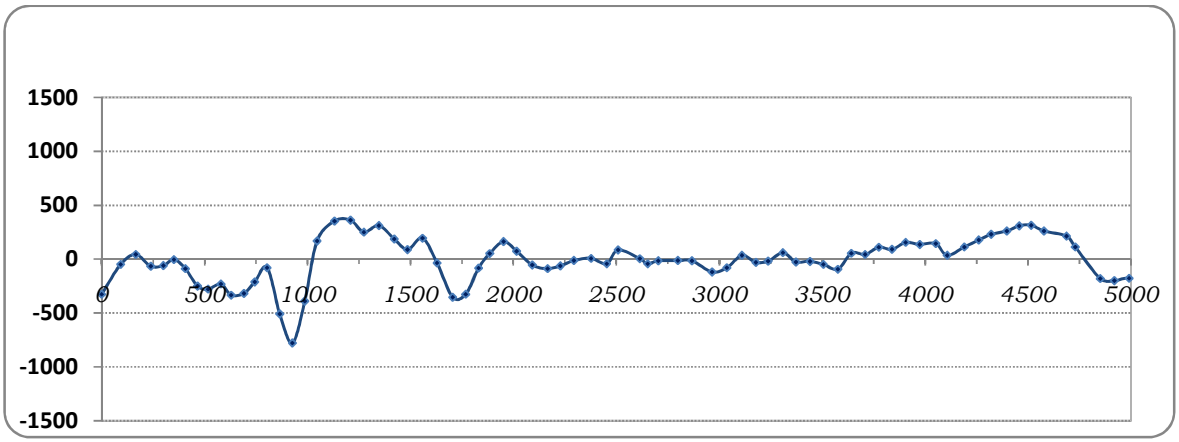

Figure 5-4: Total magnetic field anomaly profile along line-1

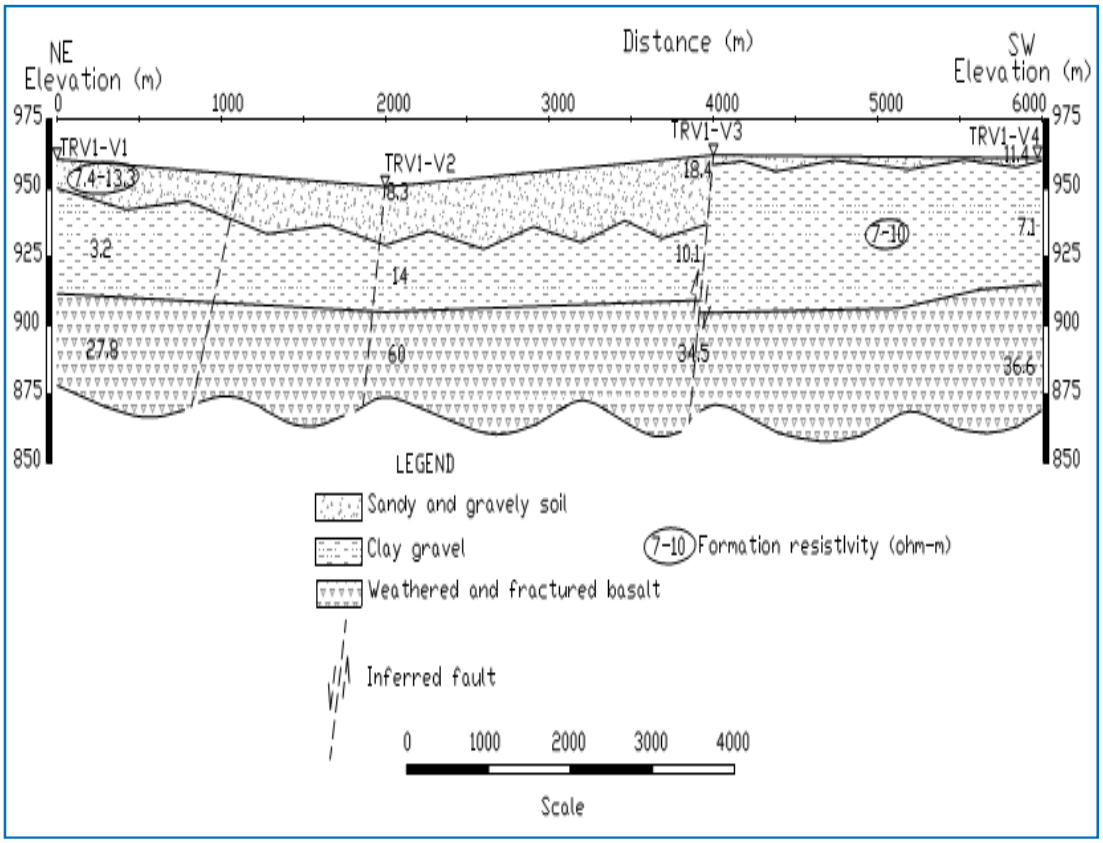

Figure 5-5: Geo-electric section constructed along TRV1 (Mermero line one)

Table 5-1: Lithological Description of Mermero (BTW2)

S/N	Depth	Lithological Description	Remarks
1	0-2	Fine gravel with sandy soil	
2	2-26	Medium grained gravel with fine sand	
3	26-46	coarse to medium grained gravel	
4	46-62	Medium grained gravel	
5	62-78	coarse, angular to sub rounded gravel deposit, transported materials of different origins	
6	78-94	deeply weathered & fractured basalt aquifer	
7	94-104	Highly compacted reddish to brownish clay soil	
8	104-110	Slightly Weathered & Fractured basalt aquifer	
9	110-137	Moderately fractured &weathered basalt aquifer	
10	137-142	Fresh Granitods	

From the above figure 5.4 the total magnetic field anomaly profile and figure 5.5 the geo-electric section along line -1 show the discontinuities of geological structures are almost identical in horizontal position in the curve and possible earth model. The magnetic curve and geoelectric section shows the same pattern in geological structures which may be concluded as contact, fractures or faults.

Therefore the overall picture gives an indication of a cutting structure (a probable faulting). There is also supporting evidence this fault on the magnetic profile indicated by a spatially corresponding bi-bipolar anomalous disturbance. Such bi-polar magnetic signature usually arises from a vertically polarized body which may have resulted from movement of subsurface blocks along a vertical plane like faults, figure 5.4. Both magnetic anomaly variation plot and the geo-electric section show the discontinuity or faults.

5.2.3.2. Mermero TRV2 (Profile Line2)

This pseudo section data is comprised from the four VES point data. The spacing between each VES points are averagely 2000m. According to this figure 5.6, there is a lateral variation in resistivity in the section with the prominent high resistivity exists under the TRV2-V2.The pseudo section shows an extensive low resistivity subsurface over the portion of the section and the deepest region beneath TRV2-V2 where high resistivity responses were recorded. The vast region under the section shows extensive coverage of low resistivity zone. The resistivity ranges (6-26Ω.m) of this low resistivity region are indicative of potential water saturation. The maximum value of the measured apparent resistivity does not exceed 34Ω.m.

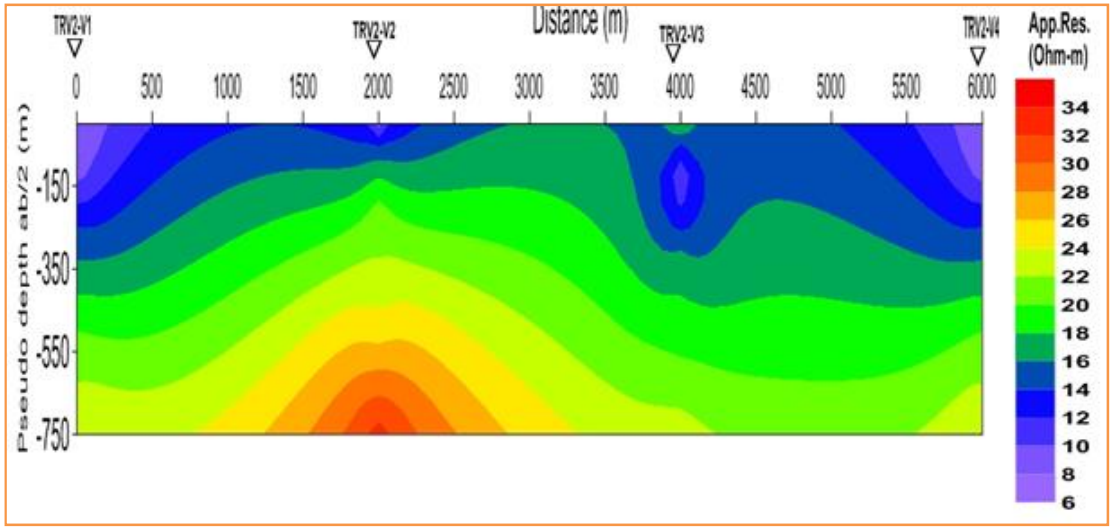

Figure 5-6: Apparent resistivity pseudo depth section

Referring from the geo- electric section the subsurface under the TRV2 represents four distnicted geo-electric layers. The top layer which is delineated with by narrow resistivity range of 7-10 Ω.m, with the average thickness of 0.9m, Overlies slightly higher resistivity horizon with variable response ranging from 11- 161Ω.m and its average thickness of this second layer 9m. This top sequence appears to represent the top soil and underlying sand and gravels. The third layer is also shown as the variable resistivity varies from the range of (12-86 Ω.m) and interpreted as brown silty clay soil and the fourth layer is interpreted as weathered and fractured basalt.

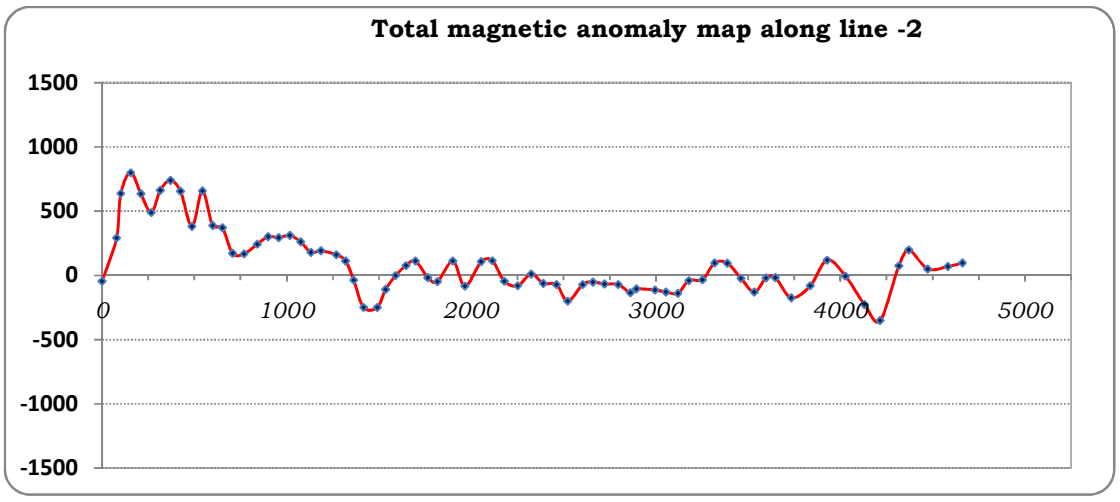

Figure 5-7: Total magnetic anomaly profile along line-2

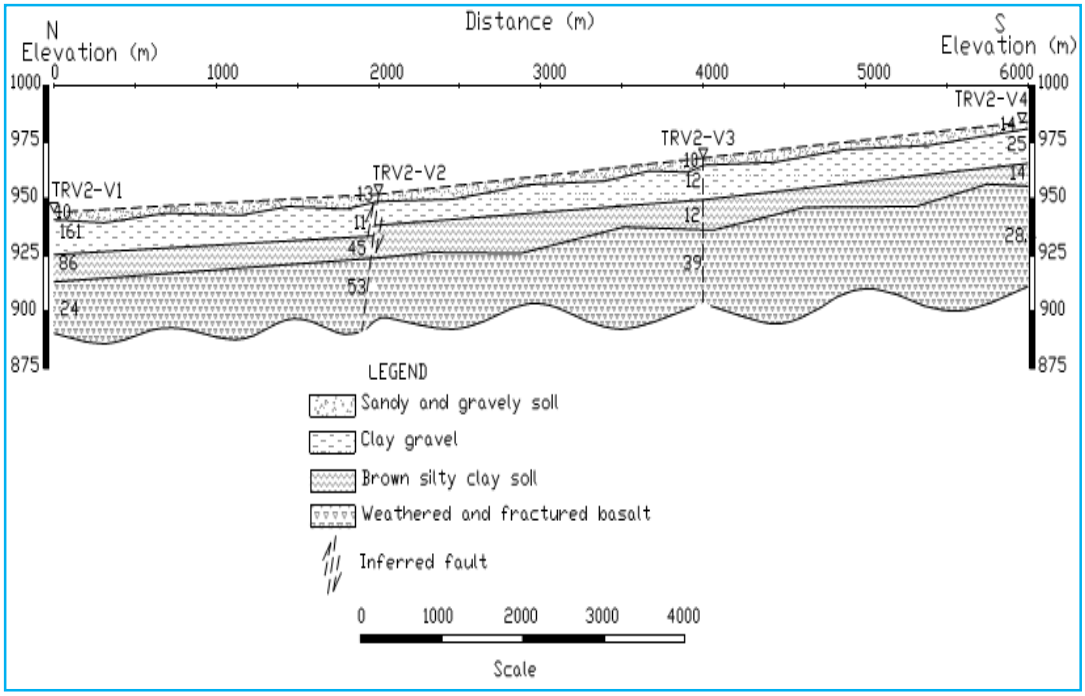

Figure 5-8: Geo-electric section constructed along TRV2-(Mermero line two)

From the above figure5.7 the total magnetic field anomaly map and figure 5.8 the geo-electric section along line -2 shows the discontinuities of geological structures are almost identical in horizontal position in the curve and possible earth model. The magnetic curve and geoelectric section shows the same pattern in geological structures which may be concluded as contact, fractures or faults. In the case of total magnetic field variation plot , there is a variation along the horizontal line.

Therefore the overall picture gives an indication of a cutting structure (a probable faulting). There is also supporting evidence this fault on the magnetic profile indicated by a spatially corresponding bi-bipolar anomalous disturbance. Such bi-polar magnetic signature usually arises from a vertically polarized body which may have resulted from movement of subsurface blocks along a vertical plane like faults, figure 5.7. Both magnetic anomaly variation plot and the geo-electric section show the discontinuity or faults.

5.2.3.3.Mermero TRV3 (profile line-3)

The data from the three VES points along NE-SW traverse line (TRV-3) is given in the form of pseudo-depth section and geo-electric section is shown below respectively.

The pseudo section shows an extensive low resistivity subsurface over the vast portion of the section, except the shallow segment under TRV3-V2 and the deepest region beneath TRV3-V3 where high resistivity responses were recorded. The maximum resistivity recorded is 110 Ωm.

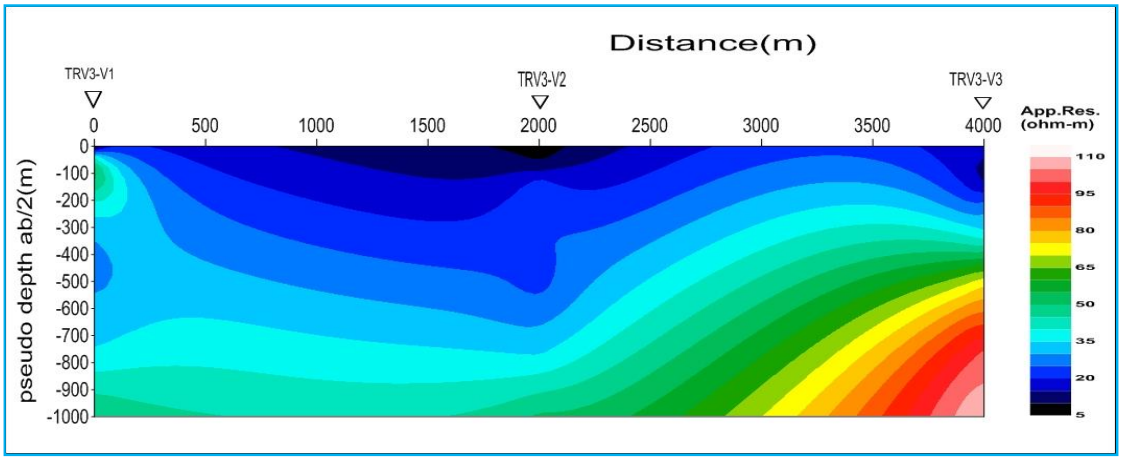

Figure 5-9: Apparent resistivity pseudo- depth sections along line-3

Referring from the Geo-electric layer the subsurface under theTRV3 is represented by four to five distinct geo-electric layers. The top layer, delineated by narrow resistivity range of (3.9 -19.05Ω.m), Overlies slightly higher resistivity horizon with variable response ranging from 10-44Ω.m. This top sequence appears to represent the top soil and underlying sand and gravels.

From the NE end mid way, there appears a third layer of elevated resistivity 369Ωm, which does not show up beneath TRV3-V3. The fourth geo-electric horizon is marked by uniformly low formation resistivity response, 17.9-19.9 Ω.m and has an average thickness

of 184.1m.Mostly such vast conductive horizons; in this area are the likely response of fragments of weathered volcanic rocks with clay silt and sand. The substratum which underlies the abovementioned vast conductive layer is characterized by variable resistivity (128.3-1253Ω.m) increasing from NE to SW.

The resistivity response of different subsurface layers provides a means of assess their suitability to host adequate amount and potable groundwater. Even though it may not be feasible to exclude the presence of fluid, formations with low resistivity, such as the vast fourth layer described above, do not usually host adequate amount of groundwater. Most commonly such pronounced drop in the subsurface electrical resistivity are related to high clay content that makes the host formations a very poor aquifer.

The reduced total magnetic field values for the TRV3 area is presented in the figure 5.10 in the form of profile plot and correlated with the geo-electric section.

The magnetic field response of the survey area shows strong low and high amplitudes towards either flanks of the line specially, at the transition zones from high to low and again high resistivity horizons exhibited on the accompanying pseudo-section and the geo-electric section. Both magnetic anomaly variation plot and the geo-electric section also show the discontinuity or faults.

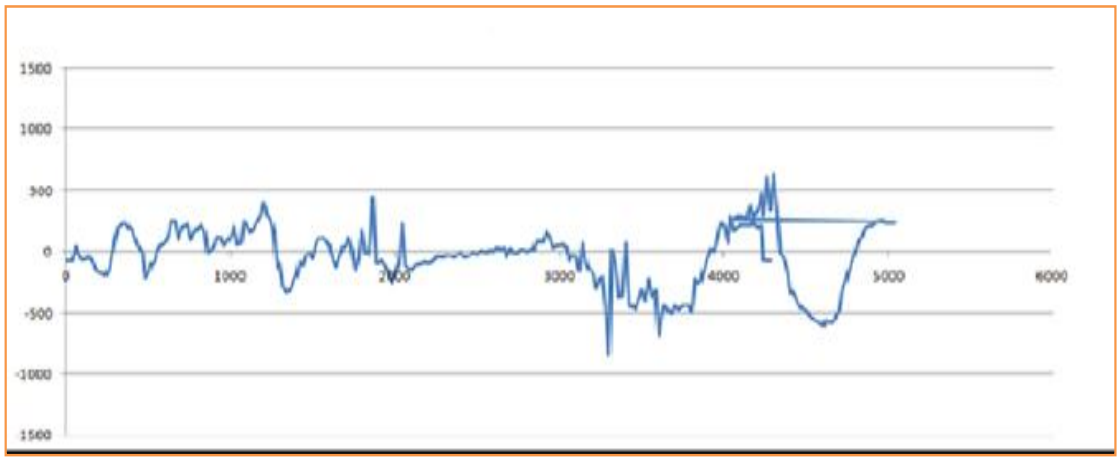

Figure 5-10: Total magnetic field anomaly profile along line-3

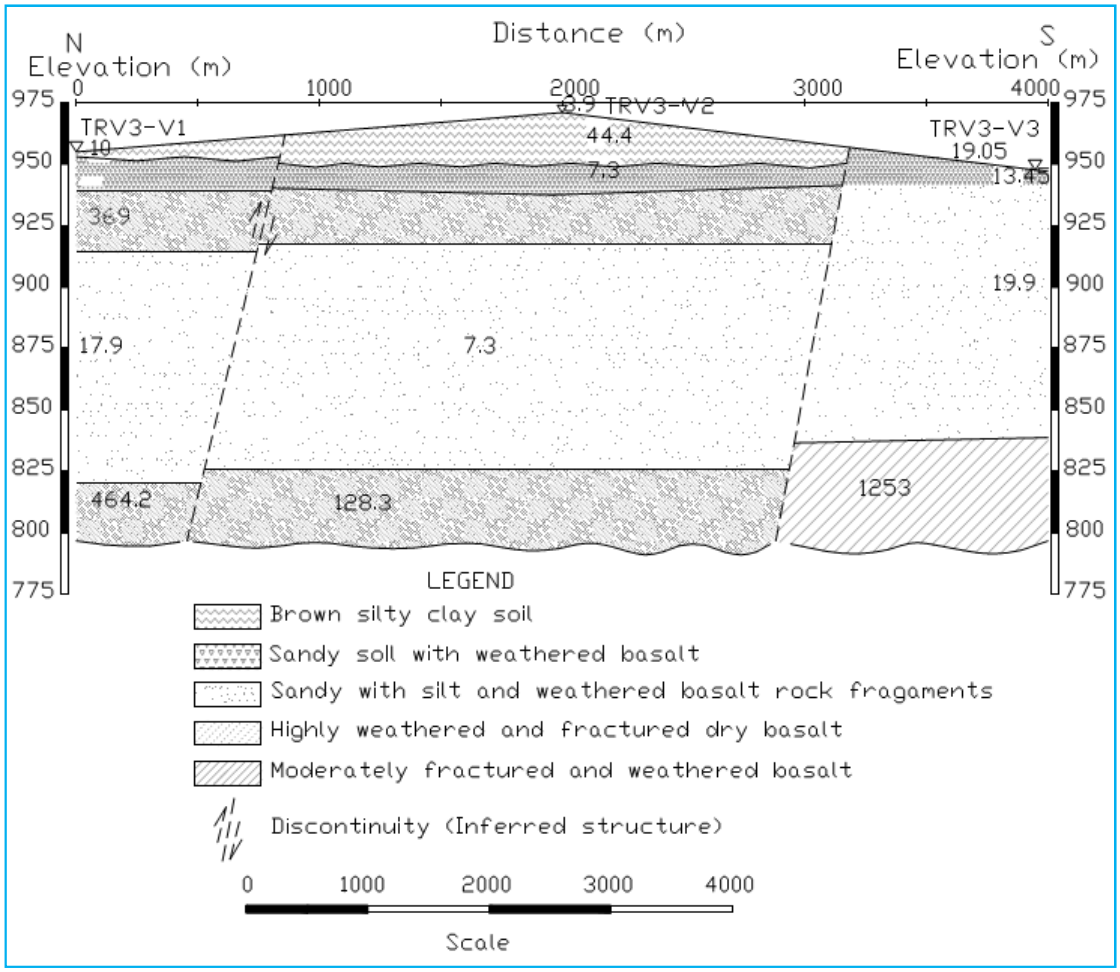

Figure 5-11: Geo-electric section constructed along TRV3

5.2.3.4.MermeroTRV3A

There are three VES points on the SW-NE trending traverse denoted as TRV3A. The spacing between each VES are averagely 2km. The pseudo depth section plot constructed using the raw data from these three VES are shown in figure 5.12 below. The figure shows an extensive region of low resistivity over most part of the section, except the high resistivity under VES-2, overlaying a uniform resistivity horizon at larger electrode spacing. Moreover, the symmetry between bow-shaped region of enhanced resistivity and the identical shape depression over the bottom resistivity horizon underneath VES-2 may indicate possibility of structural features.

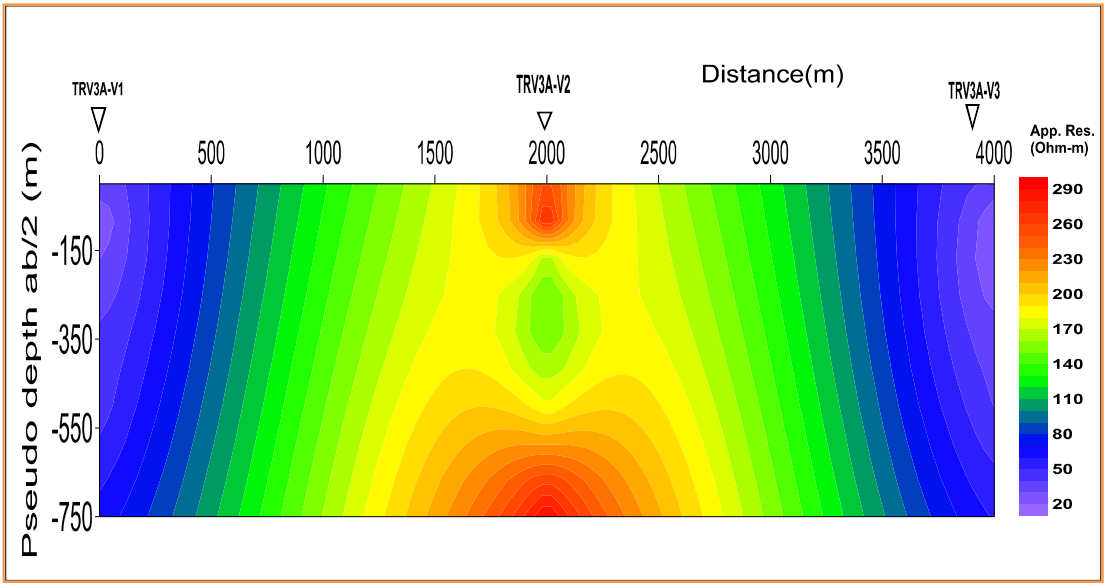

Figure 5-12: Apparent resistivity pseudo-depth sections

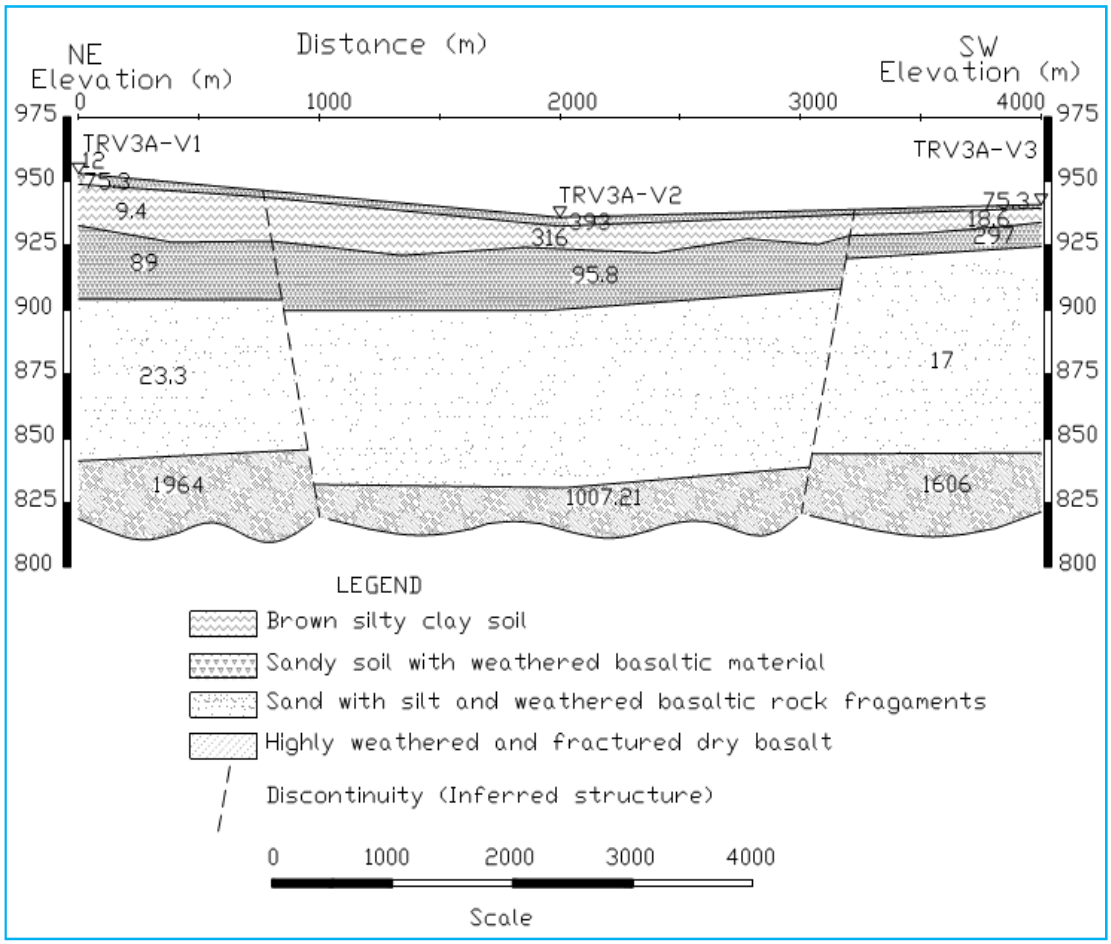

Figure 5-13: Geo-electric section constructed along the survey line TRV3A

The geo-electric section shown in figure5.13 displays near horizontal stratification of four to five subsurface geo-electric layers. The top variable resistivity (12-75Ω.m) thin soil covers is shown to be underlain by another thin layer of relatively higher resistivity (75.3-393Ω.m). The third geo-electric layer is represented by the conductive horizons. The formation resistivity again rises to range (89- 297Ω.m) with an average thickness varies up to 55.1m under VES2 in the fourth layer. The likely explanation for such fluctuation in resistivity could be the variation in grain size and texture in the top beds of sediments.

Below this an immense layer of uniform low resistivity i.e.17-23 Ω.m with an increasing the thickness under each VES. As shown from the geo-electric section the thickness increases successively to SW below TRV3A-V1 to TRV3A-V3.

5.2.3.5.Mermero TRV3B

TRV-3B is the third segment amongst the survey lines located in the central Mermero area. This traverse is oriented in E-W direction and also comprised of the three VES points with the spacing between the sounding points is averagely 2000m.

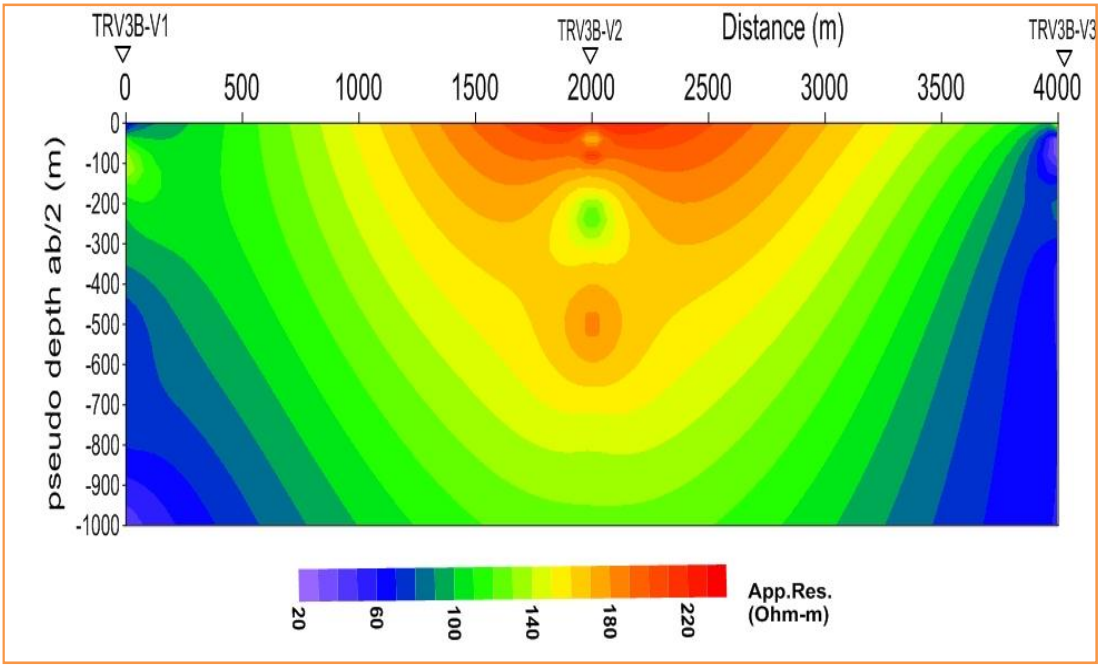

Figure 5-14: Apparent resistivity pseudo-section along TRV3B

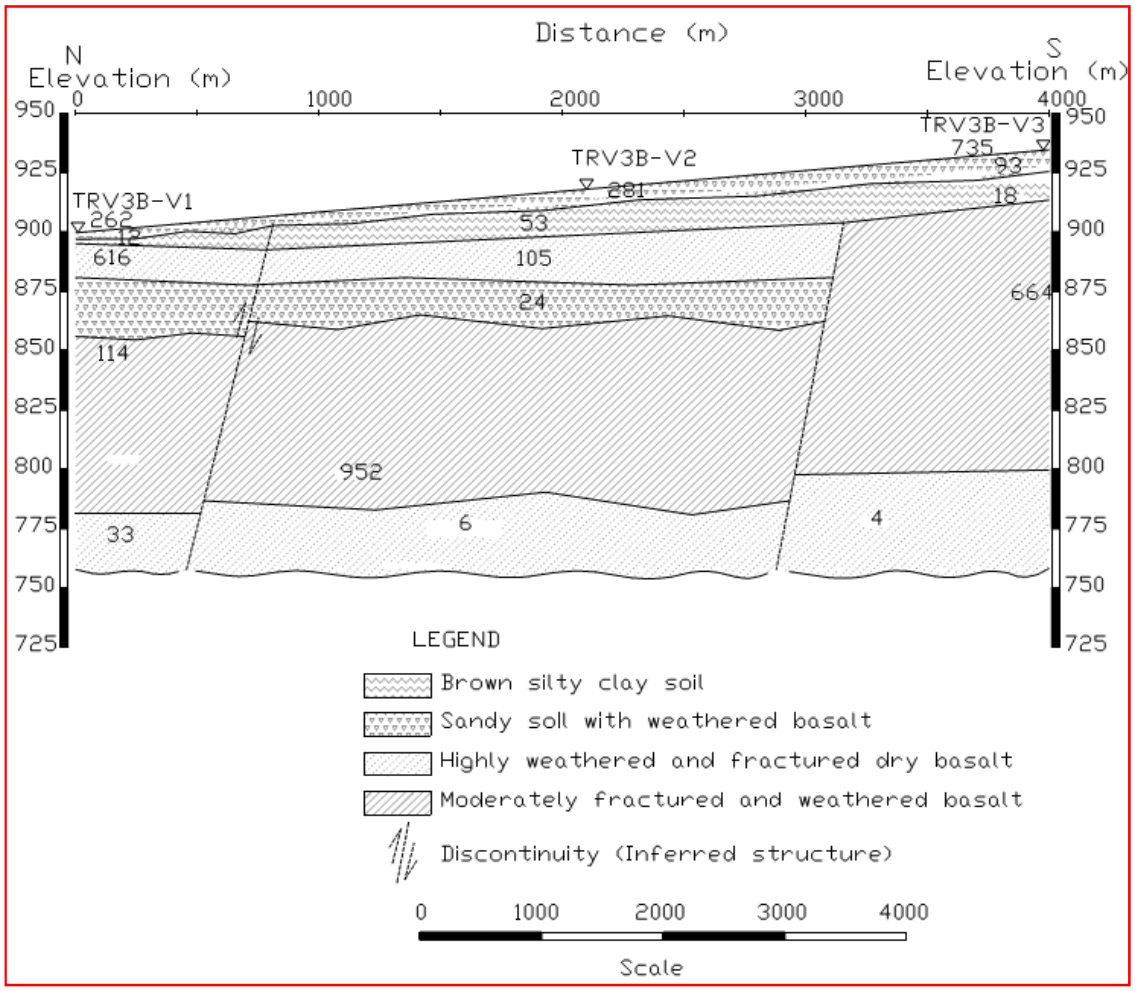

Figure 5-15: Geo-electric-section constructed along TRV3B

Figures (5.14) and (5.15) respectively show, the apparent resistivity pseudo-depth and the geo-electric section constructed using the measured raw data and the interpreted model parameters of the VES. Contrary to those sections obtained from TRV-3 and TRV-3A, the pseudo-depth section for this line as shown in the above the pseudo section figure 5.14, an extensive region of high resistivity in the central part of the section flanked by low resistivity zones. Furthermore, the high resistivity zone below TRV3B-V2 also extends to larger depth suggesting that this zone is devoid of moisture or groundwater. The area below TRV3B- V1 and TRV3B-V3 as mentioned above gave low resistivity responses suggestive of water saturated regions. The observations from the apparent resistivity pseudo-section of TRV-3B are reflected on the interpreted VES which is presented as geo-electric section in figure (5.15). Accordingly, the interpreted layered model displays that the ground section beneath is electrically heterogeneous, showing frequent resistivity variations in both vertical and lateral directions. The western flank (under TRV3B-V3) on

the other hand appears to be comparatively less variable as represented by fewer numbers of prominent layers. The eastern side, the subsurface under TRV3B-V3 has been shown to be represented by stratification of six layers while the western region, beneath VES 3 has only been consisted of three geo-electric layers. However, this variation between the flanks is more visible at shallow levels. Beyond the depth of about 50m, the subsurface tends to homogenize in to a vast resistive horizon with formation resistivity ranging from 114 to 664 Ω.m.

From water prospect point of view the shallow and intermediate sections do not show favorable physical parameters for hosting groundwater. The geo-electric substratum, i.e. the bottom layer on the section may provide a suitable environment for hosting potential groundwater. The drop in electrical resistivity (4, 33Ω.m) at such larger depth (>165m) can be attributed to presence of fluids. The vertical structures interpreted from discontinuity in layer parameters may serve as percolation channel and add extra value to the bottom layer to qualify as a possible aquifer. Although the western region (beneath TRV3B-V3) also seems to have favorable resistivity response (the bottom layer resistivity of 4Ω.m),owing to the surface topography the bottom morphology, the eastern part appears the most favorable regions and as such drilling in the close vicinity of TRV3B-V1 would have a better chance of hitting the desirable target.

5.2.3.6. Mermero TRV10 (profile line-10)

Traverse TRV10 comprised of a total of eleven(11)VES and the sounding points are located at average spacing of about 2km which are except between TRV10-V6 and TRV10-V7 6km apart .This traverse line is one of the longest line.

In qualitative terms, the subsurface underneath TRV10,portrayed on the pseudo-depth section of figure 5.16 below is electrically heterogeneous. As seen from this pseudo section graphically it gives the heterogenous property, i.e TRV10-V1,TRV10-V2 and TRV10-V3 , have low resistivity at the top layer ranges (0-40 Ω.m).The next group is TRV10-V4,TRV10-V5, TRV10-V6, TRV10-V7 and TRV10-V8 almost the structures are the same which is grouped under medium resistivity layer and the last group TRV10-V9,TRV10-V10 & TRV10-V11. Depth wise,the measured apparent resistivity shows notable variations beneath the majority of of the sounding points. There are also lateral anomalous resistivity responses showing significant contrast to the sounding.

It is seen that the vast shallow and intermediate regions give low resistivity response reflecting the area of abundance in conductive constituents such as clay. The high resistivity response of the bottom layers beneath TRV10-V9, TRV10-V10.

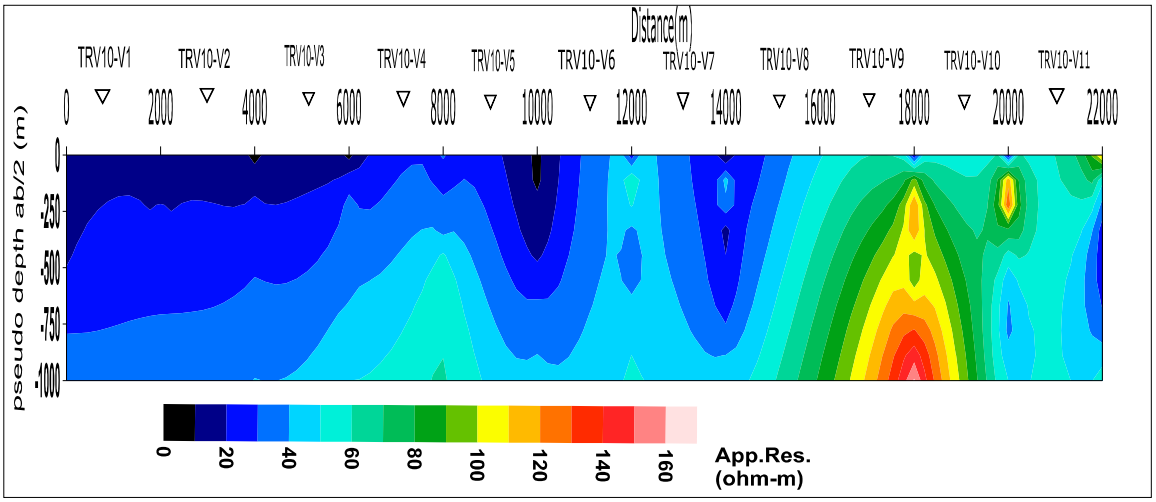

Figure 5-16: Apparent resistivity pseudo depth section plotted along TRV10

The geo-electric layer for the line TRV10 shows the subsurface with the variable resistivity response both laterally and vertically. Based on the lateral variation in the interpreted layer parameters, the subsurface under this long traverse could be broadly classified in to three major groups. Extending the same reasoning, the demarcation between these groups has been marked by vertical discontinuities indicating the possible positions of geologic structures.

According to the region under TRV10-V1to TRV10-V5 falls in the first group and is represented by four comparatively conductive layers including the geo-electric substratum. The average formation resistivity of the top 150m occupied by the top three layers is less than20Ω.m. Even across the bottom layer, the resistivity response shows only small increments to a range between 30-120Ω.m. Categorized in the second group is the ground section mapped under TRV10-V4, V5 and V6. In comparison to group one, the formation resistivity of the layers rises, except the thick third layer which is persistently conductive all along the traverse line. Particularly, the resistivity response that delineates the substratum rises ranging from 13-100Ω.m.

From geo-electric point of view, the third layer, whose resistivity responses vary between 5-21 Ω.m may qualify as a possible water bearing horizon. Its considerable thickness, persistent over the entire length of the profile, except around VES-9 and VES-10, can be considered yet another attraction. However, very low resistivity values do not necessarily

lead to striking subsurface water and decisions on well sitting needs a careful examination and consideration of subsurface lithology. Such pronounced reduction in resistivity response in hard rock area could also be a result of enrichment in electrically conductive minerals. Moreover, the relative drop in resistivity response along the geo-electric substratum (the bottom layer) may be used as a more reliable clue to speculate fluid saturation. These deep, low resistivity portions which are also close proximity to the likely to the vertical discontinuities should beneath VES-4 and VES-10 appear to be most attractive from the point of view of the objective of the survey.

Referring the total magnetic field variation plot along line-10, it shows the variation of the anomalous body. This variation of the anomalous body shows the high anomalies discontinuities of geological structures are almost identical in horizontal position in the curve and possible earth model. The magnetic curve and geoelectric section shows the same pattern in geological structures which may be concluded as contact, fractures or faults.

As seen in the pseudo-depth section and Geo-electric section this line shows the heterogeneous property. As observed from the geo-electric section and pseudo depth section, starting from VES1 up to VES 11, there is heterogeneous property. The overall picture gives an indication of a cutting structure (a probable faulting). There is also supporting evidence this fault on the magnetic profile indicated by a spatially corresponding bi-bipolar anomalous disturbance. Such bi-polar magnetic signature usually arises from a vertically polarized body which may have resulted from movement of subsurface blocks along a vertical plane like faults; figure 5.18 the magnetic anomaly variation plot support the geo-electric section which shows the discontinuity or faults.

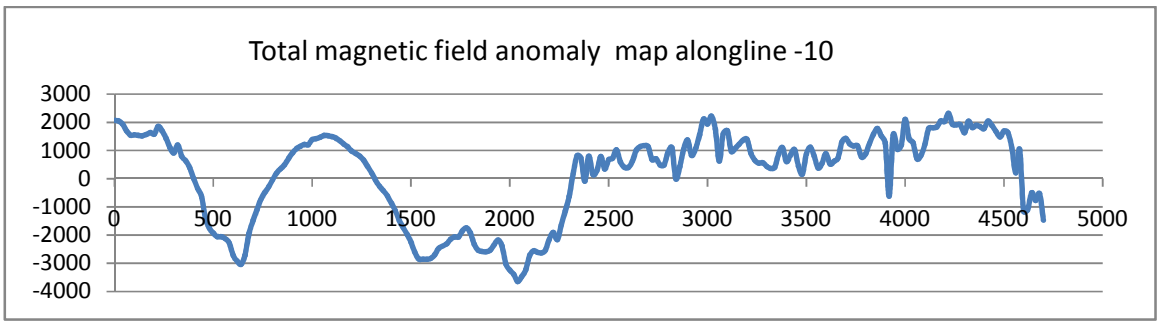

Figure 5-17: Total magnetic field anomaly profile plot for Line-10

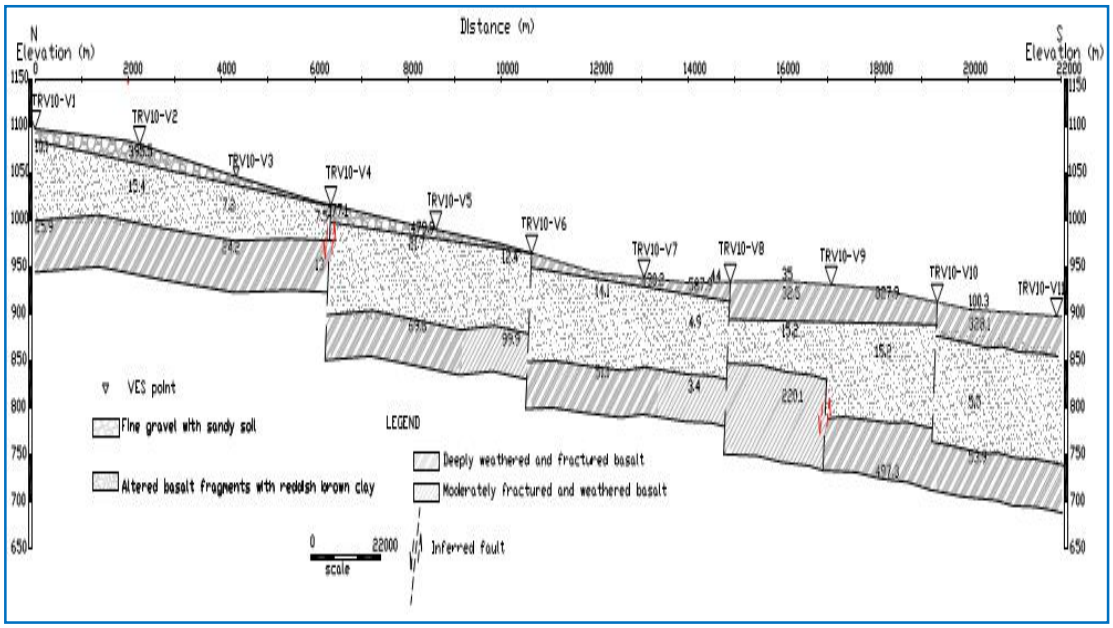

Figure 5-18: Geo-electric section constructed along line-10.

5.3. Discussion and interpretation of magnetic data

5.3.1. Magnetic data presentation

After the removal of all corrections, the residual data were processed and plotted on oasis Montaj v.6.4. The results are presented in contoured forms for visualization and further enhancements.

5.3.2. Results and Interpretations of Different magnetic Anomaly Maps

An important objective in the interpretation of potential field data is to improve the resolution of observed data. In magnetic prospecting, in areas of limited exposure, delineating lateral change in magnetic susceptibilities provides information not only on lithological changes but also on structural trends (oruc et.al., 2011).

The main target of the survey was to identify and delineate qualitatively the basement rock structures, their distribution and trends, in the study area. After applying all the necessary reductions, the magnetic anomaly maps are prepared.

The processed geophysical data were used to produce different anomaly maps, which show contrast in the susceptibility, magnetization direction and remanence of the subsurface rocks. In this case the interpretation and the result of the magnetic anomaly maps are presented below.

5.3.2.1.Total Observed magnetic field anomaly maps

The observed total magnetic field intensity map was created after the diurnal corrections and removal of the IGRF model field from the field- collected. As shown in the map, the total magnetic field intensity varies from 33699 to 35939 nT.

The total magnetic field intensity map shows low anomalies in north east, northwest and some part of the central of study area. The intermediate magnetic intensity over study area encloses the low magnetic intensity of northern and western part and the high magnetic intensity observed at the eastern, south southeastern(E-SSE) part of the map. But between east and south-southeast very low anomalies body is observed.

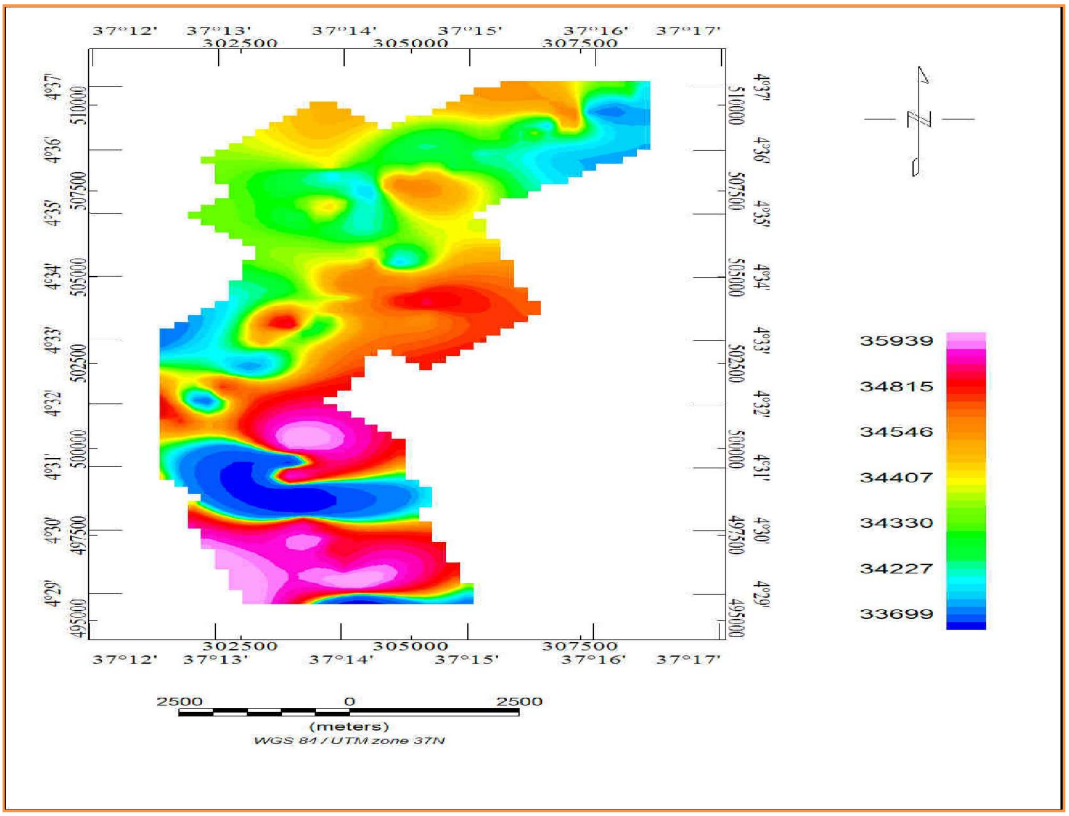

Figure 5-19: Observed total magnetic field intensity map.

5.3.2.2. Residual anomaly map

The residual magnetic field anomaly map was created after subtracting third order trend of the regional magnetic map as shown in figure 5.20.i.e the observed data was corrected by using the dinuar correction and IGRF correction.

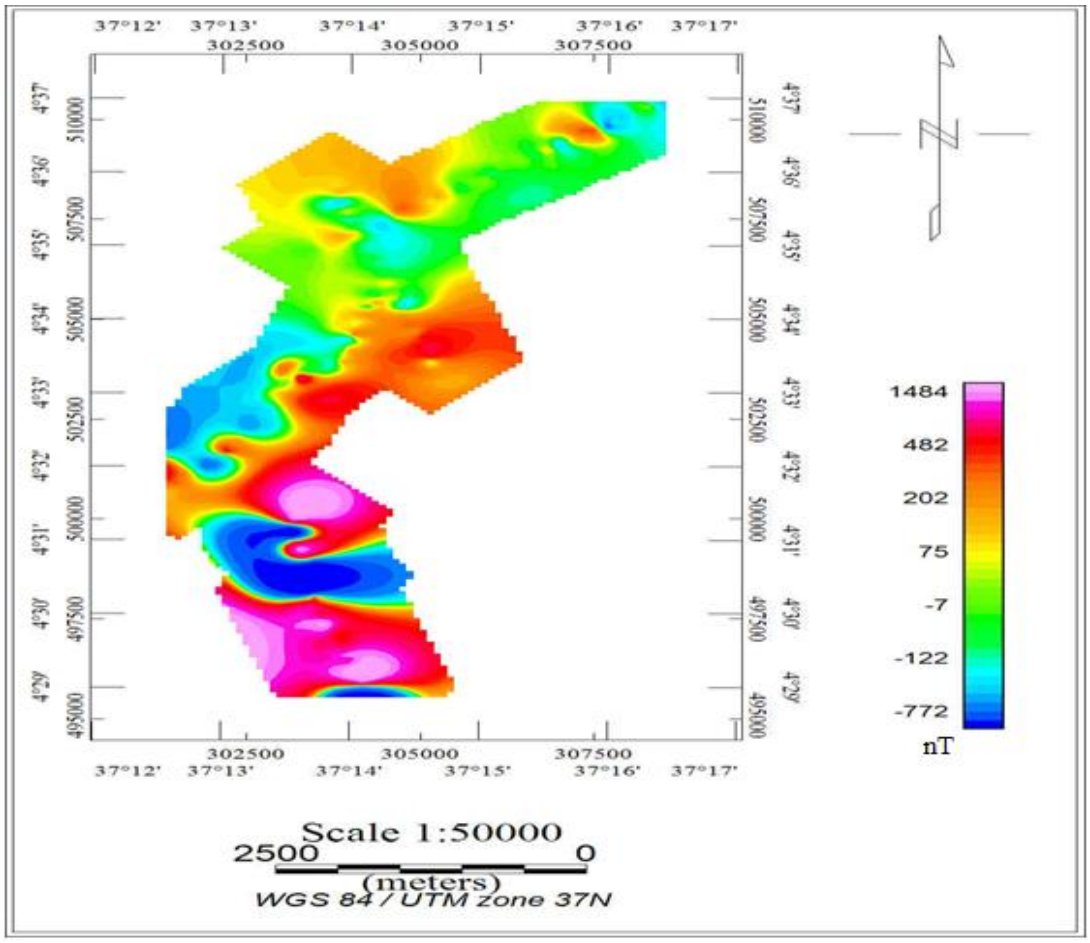

Figure 5-20: Residual magnetic anomaly maps.

As shown from the above map, the residual magnetic anomalies vary from -772 to 1484nT. This variation is from the negative anomalies body to the positive anomalies. In this case the interpretation is very difficult with the residual anomalies is that are dipolar .i.e. anomalies having positive and negative components, such that the shape and the phase of the anomalies depends in part on the magnetic inclination and presence of any remnant magnetization. This anomaly complexity makes interpretation more difficult because the body and its edges do not necessarily coincide with the most obvious mapped feature. Therefore, in order to accentuate/ emphasize the magnetic signature of the linear geologic

structures, the analytic signal has been calculated from residual values and interpretations were made based on this map.

5.3.2.3.Analytic signal map

The analytic signal method, known also as the total gradient method, as defined here produces a particular type of calculated gravity or magnetic anomaly enhancement map used for defining in a map sense the edges (boundaries) of geologically anomalous density or magnetization distributions (e.g., basement fault block boundaries, basement lithology contacts, fault/shear zones, igneous and salt diapirs, etc.). The analytic signal or total gradient is formed through the combination of the horizontal and vertical gradients of the magnetic anomaly. The analytic signal has a form over causative body that depends on the locations of the body (horizontal coordinate and depth) but not on its magnetization direction (Ansari and Alamdar, 2009).

The analytic signal method, known also as the total gradient method, produces a particular type of calculated magnetic anomaly enhancement map used for defining the edges (boundaries) geologically anomalous magnetization distributions. Analytic signal maxima have the useful property that they occur directly over faults and contacts, regardless of structural dip which may be present, and independent of the direction of the induced and/or remnant body magnetizations (Saad et al., 2010).

As shown from the analytic map shown figure 5.21 the magnetic anomalies vary from 0.1nT to 5.4nT. In the total observed magnetic map there are two dipolar anomalies presented which by application of the analytic signal this dipolar pattern has been removed completely.

When the analytic signal applied to the observed (residual) magnetic field, the method generally generates good horizontal locations for contacts and sheet sources regardless of their geologic dip or geomagnetic latitude. From this map in the direction of SE-NW there is a contact line and between the coordinates 497500 and50000 there is a high anomaly response. That the high anomalies responses as shown from the analysis signal map, it ranges from (2.7-5.4 nT). But some part of the north western and north eastern shows the low anomalies. This analytic signal map supports for each profile lines there is a contact as shown in Geo-electric section, under the interpretation of the electrical sounding.

Therefore the analytic signal map clearly identifies the lithologic units and their magnetic content.

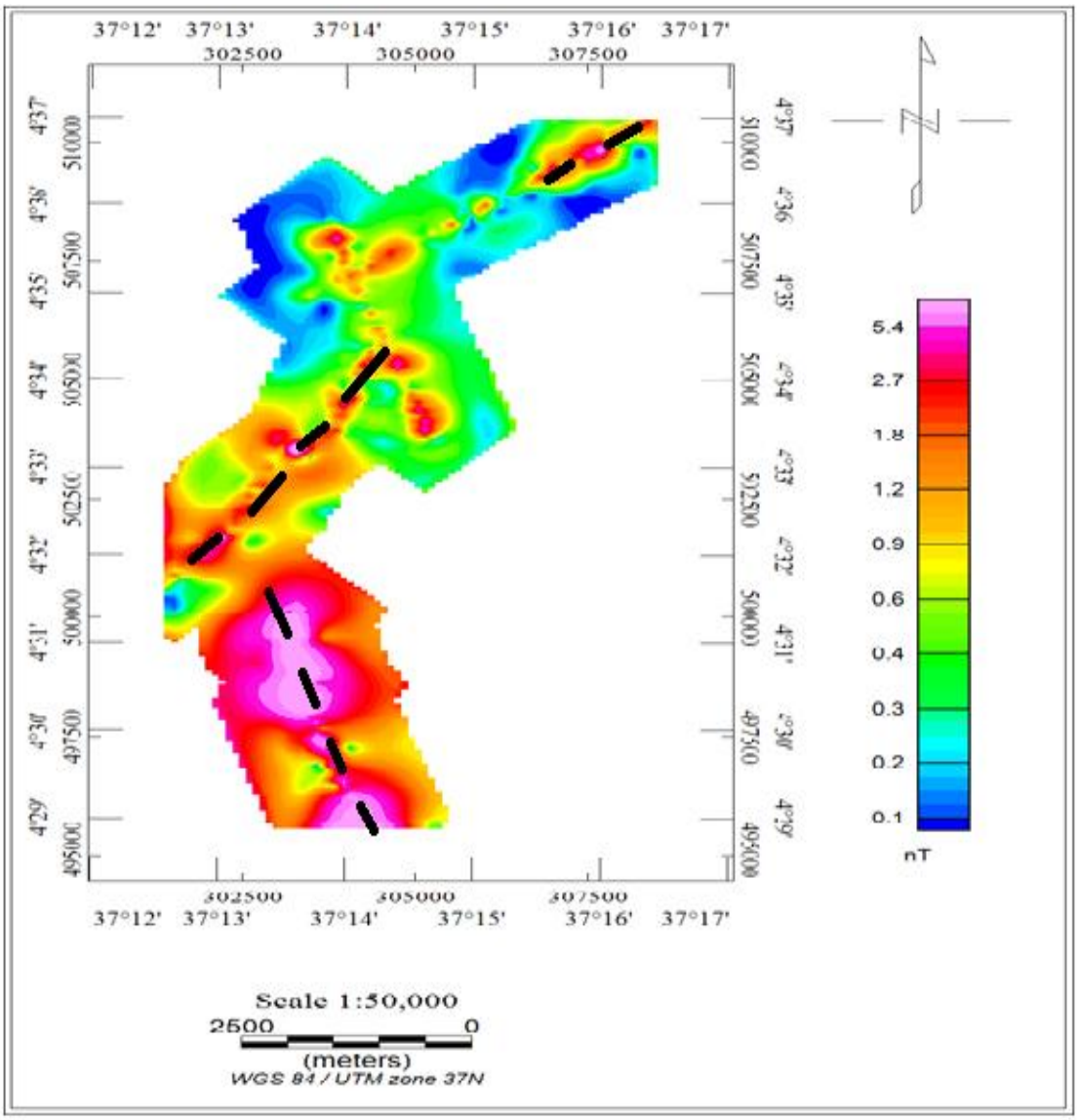

Figure 5-21: Analytic signal map

5.3.2.4.Reduced to pole magnetic (RTP) anomaly map

This method entails removing the dependence of magnetic data on the magnetic inclination i.e. converting data which were recorded in the inclined Earth's magnetic field to what they would have been if the magnetic field had been vertical. As shown the figure 5.22, this reduced to pole map shows the similar map with the analytic signal map.

From this map in the direction of SE-NW there is a contact line and between the coordinates 497500 and 50000 there is a high anomaly response. That the high anomalies

responses as shown from the analysis signal map, it ranges from (2.7-5.4 nT). But some part of the north western and north eastern shows the low anomalies.

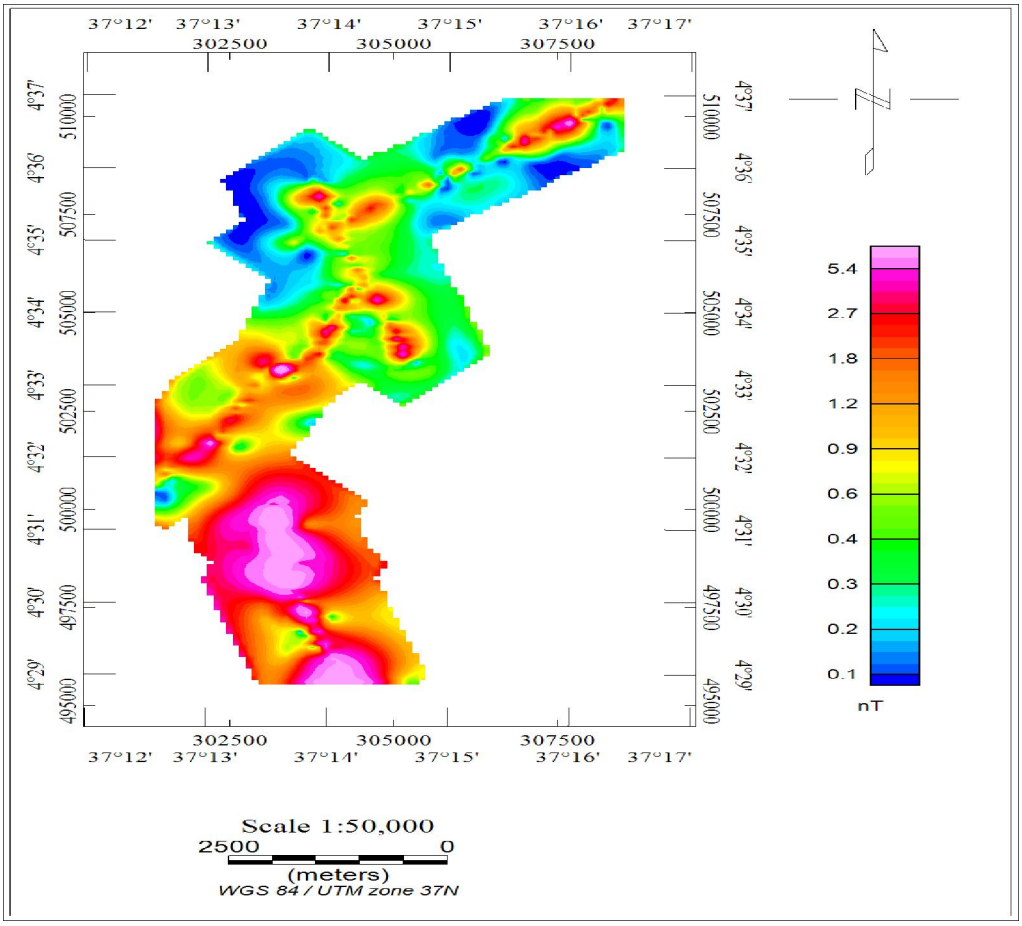

Figure 5-22: Reduced pole magnetic anomaly map

5.3.2.5. 2D Profile modeling along profile line-1

Modeling is done using the GM-SYS modeling software. It is an interactive forward modeling program which calculates the magnetic response from a user defined hypothetical geological model. Any difference between the model response and the observed magnetic field are reduced by refining the model structure. It should be noted that magnetic models are non-unique, i.e. many earth models can produce the same magnetic response, and similarly, several geological lithology may be interpreted from a given model block's susceptibility properties. It is therefore important to use as many independent source of information as possible to help constrain the model.

According to 2D magnetic modeling is developed along profile-1 from the analytic signal map as shown in Figure5.23. This model is developed based on the information from the inverted model section of electrical resistivity, geoelectric section and the borehole data (BTW2) which is described in table 5.1.

This model is developed based on the information from the borehole (BTW2) and geo-electric section of profile line one and profile line two. The developed model perfectly matches with all the maps and curve developed along each profiles from the different methods in displaying the layering, fault and contact location.

As discussed in profile line-1 in both the geo-electric section and in total magnetic variation plot, with correlating the lithologic log of Mermero BTW2, the aquifer is not fully penetrated. Therefore the 2D- modeling along these profiles supports the both geo-electric section and the total magnetic variation plot. Based on the lithologic log and the geo-electric section, the above layer is sandy and gravel soil, which interpreted as the top soil, the second layer is clay soil .As seen from the figure 5.23, up to the end of the clay soil there is a contact or a fault structure is shown. This fault line is also shown in both magnetic plots, with an interval of 0-1500m to 4500-6000m in figure 5.4 and also in geoelectric section between VES1 and VES2 in figure 5.5.

Finally the third layer is modeled as weathered and fractured basalt. Since these model is modeled based on the information of table 5.1. Lithological log description of BTW2 which has a depth of 141m and the resistivity well log is annexed in appendices; the aquifer is not fully penetrated.i.e. From the geoelectric section, the bottom layer shows low resistivity. But when the bottom layer shows low resistivity the horizons are interpreted as weathered and fractured basalt.

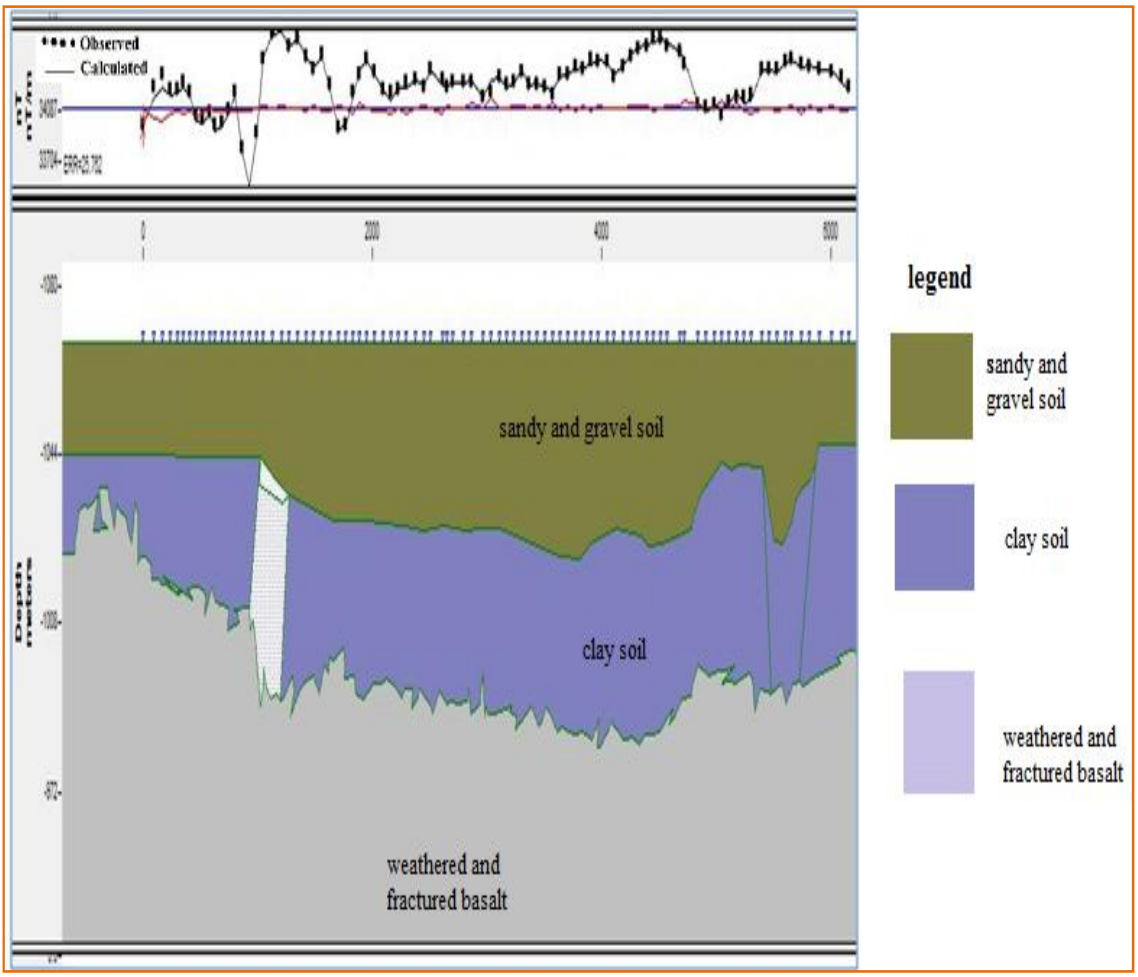

Figure 5-23: 2D magnetic modeling along profile-1

6. CONCLUSION AND RECOMMENDATION

6.1.Conclusion

Geophysical investigation for groundwater potential assessment using the vertical electrical sounding (VES) and the magnetic method were conducted to investigate groundwater potential zones at Mermero area, Borena zone, Southern Ethiopia. The main objective of this study is to determine the depth of groundwater table, to locate the groundwater potential areas and to identify the subsurface layers.

The data acquired from twenty eight (28) VES points using Schlumberger electrode array with maximum half current electrode spacing (AB/2=1000m) and 663 magnetic data points, which were interpreted both qualitatively and quantitatively in order to understand the lithostratigraphic section at the specific locality and identify aquifer bearing horizons.

The out puts of the geophysical data were used to produce different anomaly maps which show contrast in resistivity and susceptibility of the rocks.

The Vertical Electrical Sounding (VES) methods were applied to map the resistivity structure of the ground under the point of measurements. As rock resistivity is primarily dependent on the porosity and fluid saturation, it is of special interest for hydrogeological purposes. On this context, the applications the method in the present frame work allowed discriminating between the various lithologic units and, in most cases, assess variations in composition, degree of weathering and texture within the same rock types. This in turn permitted to identify the likely aquifer of the different target areas.

The major contribution of the magnetic method towards the success this of integration is to complementing the finding of the other geophysical regarding structural indication such as faults, fractures and lithologic contacts.

- From the combination of the apparent resistivity pseudo-depth and geo-electric sections and also from the magnetic map, which means the total magnetic anomaly map, the residual map and from the analytic map it has been possible to establish the likely stratification beneath the traverse line.
- From point of view the hydrogeological and the geologic interpretation was made based on the physical responses of the rock formations and the discretion made up

on the lithological log of the nearby borehole, BTW2, during the interpretations made on physical responses of the rock formations .

- From the combination of the apparent resistivity pseudo depth and geo-electric sections, and also from the magnetic map, which means the anomaly map, the residual map and the observed map, for each traverses, it has been possible to make conclusion as the preferred locations for sinking of boreholes to extract groundwater.
- The main geologic units encountered over the survey area that are likely to bear groundwater (based on the degree of fracturing and weathering) are basalts and sand.
- Referring to the discussion on the most of the geo-electric sections from the target area, the third or the fourth layers have been characterized by low electrical resistivity. At shallow depth, the reduction in resistivity could be due to intensive weathering and alteration of the volcanic rock fragments which may have resulted in clay enrichment.
- Comparison of the geophysical interpretations with drilled borehole results show that the results of geophysical survey are good correlation with the borehole lithologic logging results.
- Thick sediment deposition and intercalation of clay materials within the volcanic succession, subsurface in this target area happened to be quite conductive. As a result, the current penetration was quite shallow and it was not possible to reach the basement rock using the maximum current electrode separation of 1000m, for vertical electrical resistivity sounding (VES) survey.
- Inference of possible geological structures and their positions were made by joint consideration of both electrical and magnetic responses of the target area.

6.2.Recommendation

Based on the outcome of the study, the following thoughts are recommended.

- Additional VES survey is recommended in the perpendicular direction of the existing traverse for detail investigation for the extension of low resistivity zones. i.e with the spacing of AB/2=1000m along the profile line-1 the aquifer is not penetrated perfectly, it shows very very low resistivity at the bottom layer. Because of these additional VES with the spacing of 1500m is recommended to fully penetrate the aquifers.

- Five boreholes are recommended for drilling in the following order.
  The recommended boreholes with its UTM coordinates : at TRV3-VES1, (304227, 505193),TRV3B_VES1(297187,487164),VES3,(294372,487150),TRV10VES1,(305765,526294) andVES5(306399,515870).

- Further regional hydrological and hydrogeological investigations are recommended to understand the basin, amount of precipitation and evaporation which are used to estimate the percolation of surface water to the groundwater.

.

REFERENCES

Abebe Ketama ., (2011). Borena Volcanic Plain Groundwater Study project. Oromia water works design and supervision Enterprise.Addis Ababa, Ethiopia.

Andrew L. Herczeg and Leaney F. W.,(2010). Environmental tracers in arid-zone hydrology: Hydrogeology Journal.

Aubert, M., (1984). Resistivity and magnetic surveys in groundwater prospecting in volcanic areas. Case history Maar of Beanit,puy de Dome, France, Geophysics. Prospect.**32**:63-554.

Baker, R.D., (1991).Depth of investigation of collinear symmetrical four-electrode arrays, Geophysics, 54:1031-1037.

Bernard, J., (2003).Short notes on the principles of geophysical methods for groundwater investigations.

Coppock. L D., (1994). Synthesis of pastoral research, development and change in the Borena plateau of southern Ethiopia, the Borena Plateau of southern Ethiopia.

Davidson, A., (1983). The Omo River Project Reconnaissance geology and geochemistry of parts of Illubabor, Kefa, Gamu Gofa and Sidamo, Bulletin/ No. Ministry of Mines and Energy, EIGS.

Fetter, C.W., (2001). Applied Hydrogeology, 4th Edition. Prentice-Hall, Inc. London, UK. Pp 1-20.

Gibson, I., (1969). The structure and volcanic geology of an axial portion of the Main Ethiopian Rift, Tectonophysi*cs*. **8**:561–565.

Hailemeskel, Awoke., (2007). The geology of Yabello map sheet.(Unpublished), Geological Survey of Ethiopia, Addis Ababa.

Helland et al.,(1980b).Deep wells in the particular area for social organization and retinal. Addis Ababa, Ethiopia: EIGS.13.

IRIS Instruments, (2006).The Syscal R1 plus Switch 72 IP and Resistivity unit, www.iris-instruments.com.

Kazmin,V**.**, (1979), Stratigraphy and correlation volcanic rocks in Ethiopia. Addis Ababa, Ethiopia: EIGS.13.

Kirsch,R**.,(**2006).Groundwater Geophysics. A Tool for Hydrogeology. Springer-Verlag Berlin Heidelberg, Germany.

Koefoed, O., (1970). A fast method of determining the layer distribution from the kernel functions in geoelectrical sounding geophy.Prospecting.18:564-570.

Koefoed,O.,(1979). Geosounding Principles I: Resistivity sounding measurements. Methods in Geochemistry and geophysics. Elsevier, Amsterdam.

Kunetz,G.,(1996).Principles of direct current resistivity prospecting. GebruderBorntrager, Berlin- Nikolassee, 103 pp.

Lowrie, W.,(1997). Fundamental of Geophysics, Cambridge University press, Cambridge.

Ministry of Water Resources, (2004). Genale Dawa River Basin Master Plan Study Project.

Mohr, P.A., (1983).Perspective on the Ethiopian volcanic province. Bulletin of volcanology.46:23-44.

Mulugeta Chanie Fenta.,(2011).Application of integrated Geophysical Techniques to map Groundwater potential Zones and Geological structure at Gelchet area, Borena Zone, Southern Ethiopia. Unpublished Msc thesis. Addis Ababa University.

Nicolas, O., Mariita a,G. Randy Keller B.,(2007). An integrated Geophysical study of the northern Kenya rift. Journal of African Earth Sciences, 48, 80-94. Elsevier.

OromiaWaterWorksDeisgn and Supervision Enterprise (2008). Detailed reconnaissance geological study of Borena zone, Borena groundwater study project geology report. Oromia water works, Design and supervision enterprises, Addis Ababa, Ethiopia.(Pp1-50).

Reynold., (1997). An Introduction to Applied and Environmental Geophysics. JohnWiley and Sons limited, England, UK, pp: 160.

Robinson, E.S. and coruth, C., (1988).Basic Exploration Geophysics, John Wiley.

Roy,A. and Apparao,A.,(1971).Depth of investigation in direct current methods, Geophysics,36:943-956.

Slichter, L.B., (1933). The interpretation of resistivity prospecting method for horizontal structure. Physics, 4: 307-322.

Stefanescu,C., (1930).Schlumberger Distribution of electric field in potential horizontals layers, homogeneous and isotropic, J.Physics. radium,7:132-141 .

Tamiru Alemayehu.,(2006). Groundwater occurrence in Ethiopia. Addis Ababa University, Addis Ababa, Ethiopia.

Telford, W.M., Geldart, L.P., and Sheriff, R.E., (1990).Applied Geophysics, second Edition. Cambrige University press, Cambrige, UK.Pp 6-48,522-562.

Tigistu Haile . , (2010). Electric Resistivity Tomography: Applications (with the IRIS SYSCAL Pro R1+ Switch). Retrieved from www.mawari.net. 25 pp.

V.S.Kovalevsky et al., (2004). Groundwater Studies, Series on groundwater no7.

Vander Velpen B.P.A., (1995).RESIXIP and Win Resist software, first version; Interpex limited company.

Woldegebriel Genzebu.,(1994). The geology of Ageremariam Sheet.Geological survey of Ethiopia, Addis Ababa, Ethiopia.

Zhdanov, M.S.and Keller, G.V., (1994). The geo-electrical methods in Geophysical Exploration, Elsevier, Amsterdam.

Zohydy, et al., (1980). Application of Surface Geophysics to Ground Water Investigation. United States Government Printing Office, Washington.

Appendix 1

Interpreted VES curves of **Mermero line 1(VES -1, VES-2,VES-3,VES-4)**

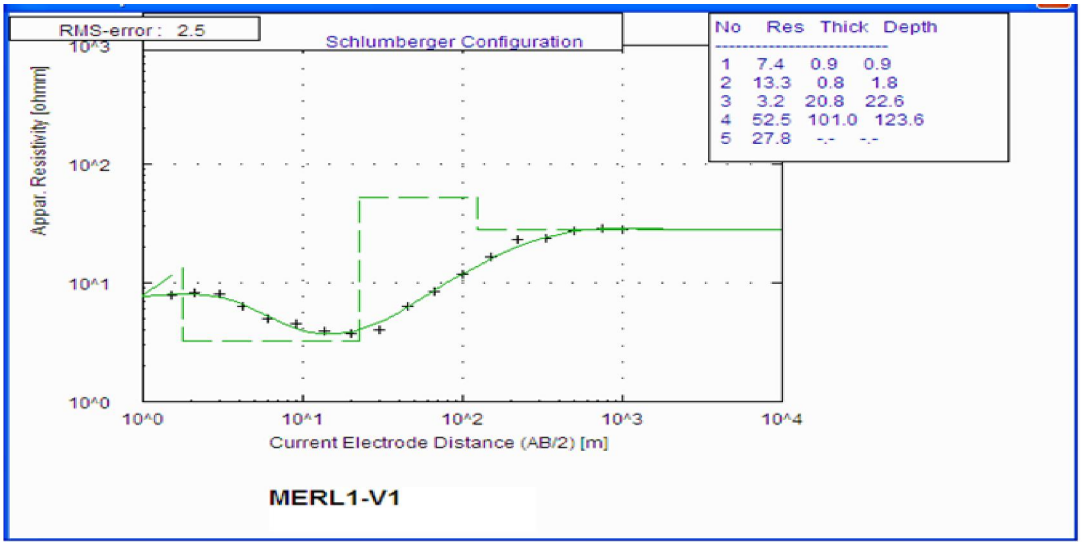

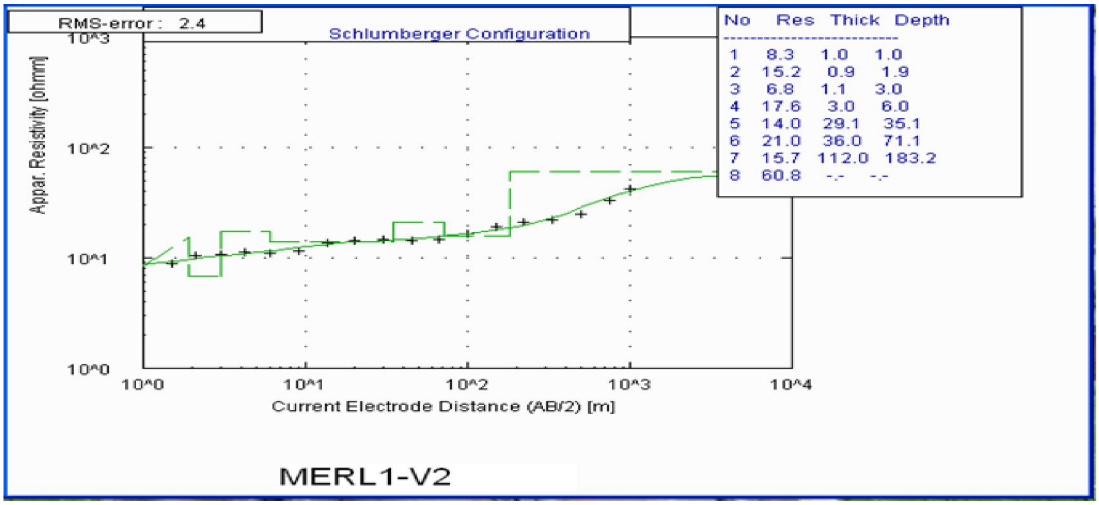

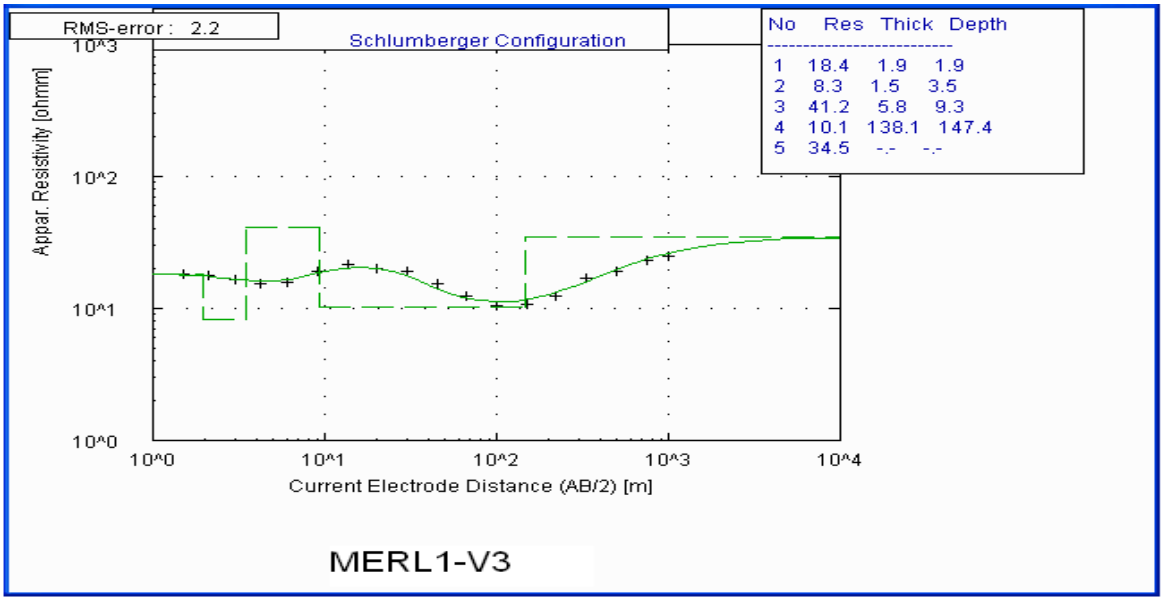
RMS-error : 2.2
Schlumberger Configuration
No Res Thick Depth
1 18.4 1.9 1.9
2 8.3 1.5 3.5
3 41.2 5.8 9.3
4 10.1 138.1 147.4
5 34.5 -.- -.-
Appar. Resistivity [ohmm]
10^3
10^2
10^1
10^0
10^0 10^1 10^2 10^3 10^4
Current Electrode Distance (AB/2) [m]
MERL1-V3

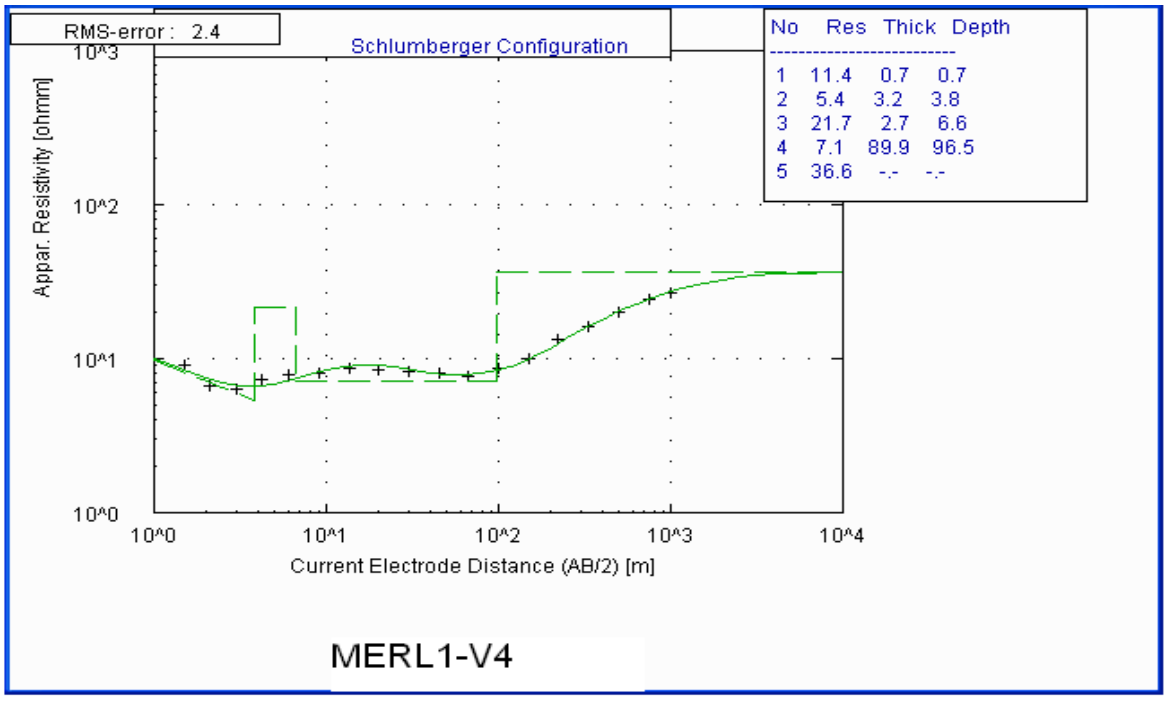
RMS-error : 2.4
Schlumberger Configuration
No Res Thick Depth
1 11.4 0.7 0.7
2 5.4 3.2 3.8
3 21.7 2.7 6.6
4 7.1 89.9 96.5
5 36.6 -.- -.-
Appar. Resistivity [ohmm]
10^3
10^2
10^1
10^0
10^0 10^1 10^2 10^3 10^4
Current Electrode Distance (AB/2) [m]
MERL1-V4

Interpreted VES curves of **Mermero line-2 (**VES -1, VES-2,VES-3,VES-4)

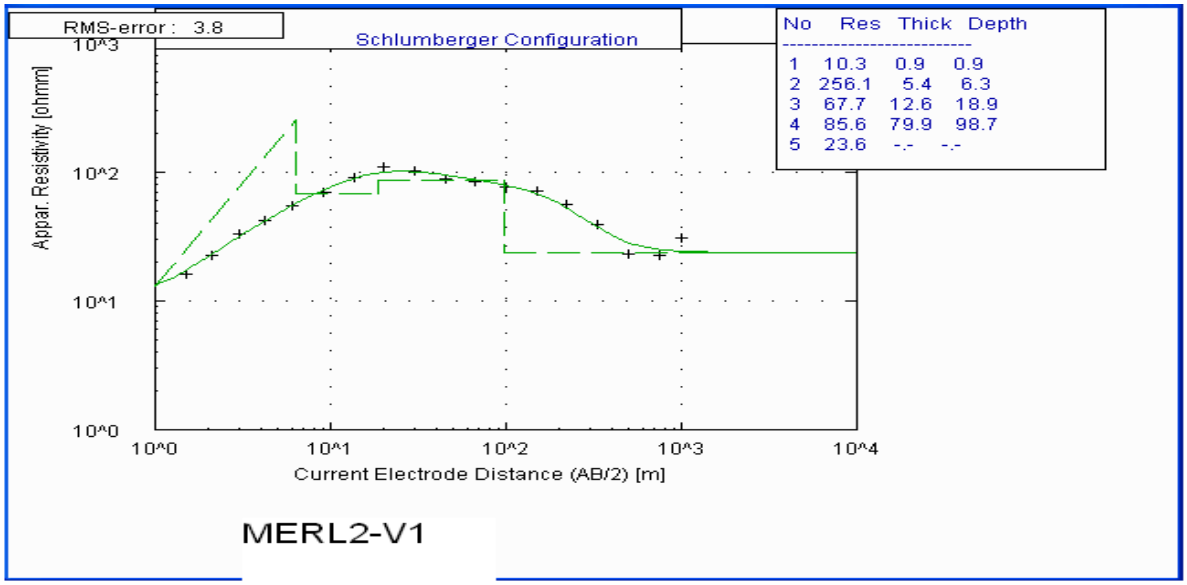

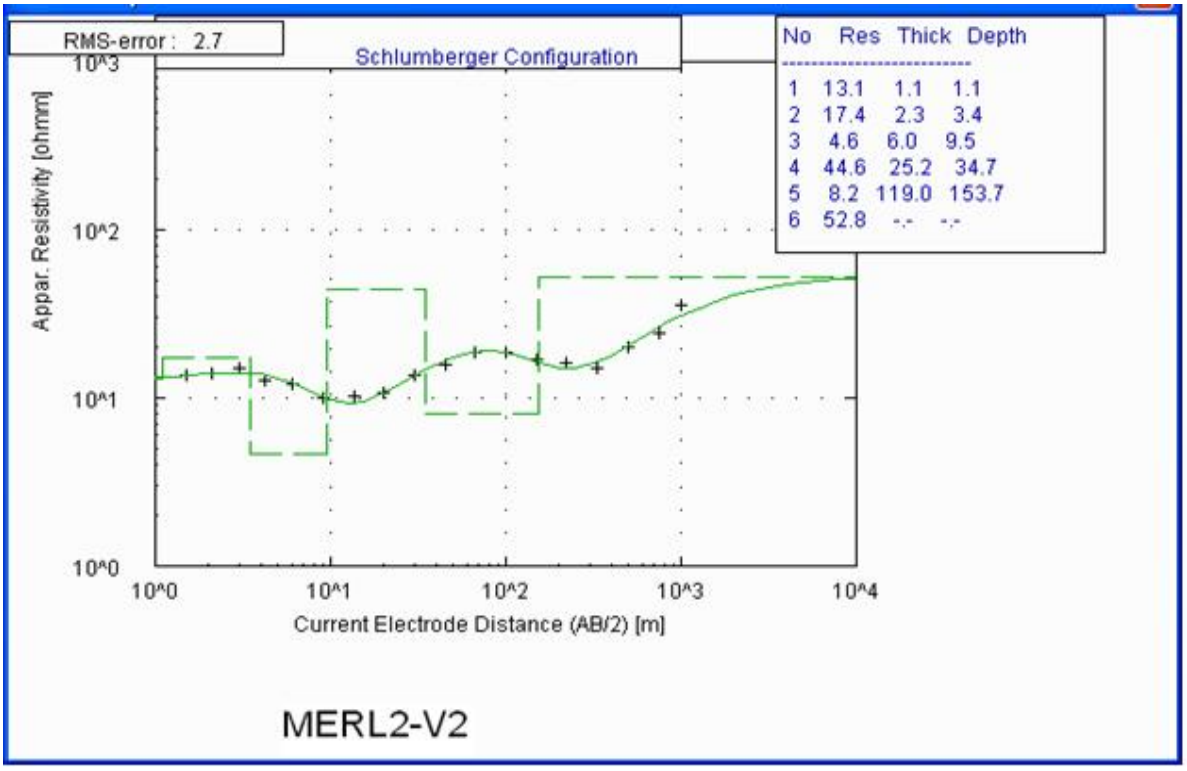

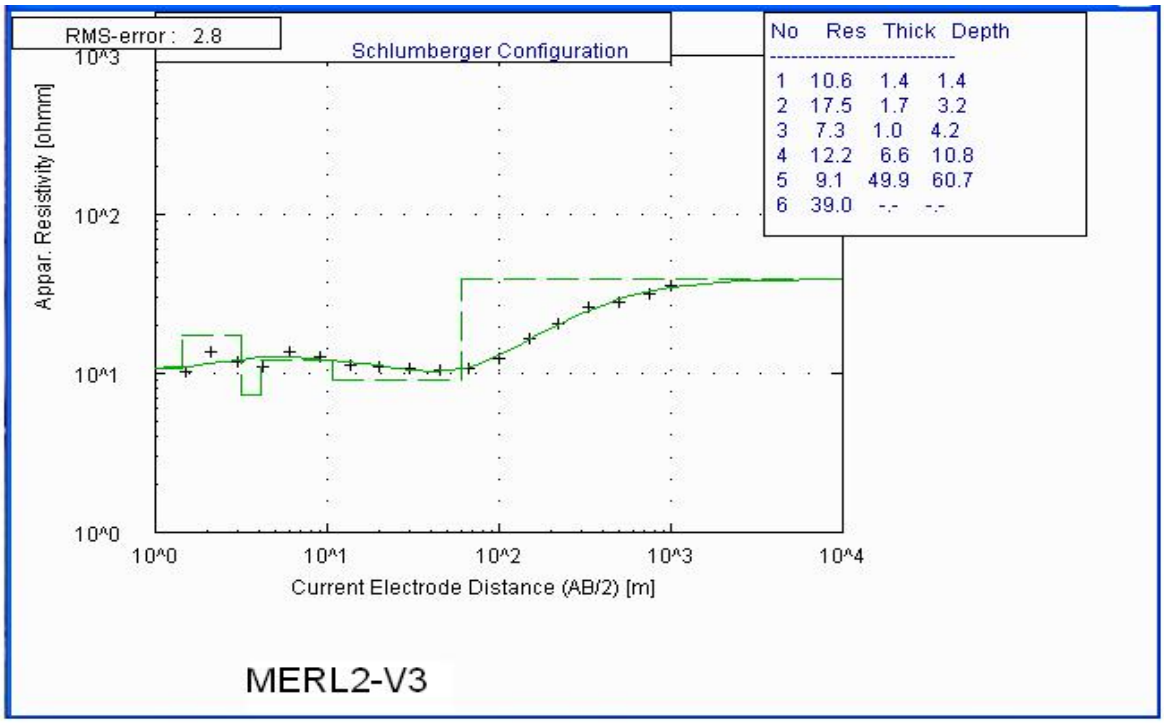
RMS-error : 2.8
Schlumberger Configuration
No Res Thick Depth
1 10.6 1.4 1.4
2 17.5 1.7 3.2
3 7.3 1.0 4.2
4 12.2 6.6 10.8
5 9.1 49.9 60.7
6 39.0 -.- -.-
Appar. Resistivity [ohmm]
10^3
10^2
10^1
10^0
10^0 10^1 10^2 10^3 10^4
Current Electrode Distance (AB/2) [m]
MERL2-V3

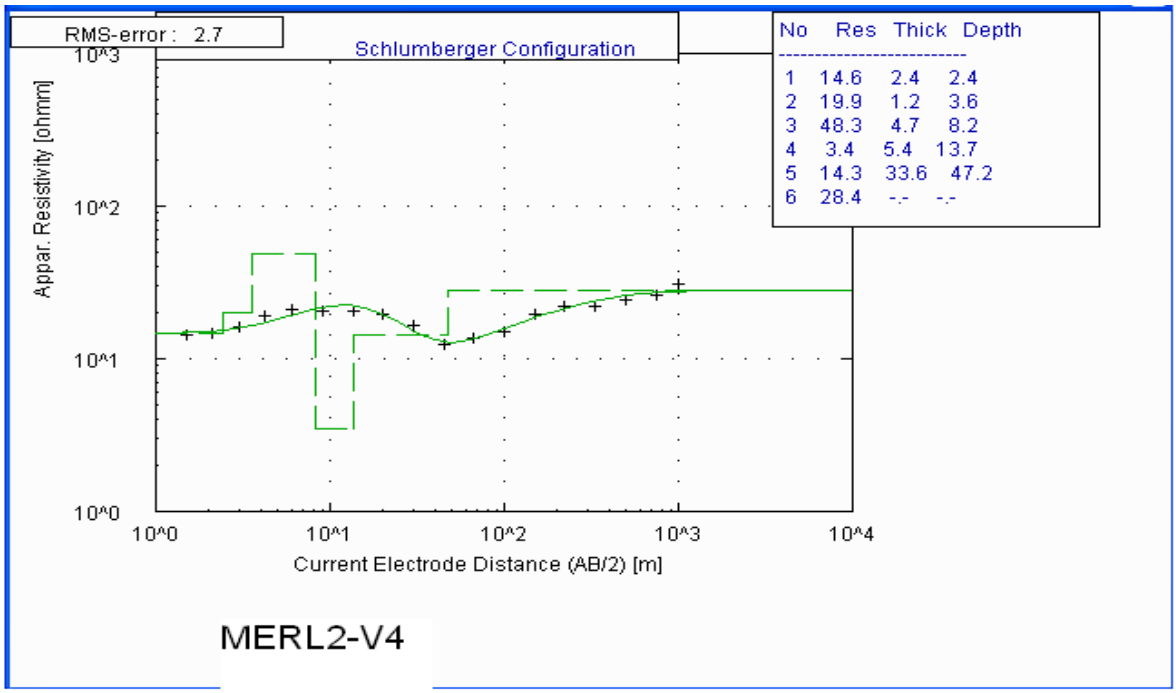
RMS-error : 2.7
Schlumberger Configuration
No Res Thick Depth
1 14.6 2.4 2.4
2 19.9 1.2 3.6
3 48.3 4.7 8.2
4 3.4 5.4 13.7
5 14.3 33.6 47.2
6 28.4 -.- -.-
Appar. Resistivity [ohmm]
10^3
10^2
10^1
10^0
10^0 10^1 10^2 10^3 10^4
Current Electrode Distance (AB/2) [m]
MERL2-V4

Mermero TRV3- (VES -1, VES-2, VES-3)

Mermero TRV3A (VES -1, VES-2, VES-**3)**

Mermero TRV3B (VES -1, VES-2, VES-3)

TRV3- V1

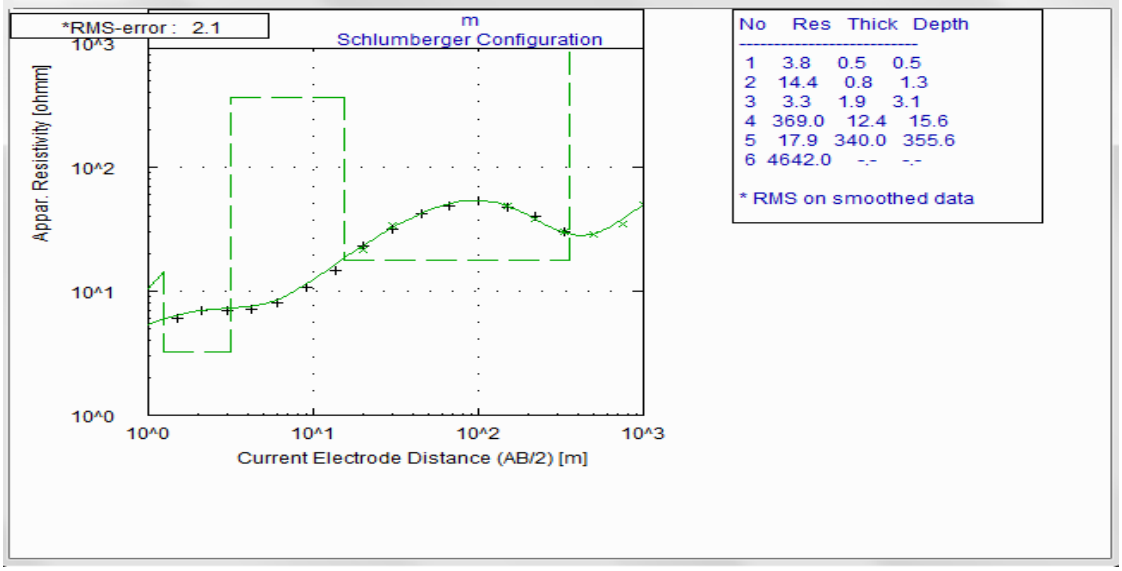

TRV3-V2

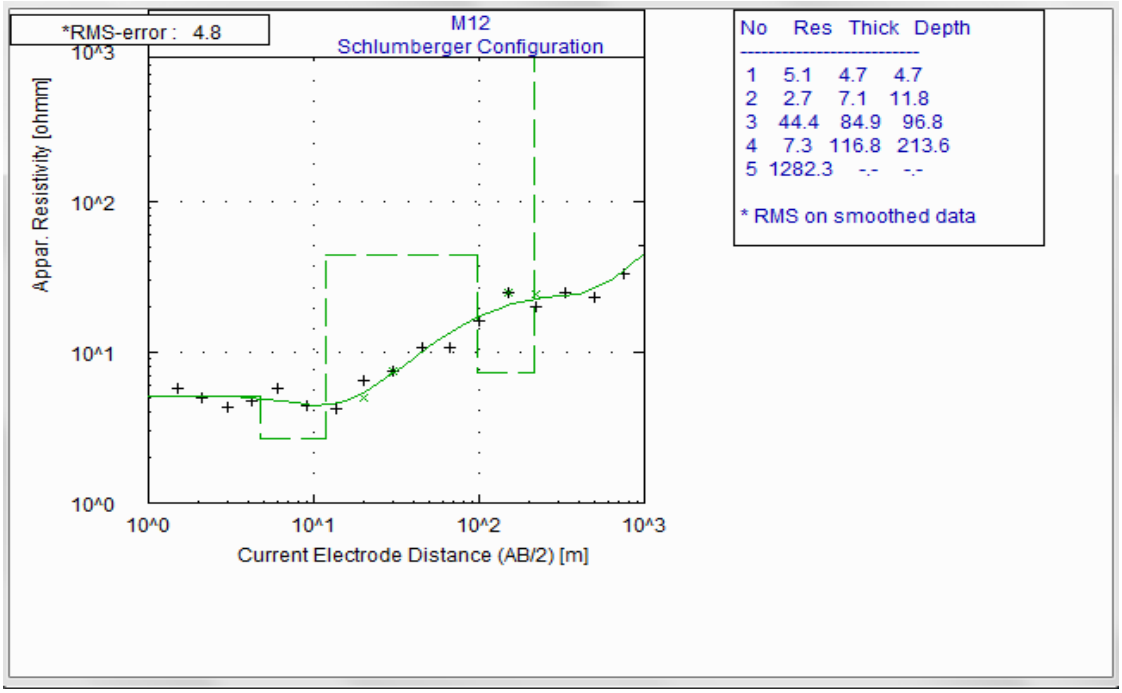

TRV3-V3

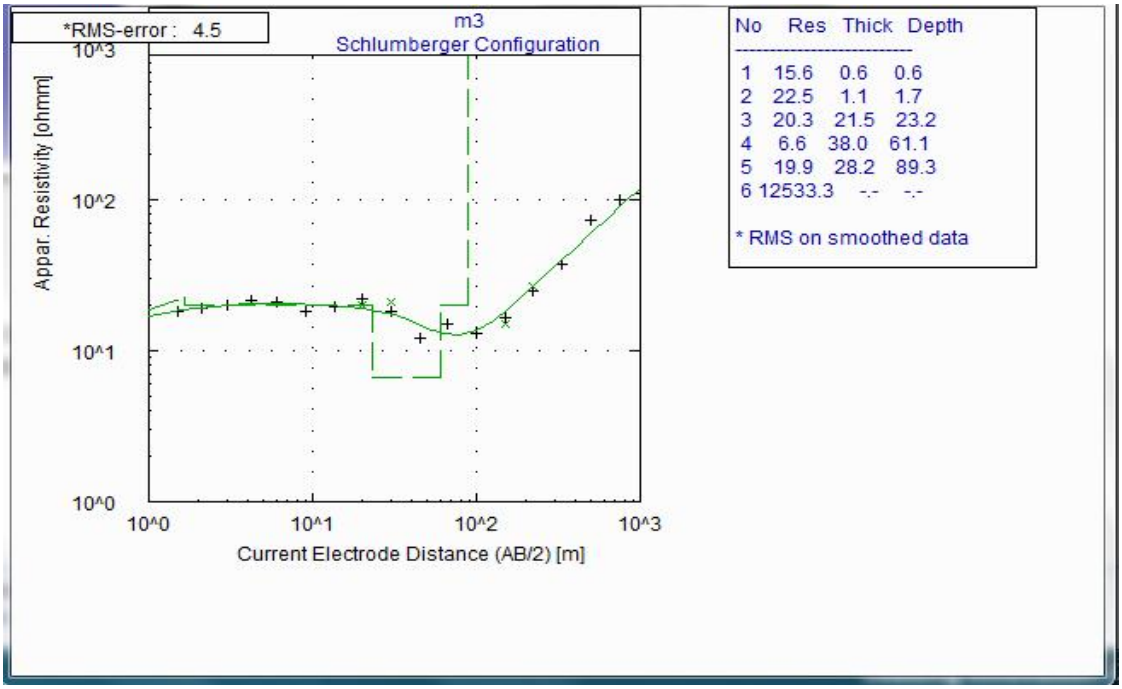

TRV3A-V1

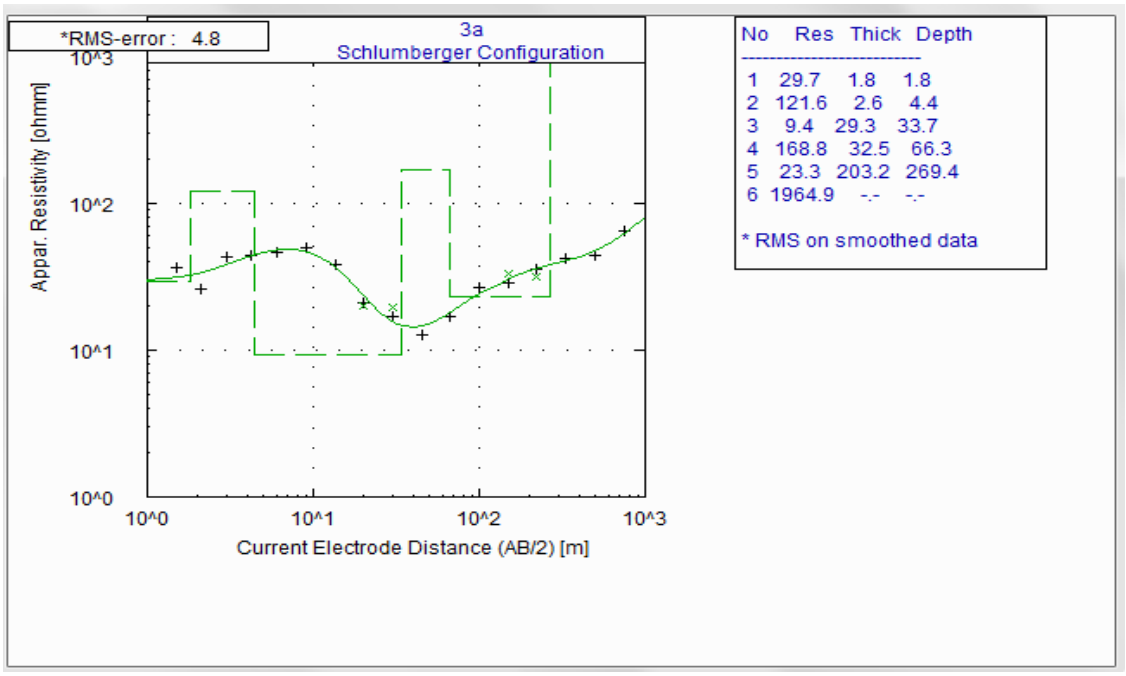

TRV3A-V2

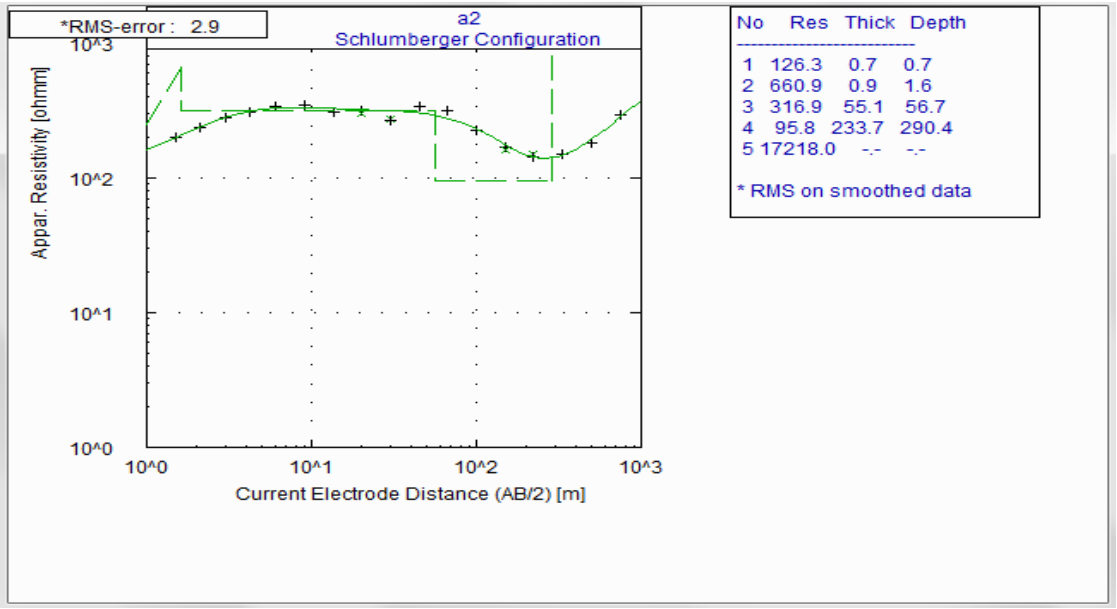

TRV3A-V3

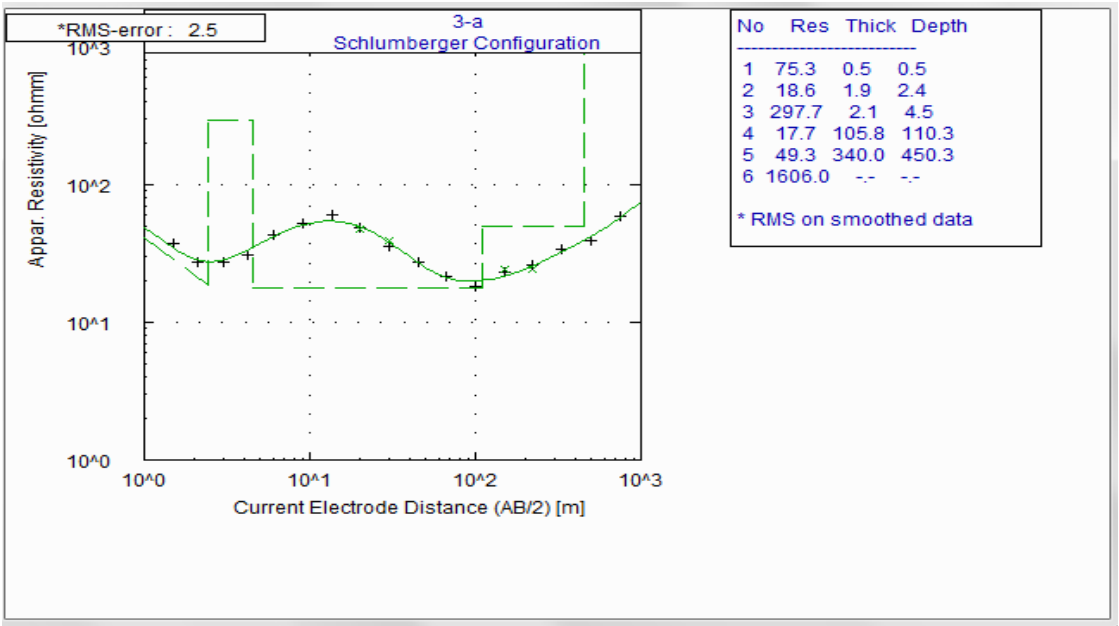

TRV3B-V1

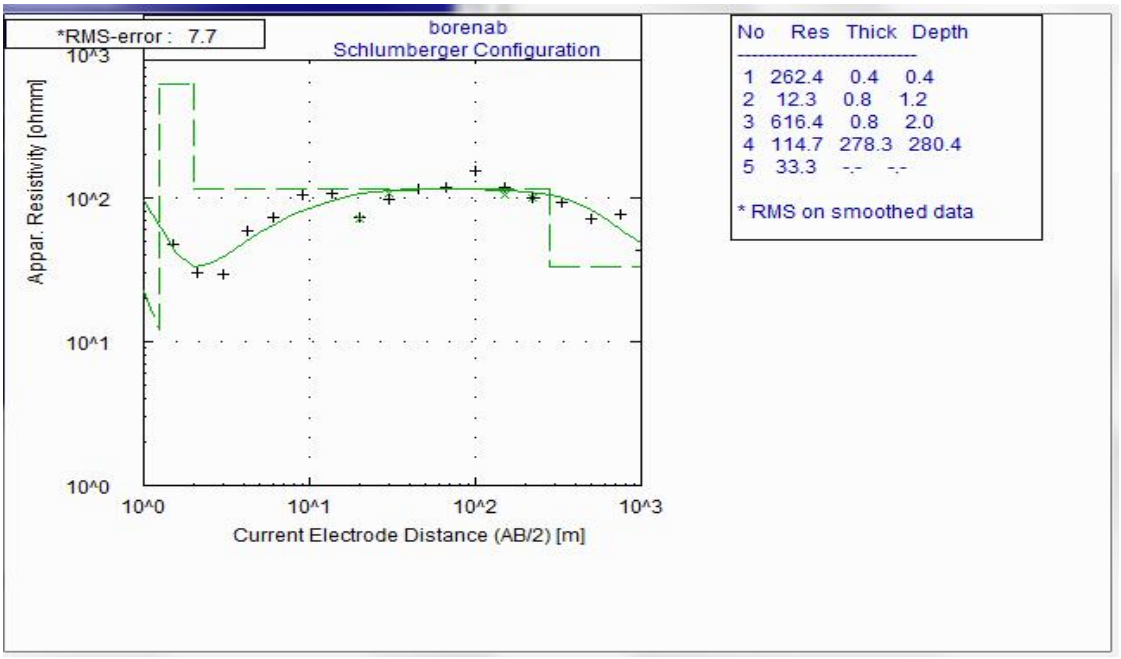

TRV3B-V2

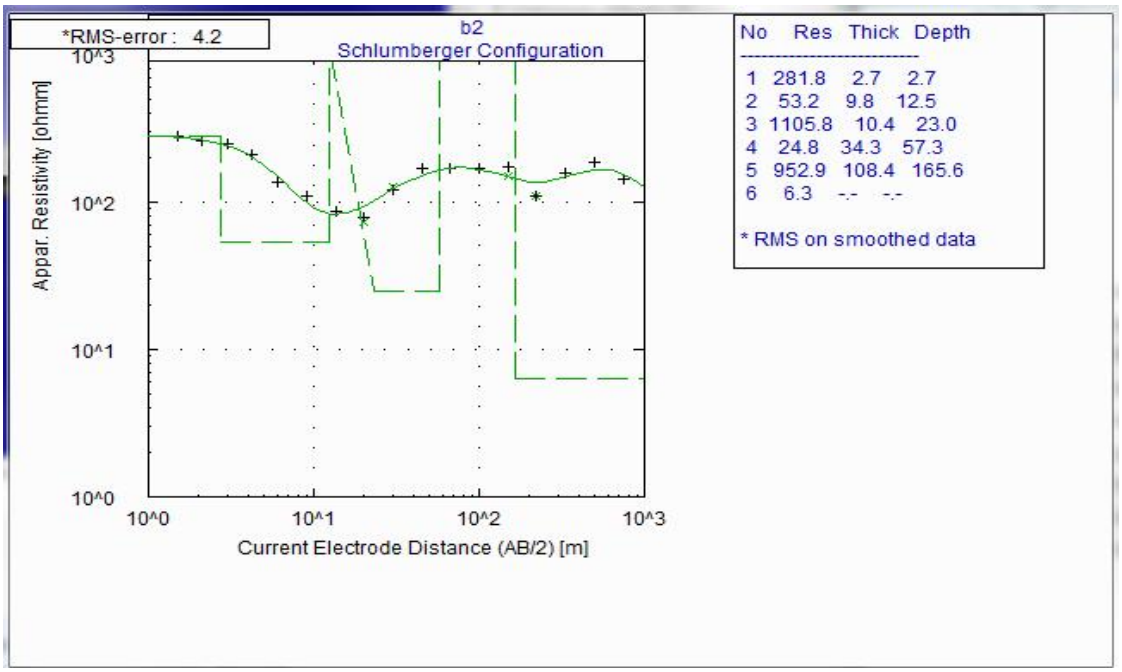

TRV3B-V3

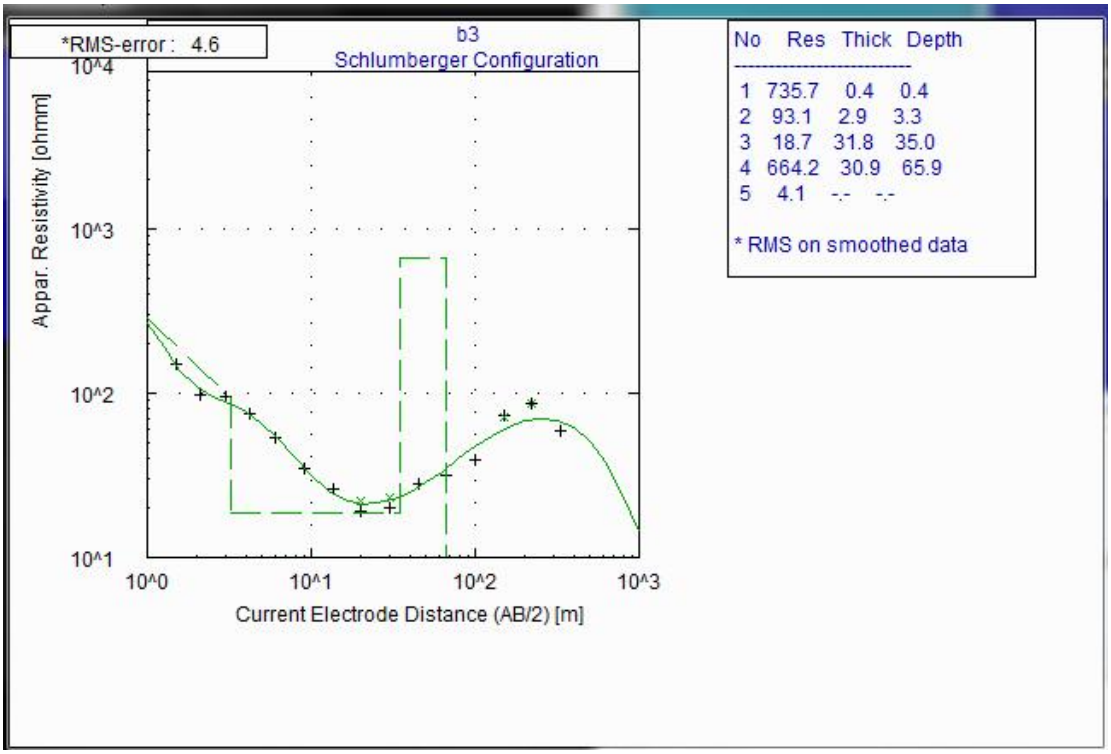

TRV-10 ,VES1

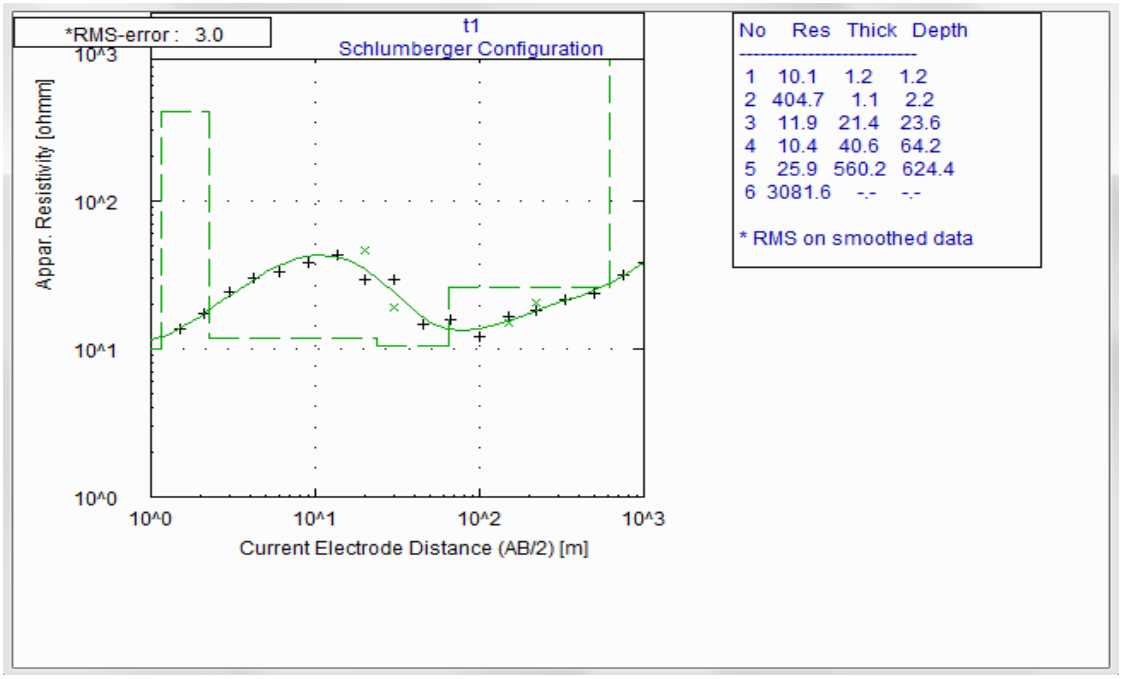

VES2

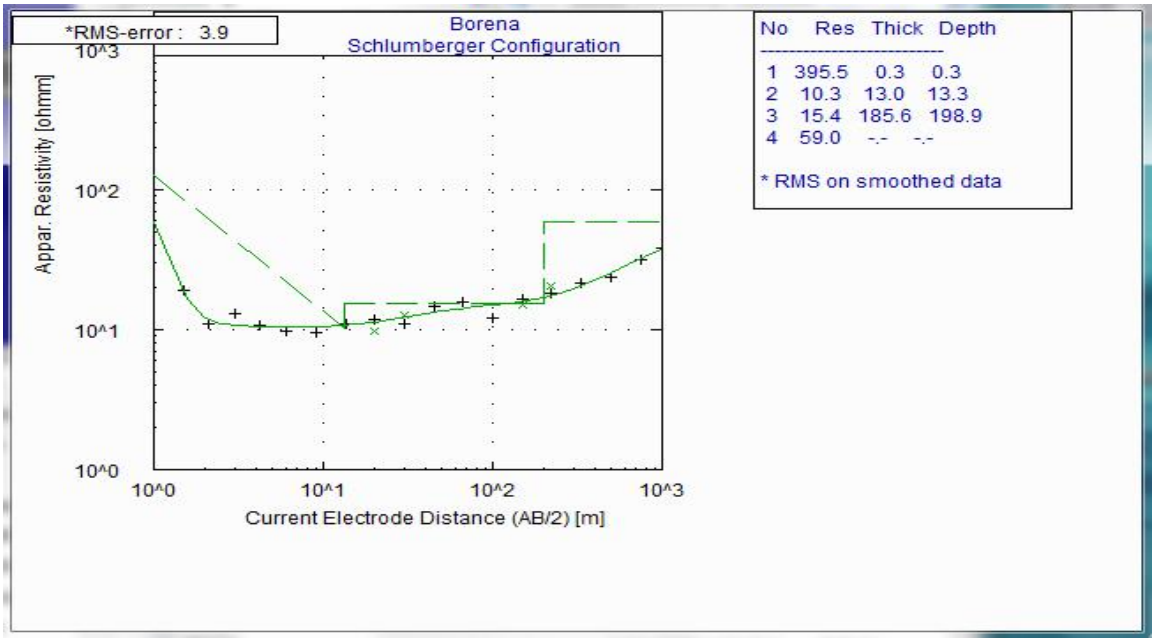

VES3

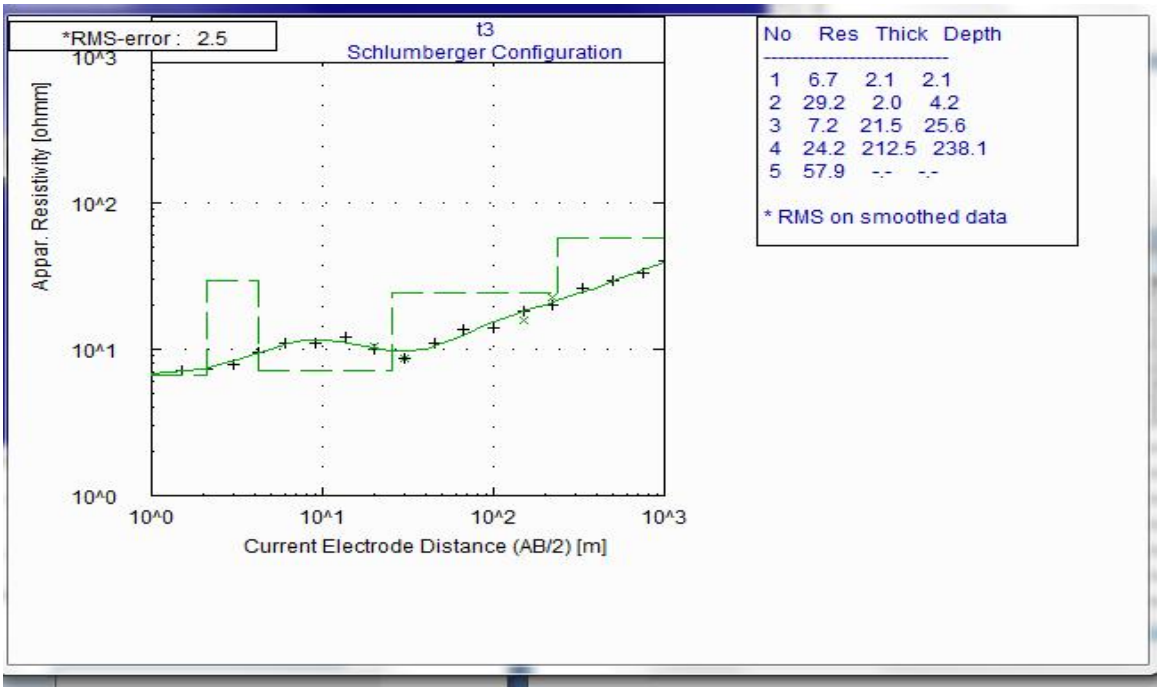

VES4

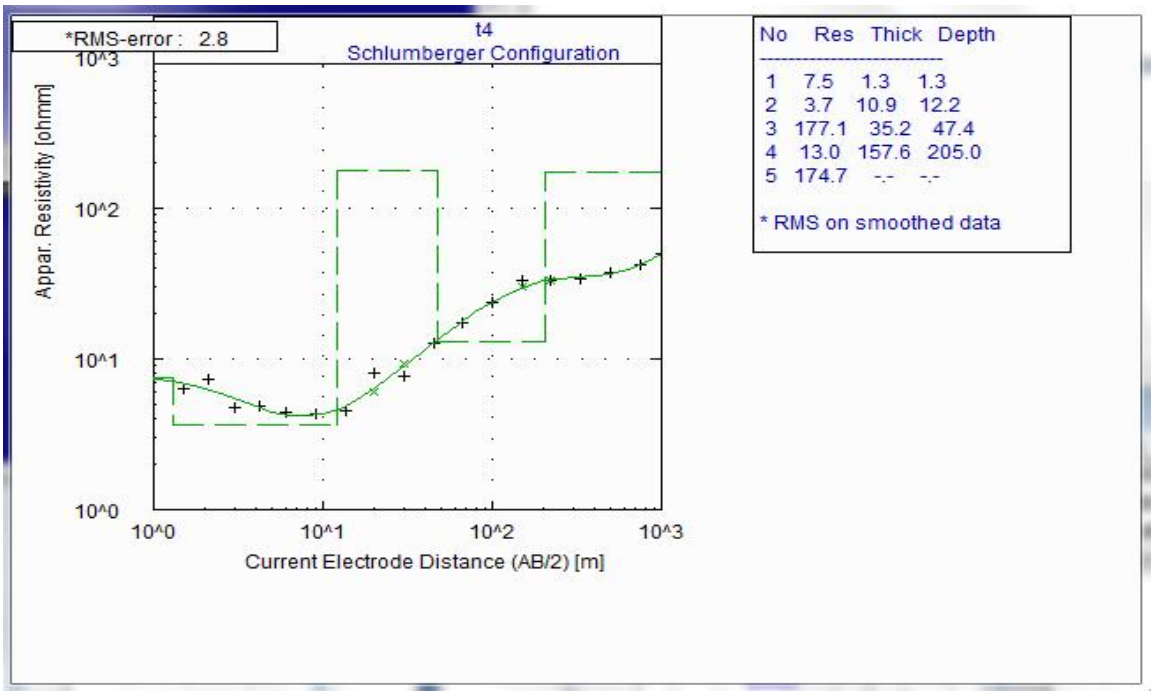
*RMS-error : 2.8
t4
Schlumberger Configuration
Appar. Resistivity [ohmm]
10^3
10^2
10^1
10^0
10^0
10^1
10^2
10^3
Current Electrode Distance (AB/2) [m]
No Res Thick Depth
1 7.5 1.3 1.3
2 3.7 10.9 12.2
3 177.1 35.2 47.4
4 13.0 157.6 205.0
5 174.7 -.- -.-
* RMS on smoothed data

VES5

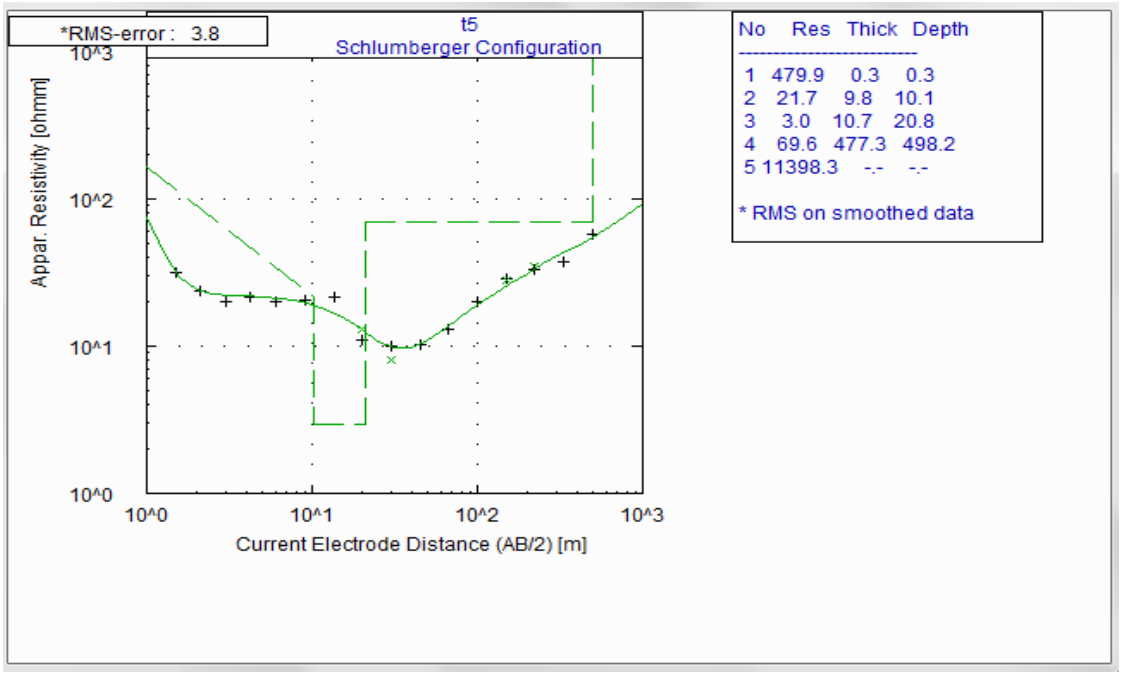
*RMS-error : 3.8
t5
Schlumberger Configuration
Appar. Resistivity [ohmm]
10^3
10^2
10^1
10^0
10^0
10^1
10^2
10^3
Current Electrode Distance (AB/2) [m]
No Res Thick Depth
1 479.9 0.3 0.3
2 21.7 9.8 10.1
3 3.0 10.7 20.8
4 69.6 477.3 498.2
5 11398.3 -.- -.-
* RMS on smoothed data

VES6

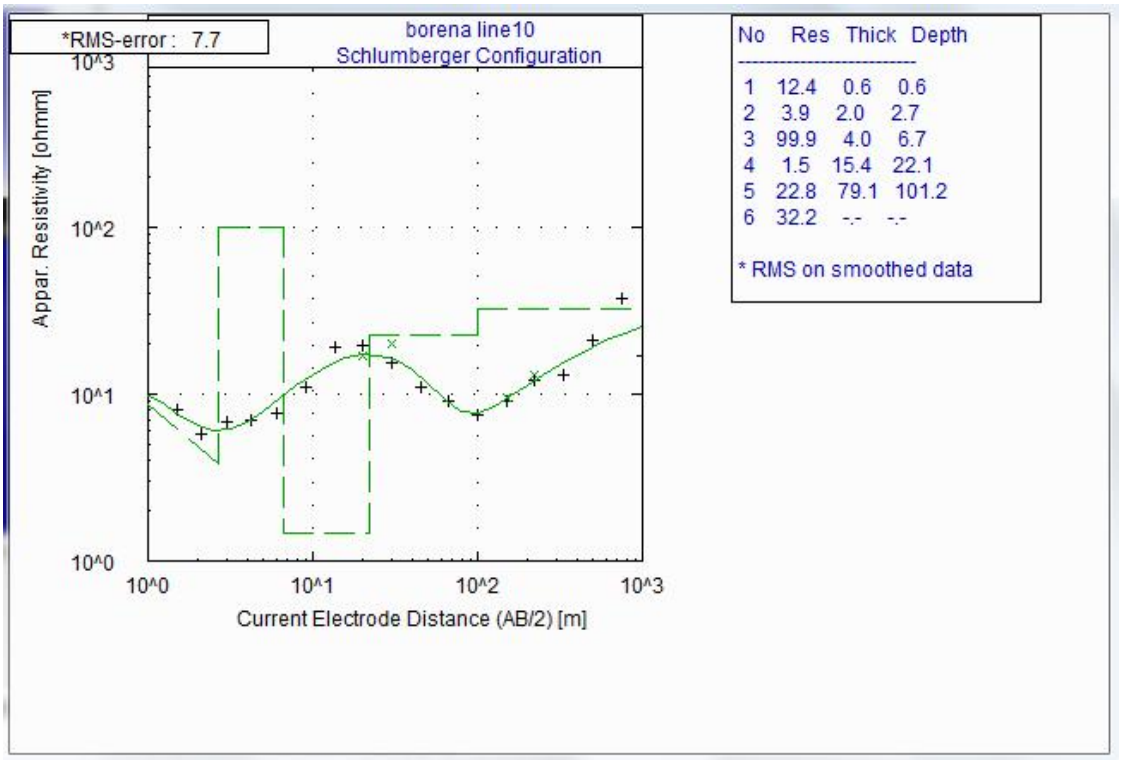
*RMS-error : 7.7
borena line10
Schlumberger Configuration
Appar. Resistivity [ohmm]
10^3
10^2
10^1
10^0
10^0
10^1
10^2
10^3
Current Electrode Distance (AB/2) [m]
No Res Thick Depth
1 12.4 0.6 0.6
2 3.9 2.0 2.7
3 99.9 4.0 6.7
4 1.5 15.4 22.1
5 22.8 79.1 101.2
6 32.2 -.- -.-
* RMS on smoothed data

VES7

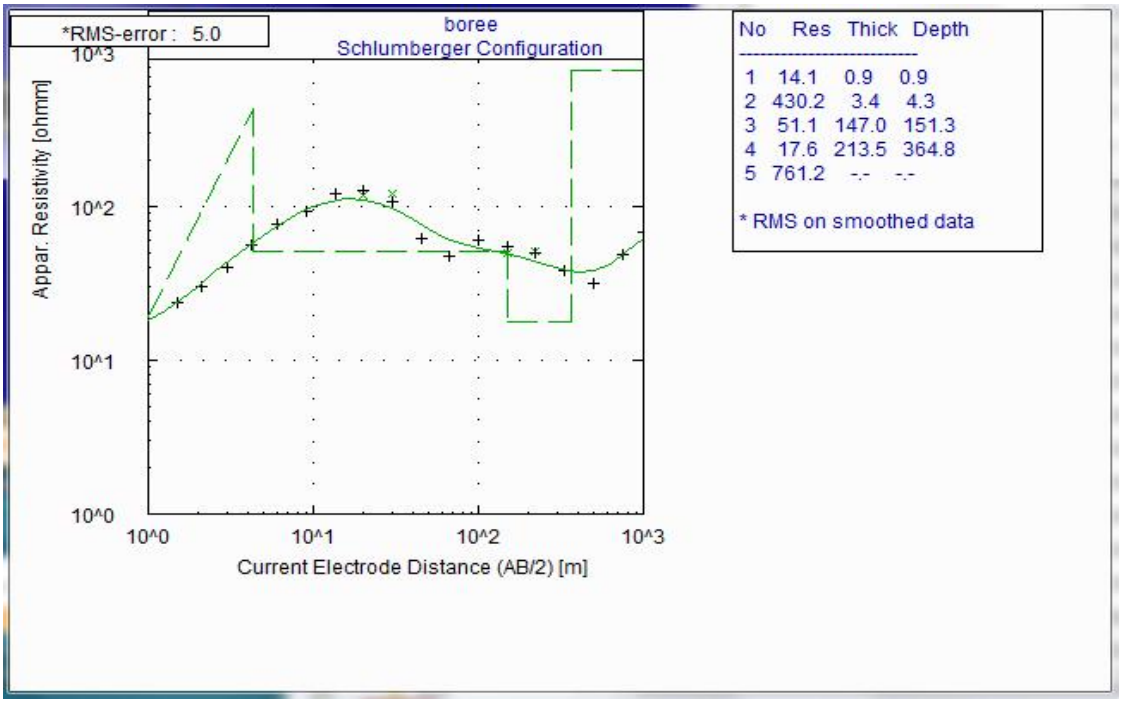
*RMS-error : 5.0
boree
Schlumberger Configuration
Appar. Resistivity [ohmm]
10^3
10^2
10^1
10^0
10^0
10^1
10^2
10^3
Current Electrode Distance (AB/2) [m]
No Res Thick Depth
1 14.1 0.9 0.9
2 430.2 3.4 4.3
3 51.1 147.0 151.3
4 17.6 213.5 364.8
5 761.2 -.- -.-
* RMS on smoothed data

VES8

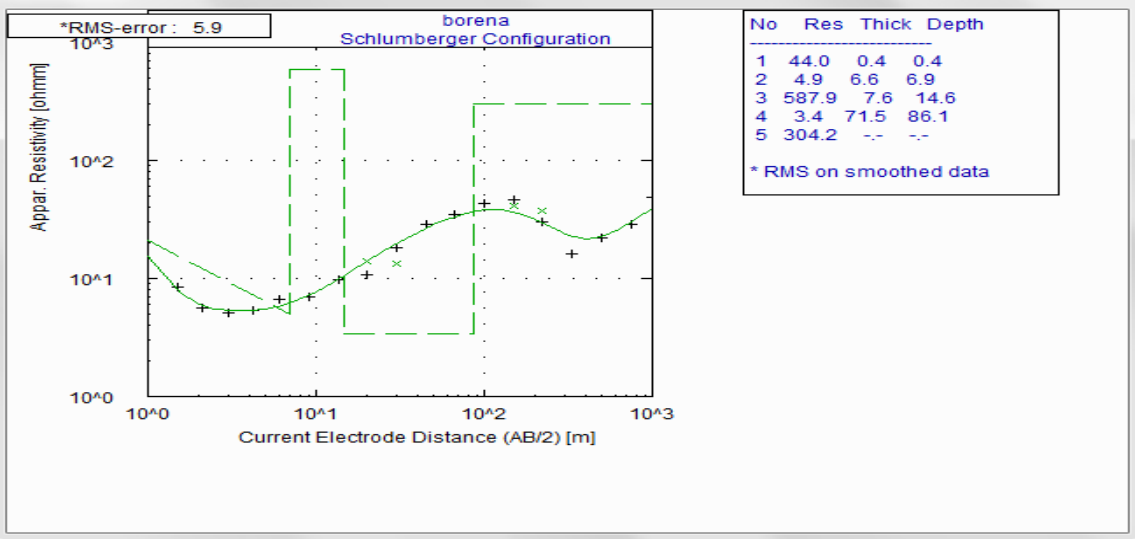
*RMS-error : 5.9
borena
Schlumberger Configuration
Appar. Resistivity [ohmm]
10^3
10^2
10^1
10^0
10^0
10^1
10^2
10^3
Current Electrode Distance (AB/2) [m]
No Res Thick Depth
1 44.0 0.4 0.4
2 4.9 6.6 6.9
3 587.9 7.6 14.6
4 3.4 71.5 86.1
5 304.2 -.- -.-
* RMS on smoothed data

VES9

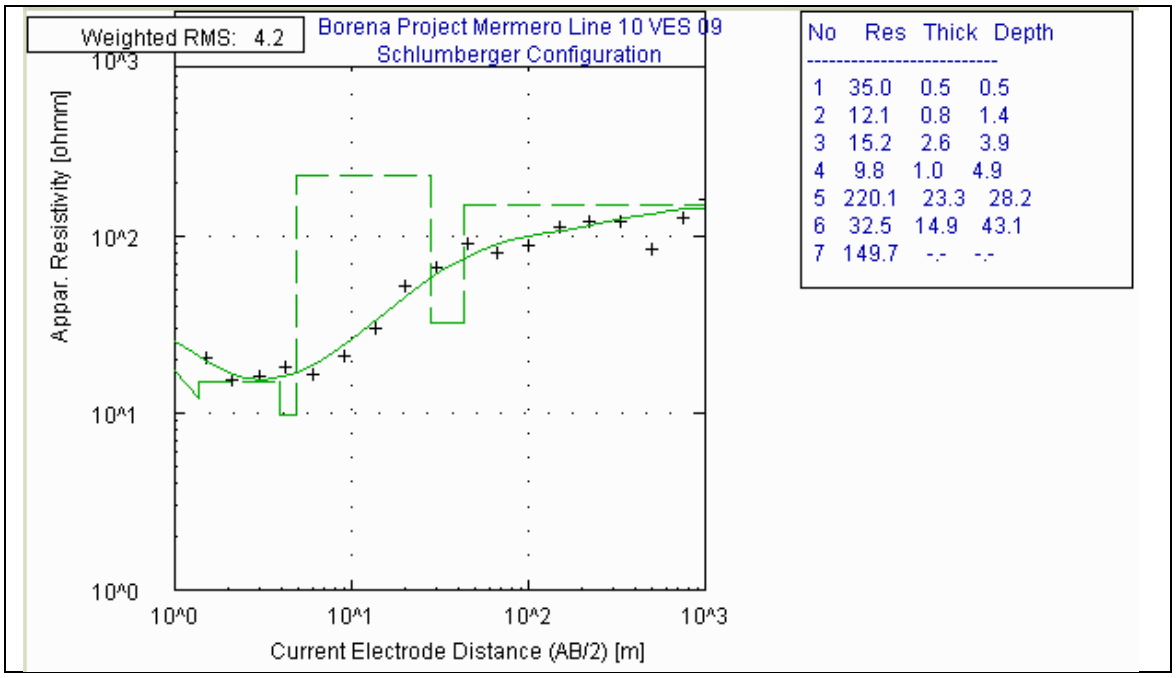
Weighted RMS: 4.2
Borena Project Mermero Line 10 VES 09
Schlumberger Configuration
Appar. Resistivity [ohmm]
10^3
10^2
10^1
10^0
10^0
10^1
10^2
10^3
Current Electrode Distance (AB/2) [m]
No Res Thick Depth
1 35.0 0.5 0.5
2 12.1 0.8 1.4
3 15.2 2.6 3.9
4 9.8 1.0 4.9
5 220.1 23.3 28.2
6 32.5 14.9 43.1
7 149.7 -.- -.-

VES10

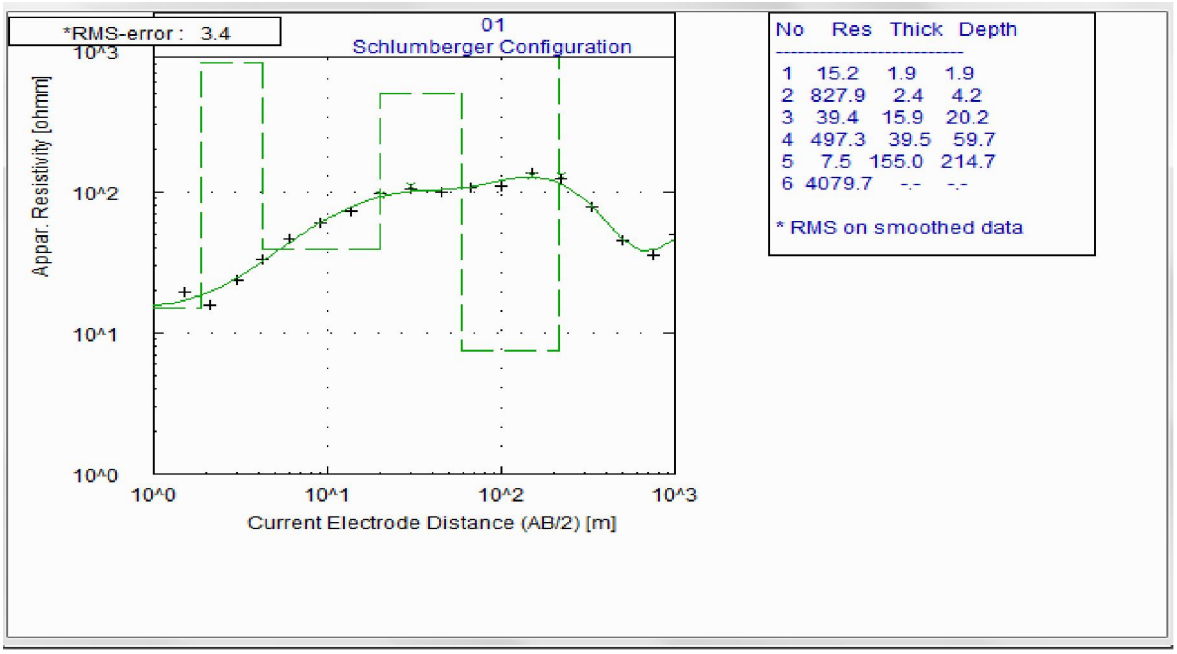
*RMS-error : 3.4
01
Schlumberger Configuration
Appar. Resistivity [ohmm]
10^3
10^2
10^1
10^0
10^0
10^1
10^2
10^3
Current Electrode Distance (AB/2) [m]
No Res Thick Depth
1 15.2 1.9 1.9
2 827.9 2.4 4.2
3 39.4 15.9 20.2
4 497.3 39.5 59.7
5 7.5 155.0 214.7
6 4079.7 -.- -.-
* RMS on smoothed data

VES11

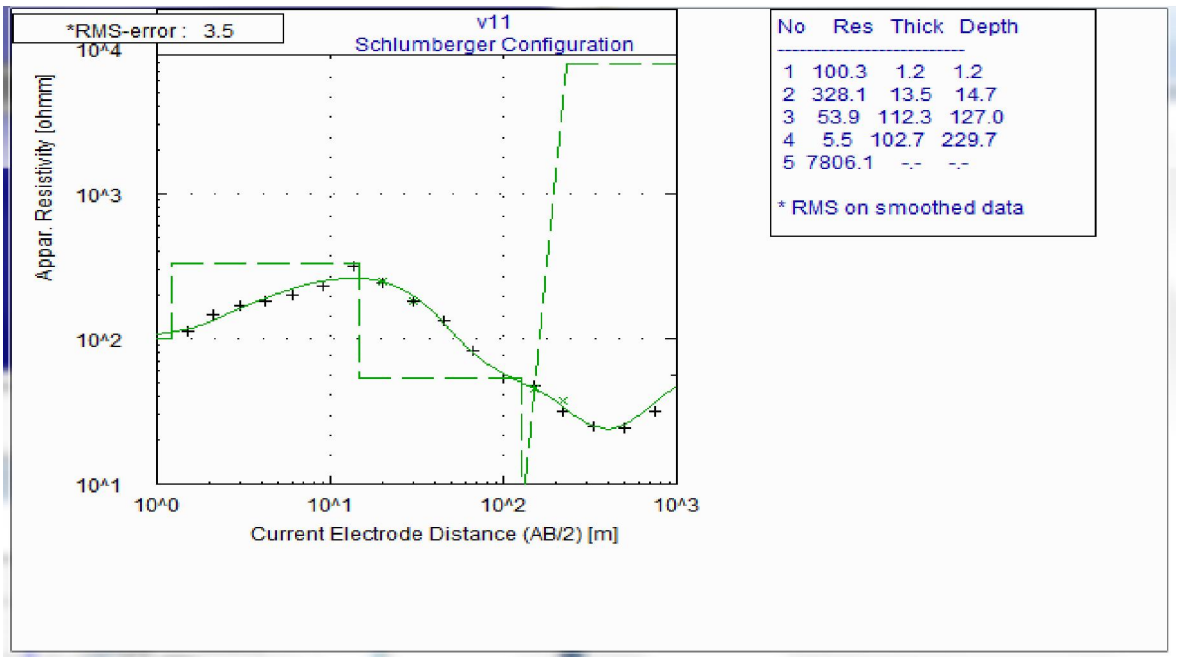
*RMS-error : 3.5
v11
Schlumberger Configuration
Appar. Resistivity [ohmm]
10^4
10^3
10^2
10^1
10^0
10^1
10^2
10^3
Current Electrode Distance (AB/2) [m]
No Res Thick Depth
1 100.3 1.2 1.2
2 328.1 13.5 14.7
3 53.9 112.3 127.0
4 5.5 102.7 229.7
5 7806.1 -.- -.-
* RMS on smoothed data

Appendix 2

Lithologic log at Mermero BTW2